Cable-supported bridges

(Hänge-, Spannband- und Schrägseilbrücken)
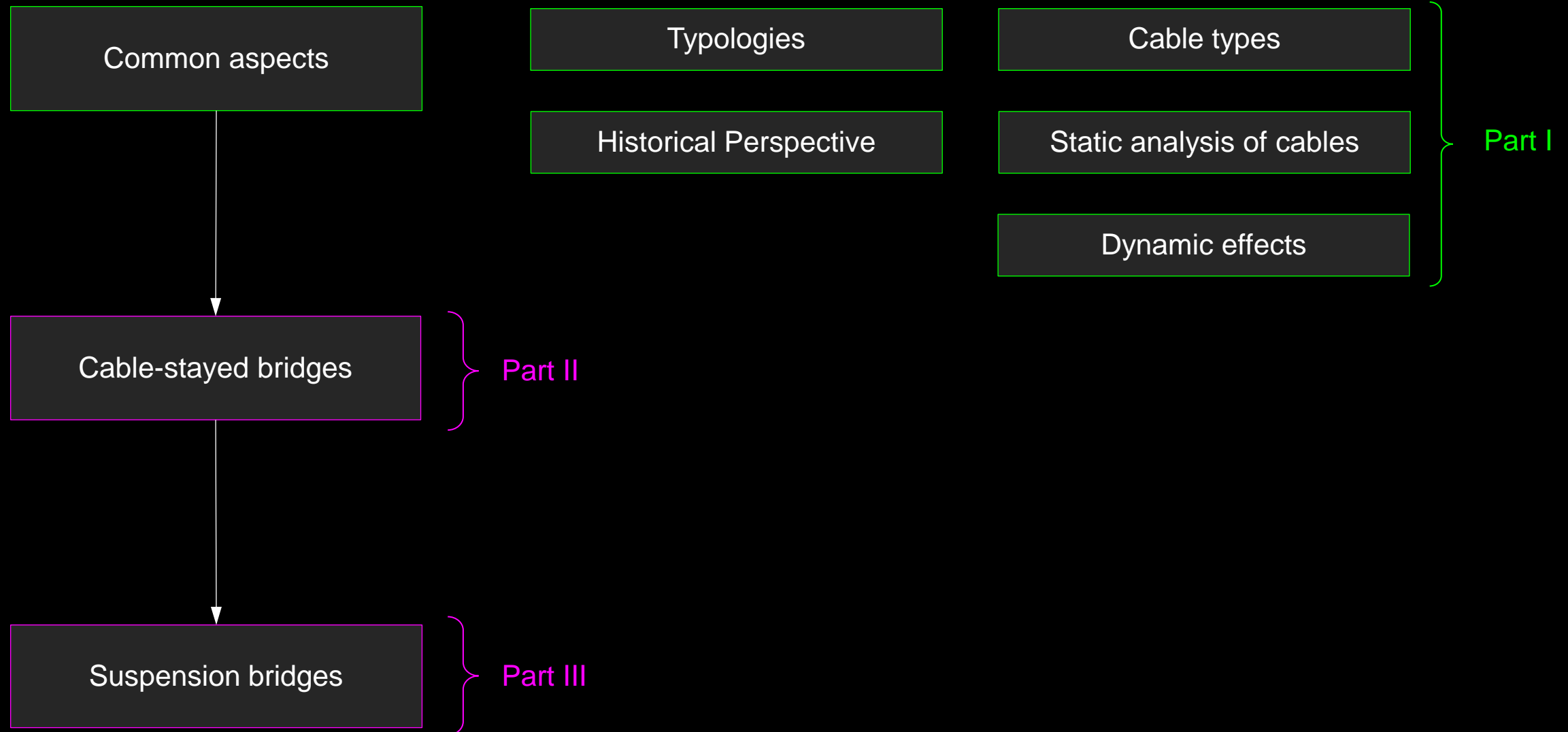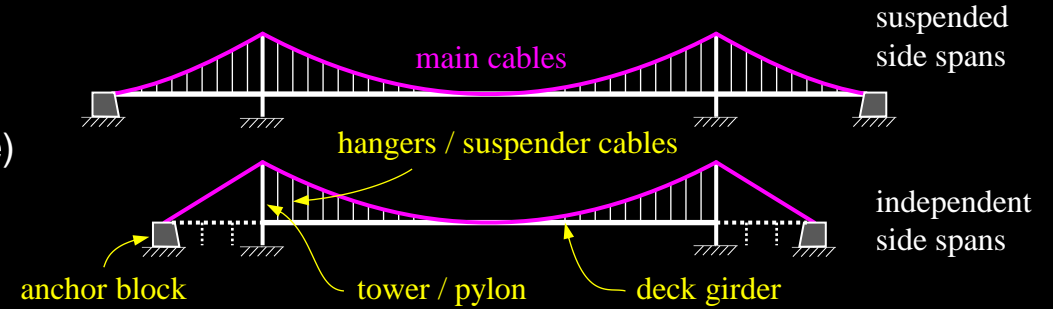
Common aspects	Typologies	Cable types
	Historical Perspective	Static analysis of cables
		Dynamic effects

Part I

Cable-stayed bridges — **Part II**

Suspension bridges — **Part III**

Cable-supported bridges

Common aspects – Typologies

Cable-supported bridges – Common aspects: Typologies

- The typology of cable-supported bridges is related to the configuration of cable system and the deck girder which, in turn, determine the loading of the cables.

- Accordingly, the following basic types of cable-supported bridges can be distinguished:

  → Suspension bridge: Sagging main cables (f/l = 1/9…1/11) spanning between towers / pylons. Main cables loaded laterally by hangers connecting the suspended deck girder to the main cables.

  → Suspended bridge / Stress-ribbon: Slightly sagging main cables, spanning between abutments without towers. Cables loaded laterally by the deck girder. The deck follows the cable profile in elevation. ("stress ribbon" commonly used for suspended bridges with prestressed concrete deck)

  → Cable-stayed bridge: Virtually straight cables connecting the deck girder to one or more pylons / towers. Cables loaded axially (primarily).

  → Stayed suspension bridge: A "hybrid" combination of suspension bridge and cable-stayed bridge.

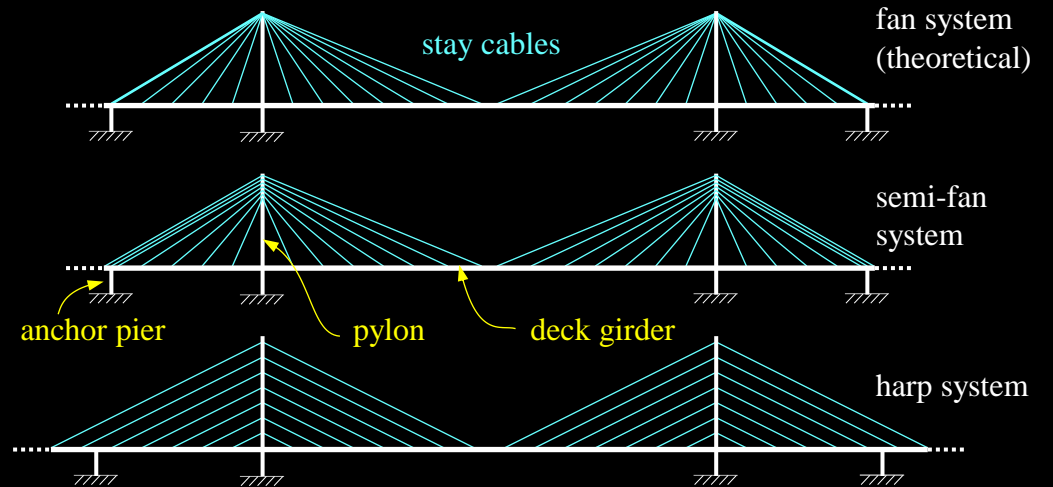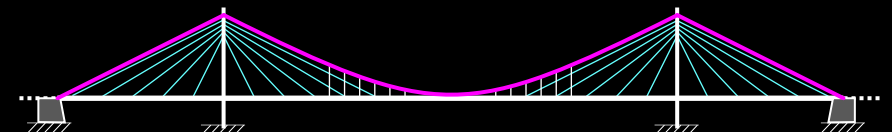Suspension bridge (Hängebrücke)

suspended side spans

main cables

hangers / suspender cables

independent side spans

anchor block   tower / pylon   deck girder

Suspended bridge (Stress ribbon) (Spannband)

Cable-stayed bridge (Schrägseil-brücke)

stay cables

fan system (theoretical)

semi-fan system

anchor pier   pylon   deck girder

harp system

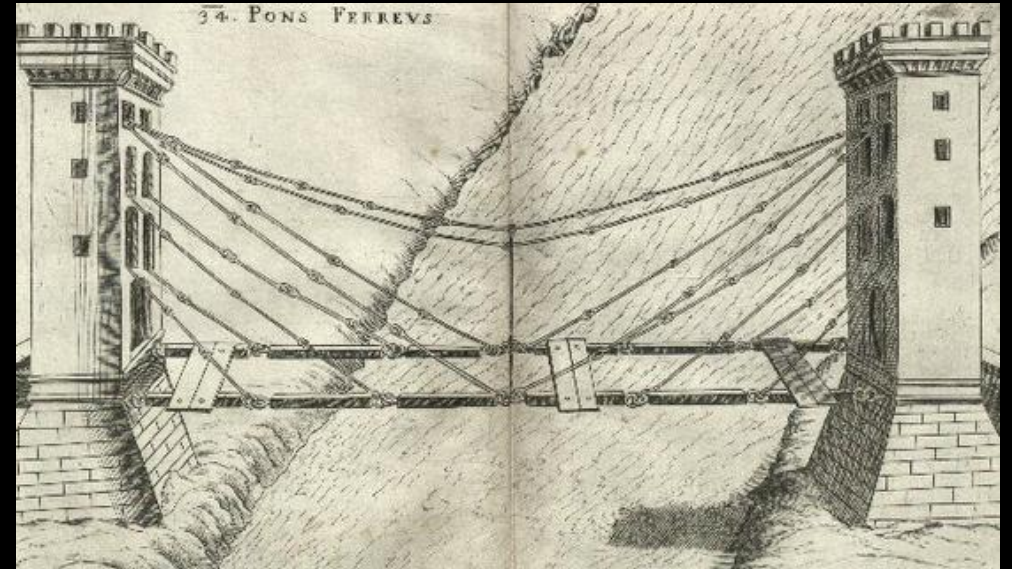Stayed suspension bridge

Cable-supported bridges

Common aspects – Historical perspective

Cable-supported bridges – Common aspects: Historical perspective

Similar to arches, suspension bridges have been built for centuries (some sources see notes):

- More than 2 millennia ago (ca. 65 n.Chr.), the first iron chain footbridge is said to have been built in Yunnan, China.

- The Incas are said to have built grass rope suspension footbridges since the 12th century, with a network of ca. 200 bridges around 1600. These bridges required regular maintenance and replacement of the ropes every 1-3 years (top photo).

- A Twärrenbrücke ("Querbrücke" = footpath along a canyon wall, suspended by means of chains) is known to have been part of the Gotthard route around 1218.

- In 1616, Faustus Verantius in a publication included a project – or rather, a vision – for a chain-supported bridge (bottom illustration).

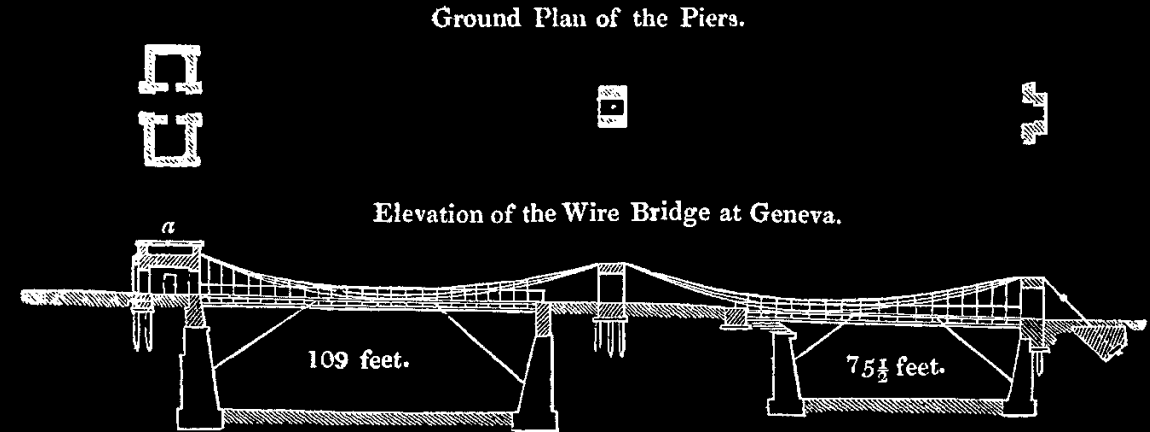# Cable-supported bridges – Common aspects: **Historical perspective**

(continued, some sources see notes)

- Thangtong Gyalpo, a Buddhist yogi known as Chakzampa (the Bridge Builder), built 58 iron chain suspension bridges throughout the Himalayan region, with spans up to 100 m, in the 15th century (top illustrations).

- James Finley built suspension bridges in the U.S., using similar chains as T. Gyalpo, already in 1796 (bottom illustrations).

- While stone arches are virtually imperishable unless their foundations are destroyed (e.g. by floods), suspension elements are much less durable and hence, hardly any of these early cable-supported bridges have survived.

- In the following, merely some milestones in the development of suspension bridges are highlighted. For a more complete overview, refer to literature.
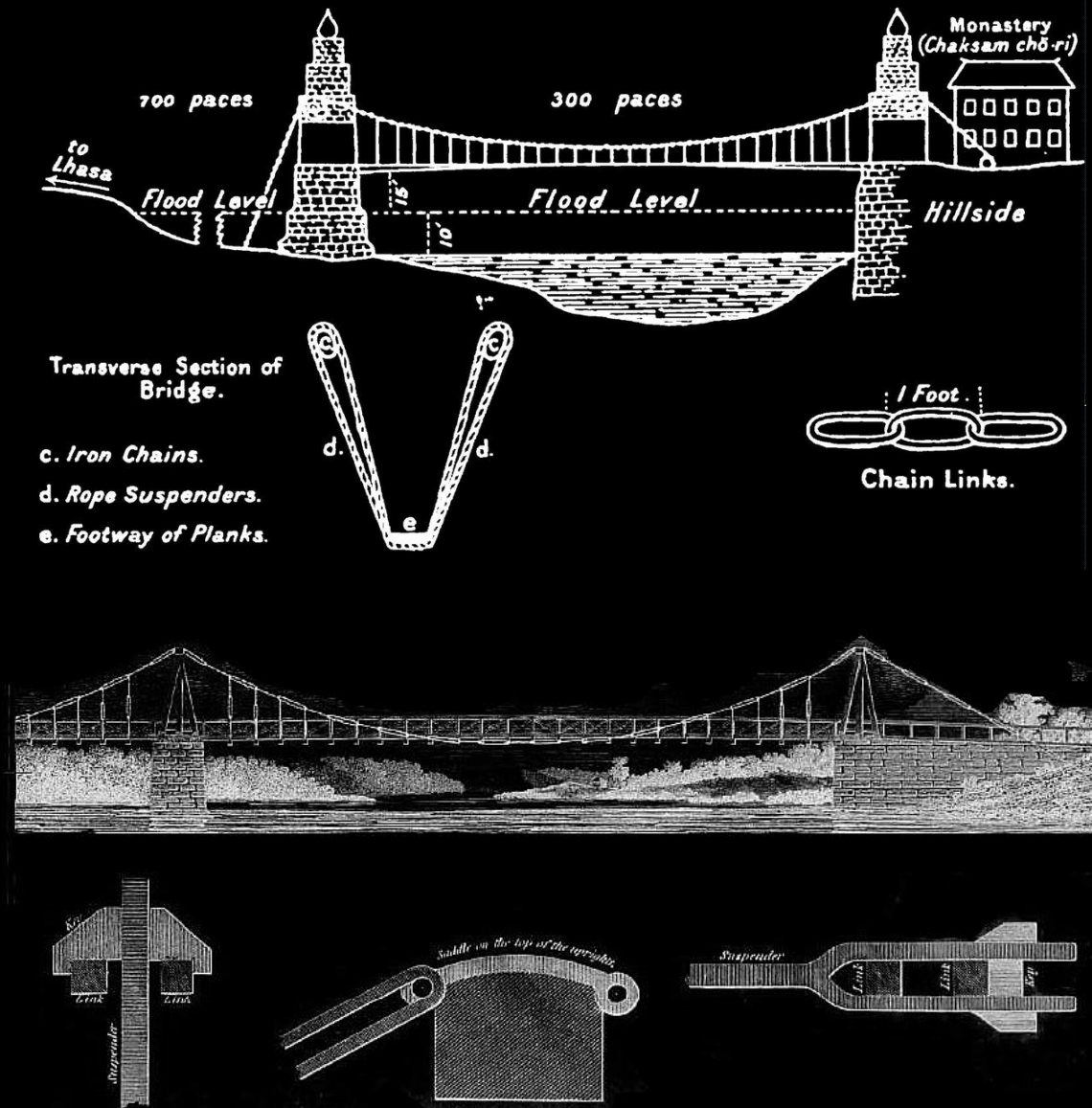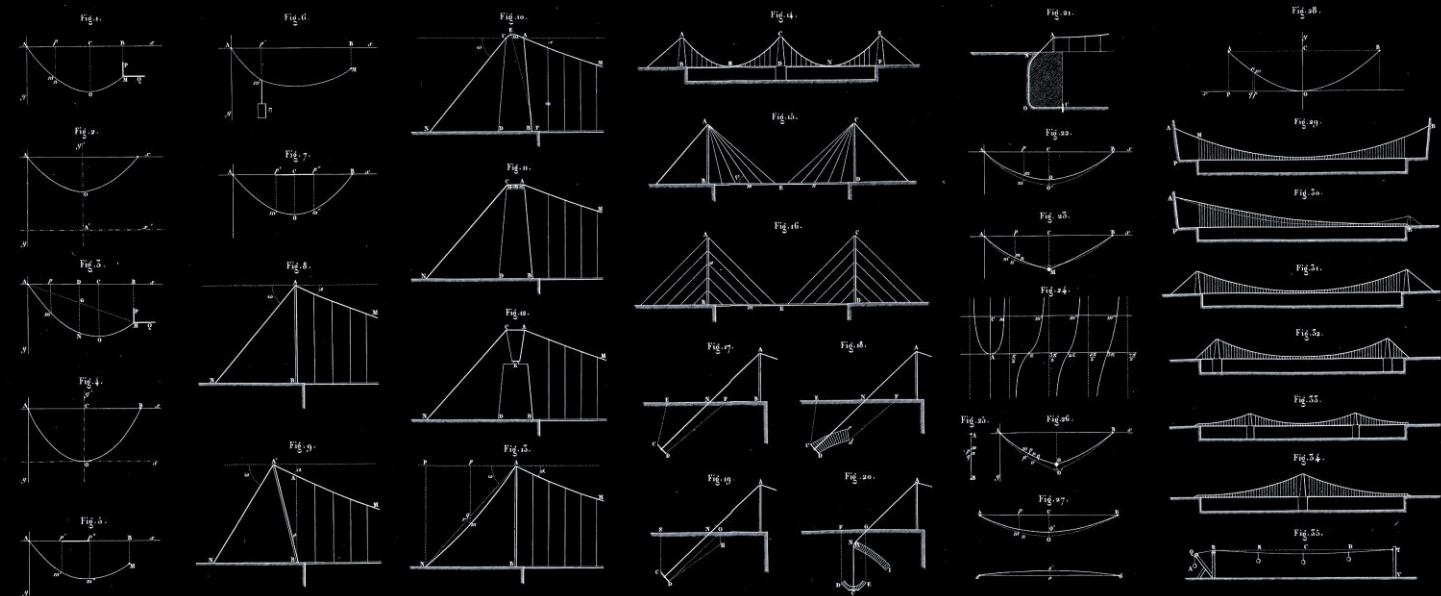
Cable-supported bridges – Common aspects: Historical perspective

- The Passerelle Saint Antoine in Geneva (1823-1850, spans 33+23 m), designed by Guillaume-Henri Dufour (based on a proposal by Marc Séguin) was the first permanent wire cable suspension bridge, see illustration at right.

- G. H. Dufour General of Swiss Army in 1847 / 1849 / 1856 / 1859) realised two further wire-cable suspension bridges in Geneva (Pont des Pâquis 1827-…., Pont des Bergues 1834-1881) and designed several others bridges.

- Marc Séguin and his brothers designed and built several further suspension bridges, e.g. the Pont de Tournon (1825, main spans 2x89 m) and the Pont d'Andance (1827, spans 2x90, oldest suspension bridge still in use in continental Europe, see photos).

Ground Plan of the Piers.

Elevation of the Wire Bridge at Geneva.

a

109 feet.   75½ feet.

Cable-supported bridges – Common aspects: Historical perspective

- The chain-stayed Saalebrücke in Nienburg (l = 80 m, Christian Gottfried Heinrich Bandhauer, 1825, top figure) was a precursor of cable-stayed bridges, though not very successful.

- The bridge collapsed on the 6.12.1825, only four months after inauguration, due to overload, faulty chains and / or oscillations caused by singing public during the celebration of St. Nikolaus. 55 people died.

- Bandhauer's design was very innovative, despite that he probably knew Claude Louis Marie Henri Navier's "Mémoire sur les ponts suspendus" (published 1823), where similar schemes were depicted (bottom figure; Navier's project for a suspension bridge over the Seine in Paris, the Pont des Invalides with 170 m span, also part of this publication, was never finished).

- A further highlight was the bascule opening at midspan, allowing large ship masts to pass.

Cable-supported bridges – Common aspects: Historical perspective

- The Menai Strait suspension bridge (1826, span 176 m), designed by Thomas Telford, is commonly recognised as the first major suspension bridge (photo).

- Earlier plans included straight backstays and a different tower design (bottom drawings).

- Telford opted for chains rather than wire cables, because he was more familiar with this type of structural element. While chains were used in several early suspension bridges (particularly in the UK), the more economical wires soon became the standard.

- The bridge initially had a lightweight timber deck, which was merely 7.4 m wide, without stiffening girders or trusses. It was highly unstable in the wind and seriously damaged in 1839.

- The deck was strengthened in 1840 and in 1893, a steel deck was installed. Major repairs were also carried out in 1999.
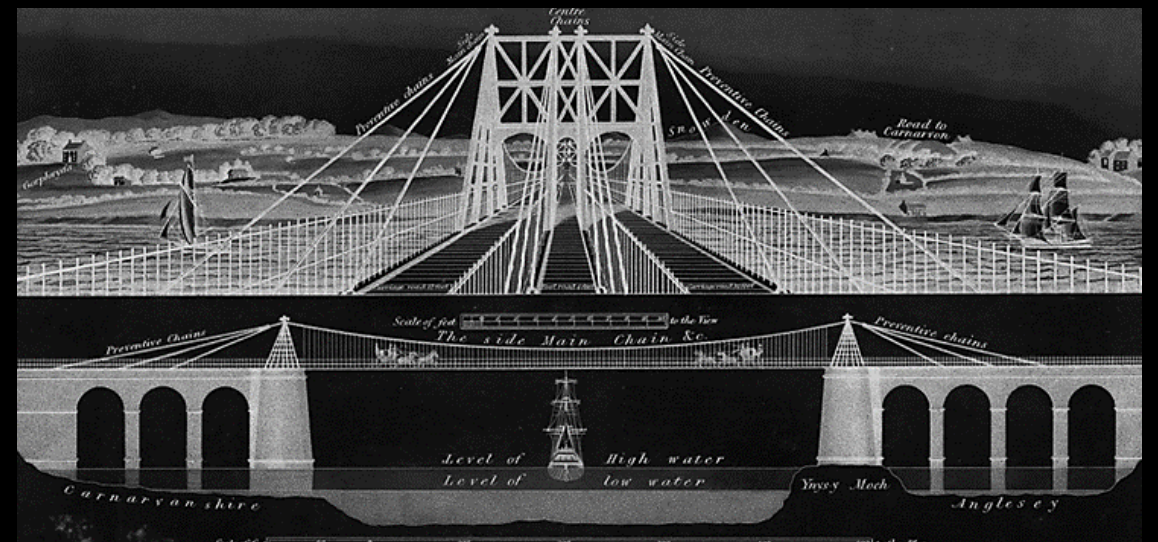
Cable-supported bridges – Common aspects: Historical perspective

- Suspension bridge chains were commonly eyebar chains, usually with direct connection by pins.

- The Menai suspension bridge originally had cast iron chains with indirect connection (bottom left photo). These were replaced by steel chains with direct connection in 1939.
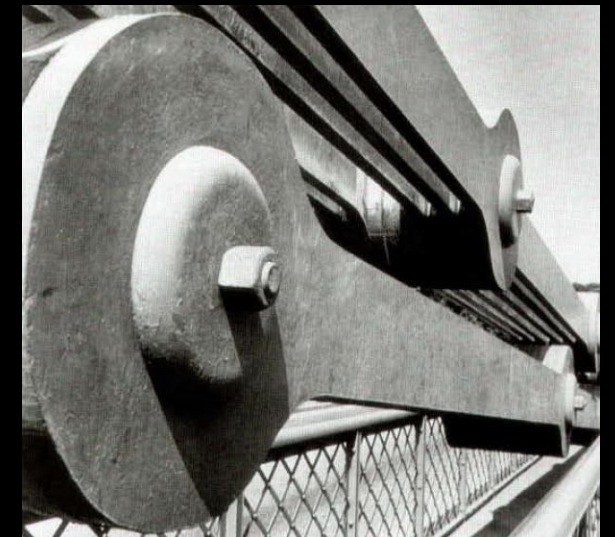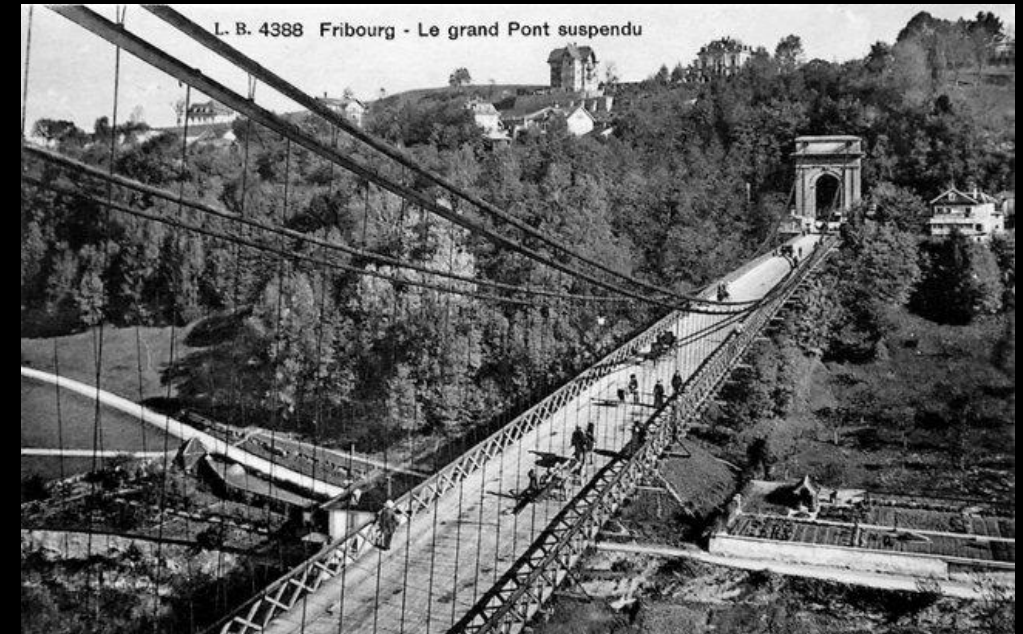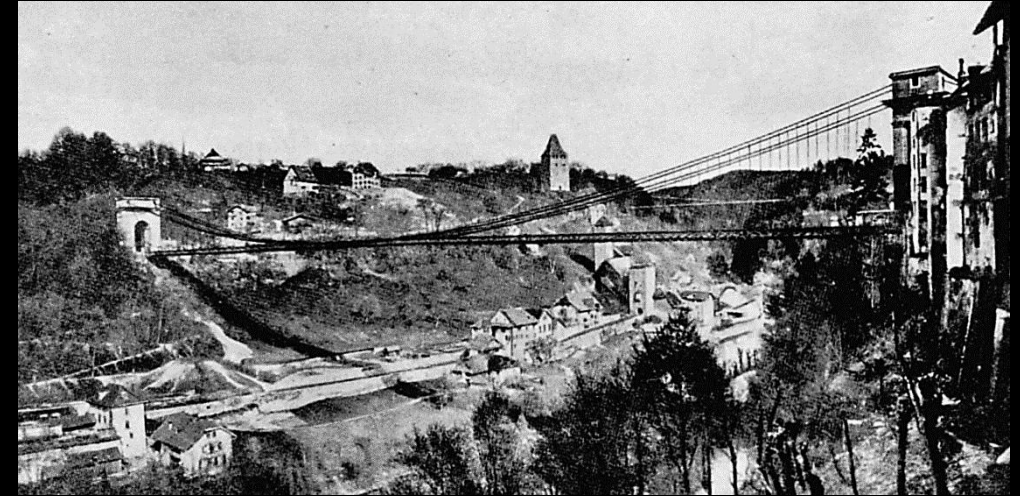
Cable-supported bridges – Common aspects: Historical perspective

- The Clifton suspension bridge (1863, span 214 m), designed by Isambard Kingdom Brunel, also used eyebar chains.

- Other relevant bridges were built before (see next slide). The Clifton bridge is mentioned here, right after the Menai straits bridge, because of the chains, and also because it should have been finished much before its opening in 1864 (see notes).

- Other than the Menai straits bridge, there are no hangers in the side spans in the Clifton bridge.

Cable-supported bridges – Common aspects: Historical perspective

- The Grand Pont Suspendu in Fribourg (1834, span 273 m, world record until 1849), designed by Joseph Chaley, was the longest suspension bridge worldwide for many years.

- Inspired by the bridges designed by the Séguin brothers, wires cables were used.

- Each of the four main cables was composed of more than 1000 wires, grouped in 20 strands.


L. B. 4388 Fribourg - Le grand Pont suspendu

Cable-supported bridges – Common aspects: Historical perspective

- The Grand Pont Suspendu in Fribourg (1834, span 273 m, world record until 1849), designed by Joseph Chaley, was the longest suspension bridge worldwide for many years.

- Inspired by the bridges designed by the Séguin brothers, wires cables were used.

- Each of the four main cables was composed of more than 1000 wires, grouped in 20 strands.
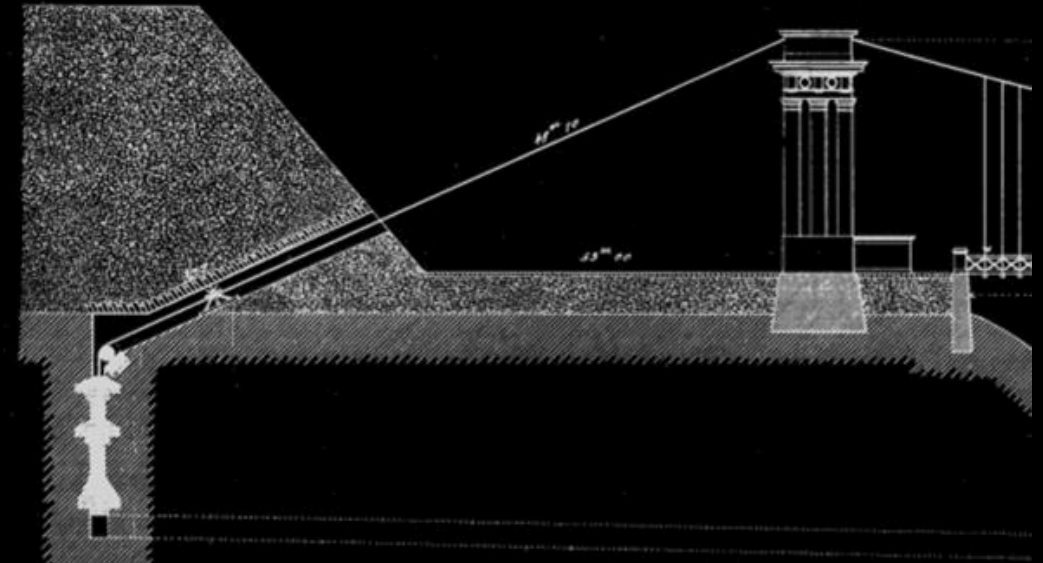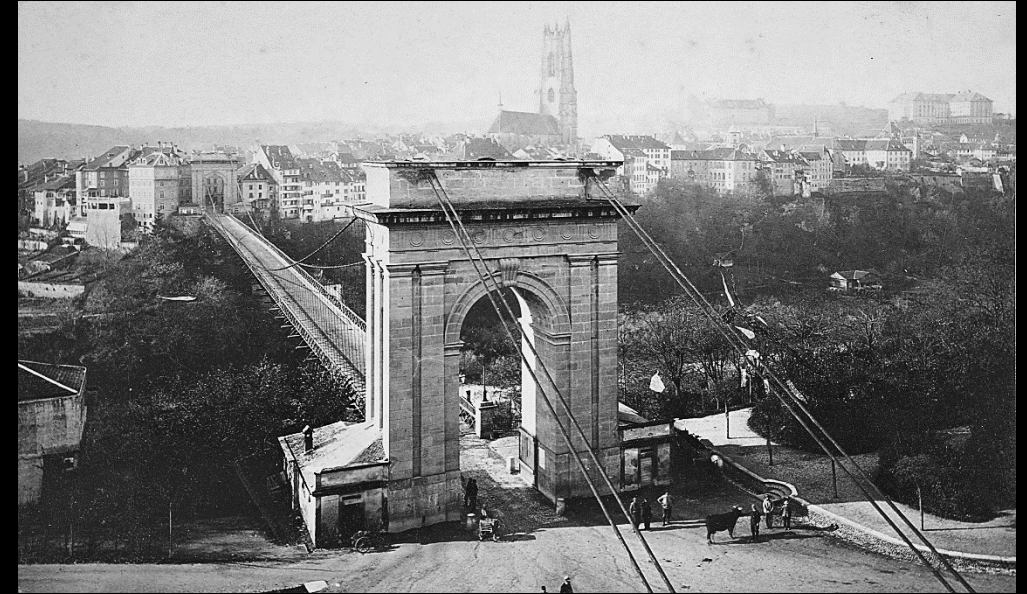
Cable-supported bridges – Common aspects: Historical perspective

- Joseph Chaley also designed the Pont du Gottéron in Fribourg (1842, 151 span with only one tower)

- This bridge had a shorter span, but only one tower.

- The bridge was severely damaged in a storm in 1895 and had to be strengthened.

- It became famous in 1919 when a truck damaged the deck and fell from the bridge (bottom right photo).

Fribourg - Le Pont du Gotteron

Edition Photoglob   826. Fribourg. Pont de Gotteron.

Cable-supported bridges – Common aspects: Historical perspective

- The Wheeling suspension bridge (1849, span 308 m, record until 1866), designed by Charles Ellet Jr., is the oldest suspension bridge still serving vehicle traffic.

- However, it had to be reconstructed after collapsing in 1854 due to wind-induced oscillations apparently similar to the Tacoma Narrows Bridge (see behind).

- In 1886, under guidance of J. Roebling, stays similar to the Brooklyn Bridge (see behind) were installed. Further strengthening was provided in 1922 and 1930.
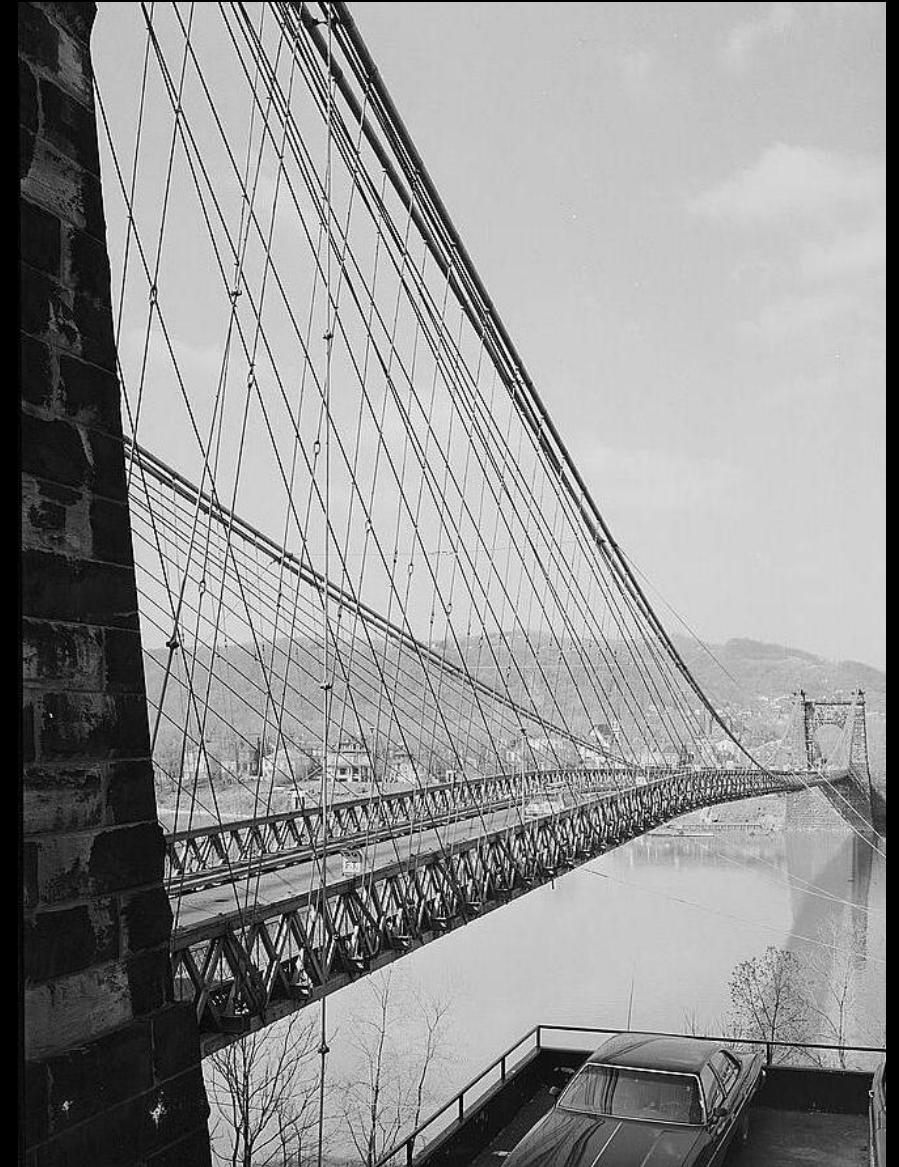
Cable-supported bridges – Common aspects: Historical perspective

- The Niagara Falls Suspension Bridge (1855-1896, span 250 m), designed by John August Roebling, was the world's first cable-supported railway bridge. It is also the first bridge with air-spun wire cables.

- Ch. Ellet Jr. had been in charge of building the bridge and had already erected a footbridge, but was forced to leave due to delays and technical concerns regarding his project. Roebling used Ellet's bridge as falsework / scaffolding.

- The bridge's original timber deck decayed rapidly and was replaced with stronger steel and iron versions by 1886. In 1897, the entire bridge was replaced by a steel arch bridge, capable of carrying heavier trains.
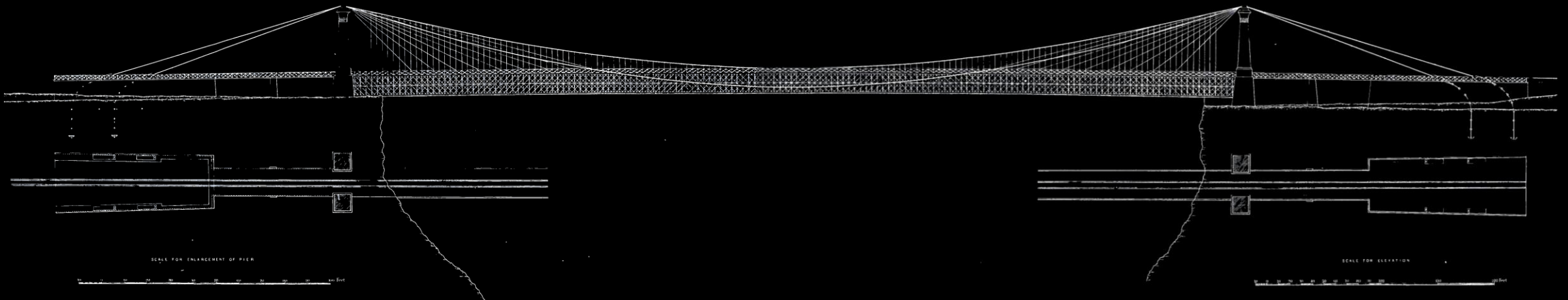
Cable-supported bridges – Common aspects: Historical perspective

- Traffic loads on railway bridges are significantly higher than on road bridges, which is a particular challenge for suspension bridges (see structural response). Furthermore, the dynamic loads may cause vibration problems.

- Roebling mastered the challenge by designing a combination of suspension and cable-stayed bridge (though the latter designation was unknown at the time), further stiffened by a truss girder. This combination became characteristic for his bridges.

- In the Niagara Falls Suspension Bridge, Roebling designed a particularly stiff deck girder (double deck forming a tube similar to Britannia bridge, but with railway on top) and provided stays running from deck to ground to reduce oscillations.
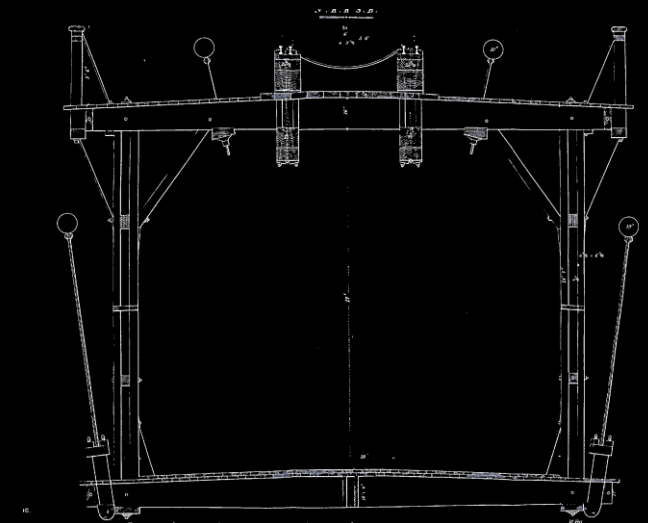
Cable-supported bridges – Common aspects: Historical perspective

- Almost at the same time, Robert Stephenson designed the Britannia Bridge, carrying railway traffic across the Menai Strait (1850, spans 70+140+140+70 m).

- In order to control deformations and oscillations, Stephenson provided a "monster tube" cross section, consisting of riveted wrought iron plates (following contemporary shipbuilding practices), inside which the trains were running.

- Originally, Stephenson's intention was to use the steel girder primarily for stiffness, and provide suspension cables or stays to carry a large portion of the self-weight.

- However, experiments by William Fairbairn to verify the buckling stability of the top chords indicated that they needed to be strengthened. Further experiments on stiffened plates (see cross-section photo) then led to a design that was stiff and strong enough to carry the entire load without any need for cables.

- While the bridge was seen as a "triumph of science" at the time, hardly any tubular bridges were built later (Conwy Railway bridge and Pont Victoria in Montreal, both designed by Stephenson).

- Unfortunately, the bridge had to be replaced after a fire in 1970, and the new design only maintained the piers.

THE TRIUMPH OF SCIENCE.

AN ACCOUNT
OF THE
GRAND FLOATATION
OF ONE OF
THE MONSTER TUBES
OVER THE MENAI STRAITS,
BRITANNIA BRIDGE,
JUNE 20th, 1849,
WITH AN ENGRAVING.
THE STUPENDOUS TUBULAR BRIDGE WAS PROJECTED
BY R. STEPHENSON, Esq., M.P.
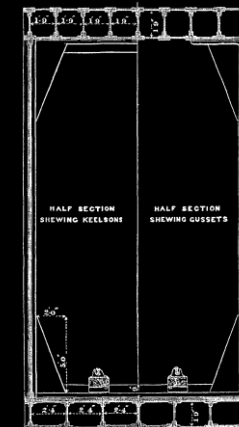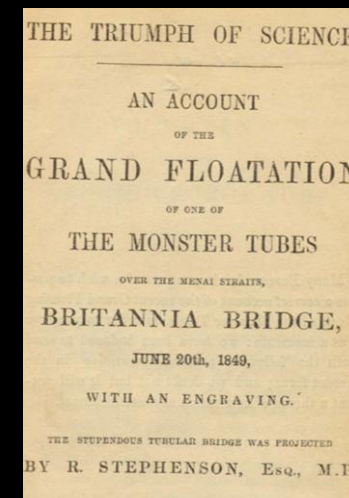
Cable-supported bridges – Common aspects: Historical perspective

- In the John A. Roebling Suspension Bridge (1866, until 1983 Covington and Cincinnati Suspension Bridge, span 322 m) over the Ohio River, Roebling used the same concept as in the Niagara Falls suspension bridge, albeit with

  → a less stiff truss girder since the bridge had to carry only carriages and pedestrians

  → suspended side spans

- The Covington-Cincinnati bridge held the span record until 1868, when the Niagara-Clifton bridge was built (Samuel Keefer, stayed suspension bridge, span 384 m). However, that bridge collapsed in a hurricane in 1889.

- In 1896, the Covington-Cincinnati bridge was widened and provided with a second set of cables. Currently, it is still used, with a weight limit of 11 t.

Cable-supported bridges – Common aspects: Historical perspective

- The Brooklyn Bridge (1883, until 1915 "New York and Brooklyn Bridge" or "East River Bridge", span 486 m, record suspension span until 1903) is certainly the most prominent bridge designed by John A. Roebling.

- Roebling again used the same concept as in the Covington-Cincinnati and Niagara bridges, combining suspension cables, stay cables and a stiffening truss.
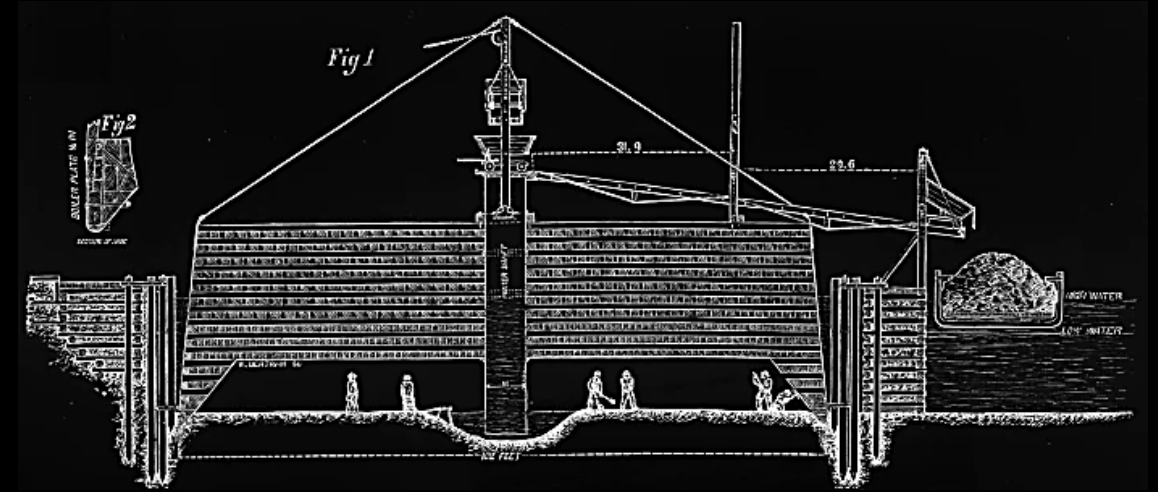
Cable-supported bridges – Common aspects: Historical perspective

- Since the bridge is wider, it has four large-diameter main cables, each consisting of 5'282 wires. The cables were air-spun as in the Niagara bridge, but for the first time bundled in individual strands (19 @ 278 wires each) before assembling them.

- The truss girder is supported by 1'520 hangers (US: "suspender cables") and 400 stays radiating from the towers.

- John A. Roebling died after an accident shortly after construction had started.

- His son, Washington Roebling, took over but became paralysed after staying in a pneumatic foundation caisson that caught fire. Washington's wife Emily Warren Roebling subsequently led the works on site.

- The bridge today carries 6 lanes of road traffic (until 1950 8 lanes), with a weight limit of 6'000 lb (2.7 t).

- Since the opening ceremony in 1883, the upper pedestrian deck tends to be overcrowded (more than 150'000 people crossed the bridge on the first day, and six days after opening, 12 people were killed in a stampede).

Cable-supported bridges – Common aspects: Historical perspective

- As mentioned, the Brooklyn Bridge was the longest span suspension bridge until 1903. However, the Forth Bridge, a cantilever steel truss bridge, designed by John Fowler and Benjamin Baker, was the world's longest span bridge after opening in 1890, with a main span of 520 m, followed by the similar Québec Bridge (1918, rebuilt after having collapsed in construction 1907) with a span of 549 m.

- Suspension bridges only returned to be the longest span typology with the Ambassador Bridge (1929, span 564 m), whose span was soon almost doubled by the George Washington Bridge (1931, 1067 m).


Longest span bridges (all typologies)
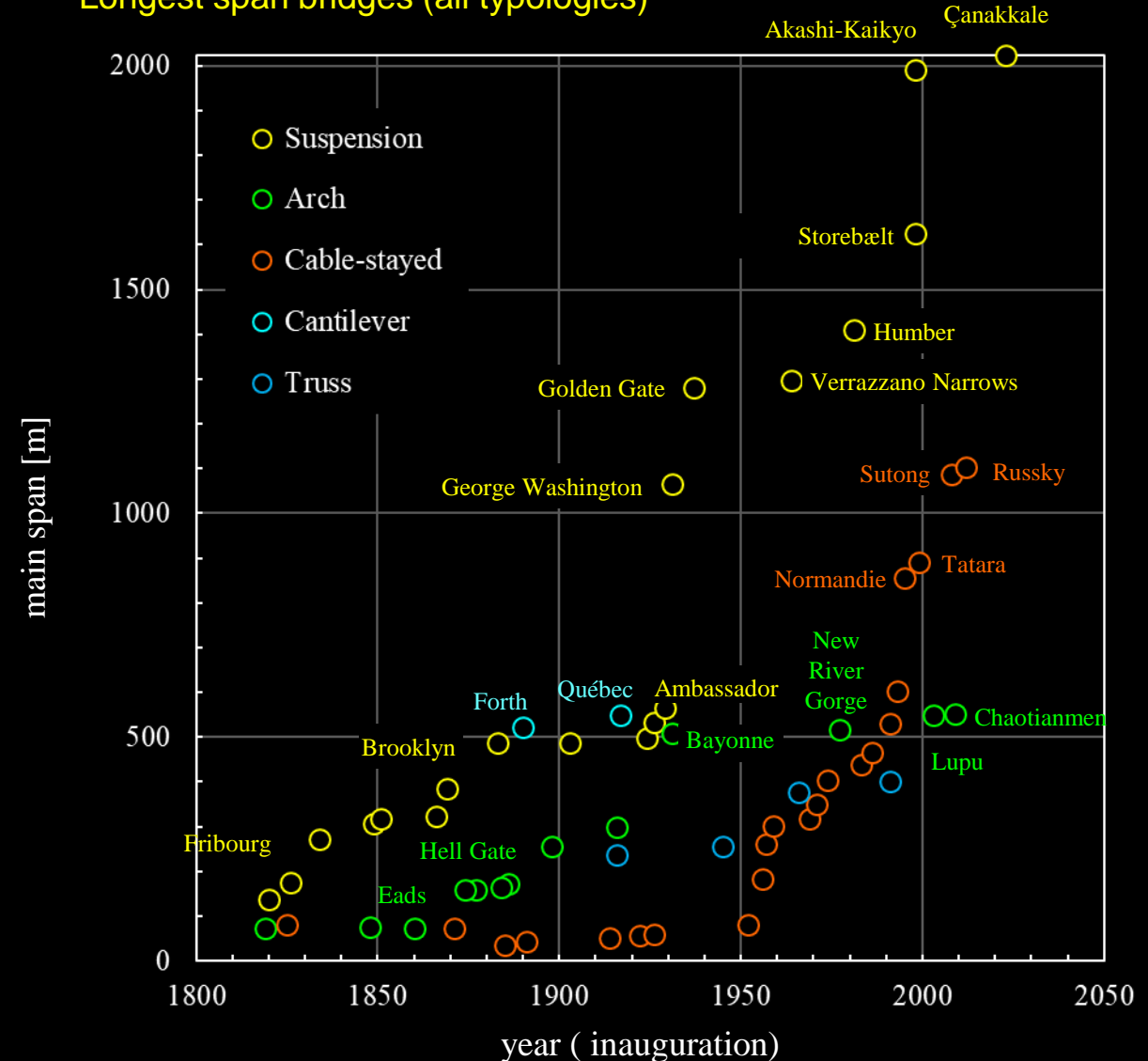
Cable-supported bridges – Common aspects: Historical perspective

- The history of suspension bridges is closely linked to the development of theories for their analysis and design – and, unfortunately, bridge failures.

- The design of early suspension bridges (e.g. Telford's Menai Straits Suspension Bridge) was primarily based on the catenary curve (Kettenlinie), known since the end of the 17th century (Hooke, Leibniz, Huygens, Johann Bernoulli), experimental tests (see Drewry's quote in notes), and intuition.

- Navier's Theory of Suspension Bridges, published in 1823, served as a basis of suspension bridge design for the next five decades. While Navier already accounted for changes in the shape of the chains or cables (under a point load at midspan), he did not account for the effect of a stiffening girder nor cable elongations.

- In early suspension bridges, lightweight narrow timber decks were standard, and traffic loads were limited to pedestrians and carriages. Hence, most of the load consisted of the chain or cable self-weight, and the deck stiffness was indeed negligible.

- However, bridge decks became wider, and traffic loads kept increasing – up to the point where neglecting the traffic loads, nor deck girder stiffness, could no longer be justified.

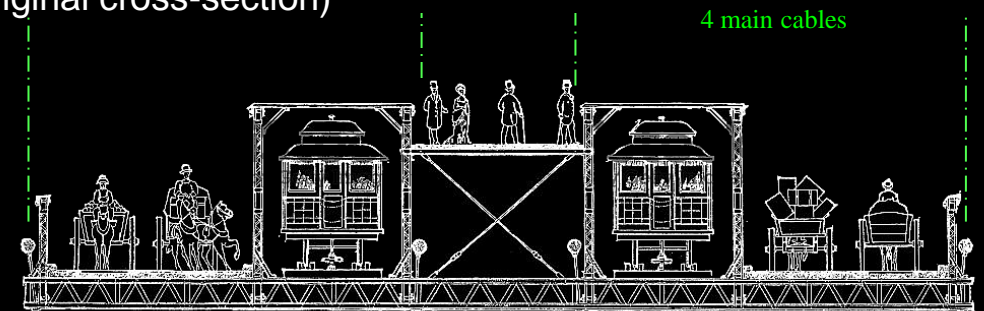Pont des Invalides, 1823 (Navier, never completed)
(timber deck on iron cross-beams)

2 main cables
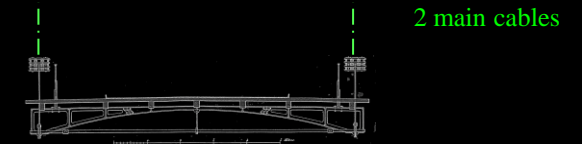
Menai Strait Suspension Bridge, 1826
(original cross-section with timber deck)

4 chains
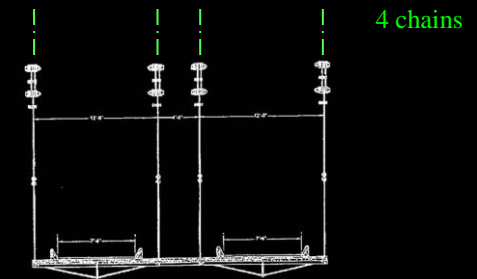
Brooklyn Bridge, 1883
(original cross-section)

4 main cables

Cable-supported bridges – Common aspects: Historical perspective

- Many early suspension bridges suffered from excessive oscillations, and several collapsed.

- Being aware of these problems, Roebling – as already mentioned – provided stays and stiffening truss girders in his suspension bridges to increase their stiffness. Hence, his designs combined three load-carrying elements:
    - → suspension cables
    - → stay cables
    - → stiffening girder

- However, at the time, there was no theory to analyse such a complex structure. Based on his engineering judgment, Roebling (except in his earlier bridges, where the stays were merely "activated" as stiffening against oscillations, for more details see reference in notes)
    - → converted all actions to a uniformly distributed load
    - → assigned most of the load to the suspension system
    - → assigned the remaining part of the load to the stays
    - → in most cases did not assign any loads to the stiffening truss

- Assuming that the truss is capable of transforming the applied loads to a uniform load, he thus implicitly used an equilibrium solution.

Cable-supported bridges – Common aspects: Historical perspective

- Rankine had published a suspension bridge theory in 1858, where he indeed used the stiffening truss to convert arbitrary loads to uniform loads in a suspension bridge (the latter carried by the cable system). However, this theory did not find much application.

- Rather, at the end of the 19th Century, the "Elastic Theory" of suspension bridges was established, among others by Maurice Lévy and Josef Melan. This theory, equivalent to the elastic theory for arches, allows accounting for the load distribution between suspension cables and stiffening girder, satisfying equilibrium and compatibility (bending stiffness of girder, axial stiffness of cables).

- However, since the theory is based on small deformations (equilibrium is formulated in the undeformed state), it does not account for the capability of cables to carry non-uniform load by adapting their shape to the load configuration).

- Hence, in designs using this theory – analogous to a a stiffened arch – stiffening girders need to resist all non-uniform load, as well as bending moments caused by deflections due to elastic cable elongation. As a result, long-span suspension bridges designed using this theory require very stiff deck girders, as illustrated by the Williamsburg Bridge designed by Leffert L. Buck (1903, span 488 m, longest suspension span until 1924).

Cable-supported bridges – Common aspects: Historical perspective

- In 1888 (refined version 1906), Josef Melan published the "Deflection Theory" of suspension bridges (Formänderungstheorie der Hängebrücken).

- This theory accounts for the beneficial effect of large cable deformations (second order deformations) in the load distribution among suspension cables and stiffening girder.

- As a result, much more slender stiffening girders could be used in bridges designed using this theory.

- Leon Moisseiff first applied the Deflection Theory in the design of the Manhattan Bridge (1909, span 448 m).

- The difference between the Manhattan bridge and the Williamsburg bridge, built only 6 years earlier and carrying even less traffic load with a similar span, is striking both visually (compare photos) as well as numerically (Slenderness h/l = 1/37.5 vs 1/56).

Cable-supported bridges – Common aspects: Historical perspective

- When applying the Deflection Theory, structural safety can be guaranteed without stiffening girder. The required girder stiffness is thus essentially governed by the limits on deflections under traffic loads – which become smaller as the self-weight of the bridge increases.

- Consequently, very slender deck girders are sufficient in large span suspension bridges with a relatively large self weight (cables + deck girder).

- Othmar H. Ammann made use of this in his incredibly slender design (h/l = 1/351, more than six times higher slenderness than in the Manhattan bridge) of the George Washington Bridge (1931, span 1067 m, record span until 1937).

- The George Washington Bridge was disruptive regarding span, but also slenderness (see notes).

Cable-supported bridges – Common aspects: Historical perspective

- In 1962, a second deck was added to the George Washington Bridge, increasing its capacity from 8 to 8+6 = 14 lanes of traffic.

- The slenderness was reduced to $h/l = 1/120$, yet the bridge still is and looks very slender.

Cable-supported bridges – Common aspects: Historical perspective

- The Golden Gate Bridge was promoted by Joseph B. Strauss, who is commonly given credit for its design. However, Strauss' initial design was unsatisfactory, and the bridge finally built was designed by Clifford E. Paine, Irving F. Morrow and Charles A. Ellis (with Othmar Amman as consultant). It set a new span record in 1937 (l = 1281 m), which would hold for almost 30 years.

- It was not as slender as the George Washington Bridge, but still much more slender than earlier bridges (h/l = 1/168). A lower deck lateral bracing was installed in 1953/54 after a storm shook the bridge strongly in 1951.

- Othmar H, Ammann himself designed further very slender suspension bridges, such as the Bronx-Whitestone Bridge (1939, span 701 m, h/l = 1/210).

- After the Tacoma Narrows Bridge Collapse (see behind), the bridge was stiffened with stays and additional truss girders, reducing the slenderness to h/l = 1/91). In 2003, aerodynamic fairings were installed and the trusses removed, recovering the initial elegance.

Cable-supported bridges – Common aspects: Historical perspective

- Several suspension bridges with slender decks built in the late 1930s experienced excessive oscillations and had to be stiffened for this reason.

- Documented examples include the Thousand Islands Bridge (1937, span 240 m) and the Deer Isle Bridge (1939, span 329 m), both designed by the renowned engineer David B. Steinman.

- The Thousand Islands Bridge was stiffened with "truss" stays shortly after the opening, due to excessive oscillations in wind. The Deer Isle Bridge was retrofitted with "truss" stays even before opening, since similar oscillations as in the Thousand Islands Bridge had been observed during construction.

- Despite these obvious problems, and the knowledge about wind-induced collapses of several early suspension bridges without stiffening girder, ultra-slender suspension bridges kept being built.
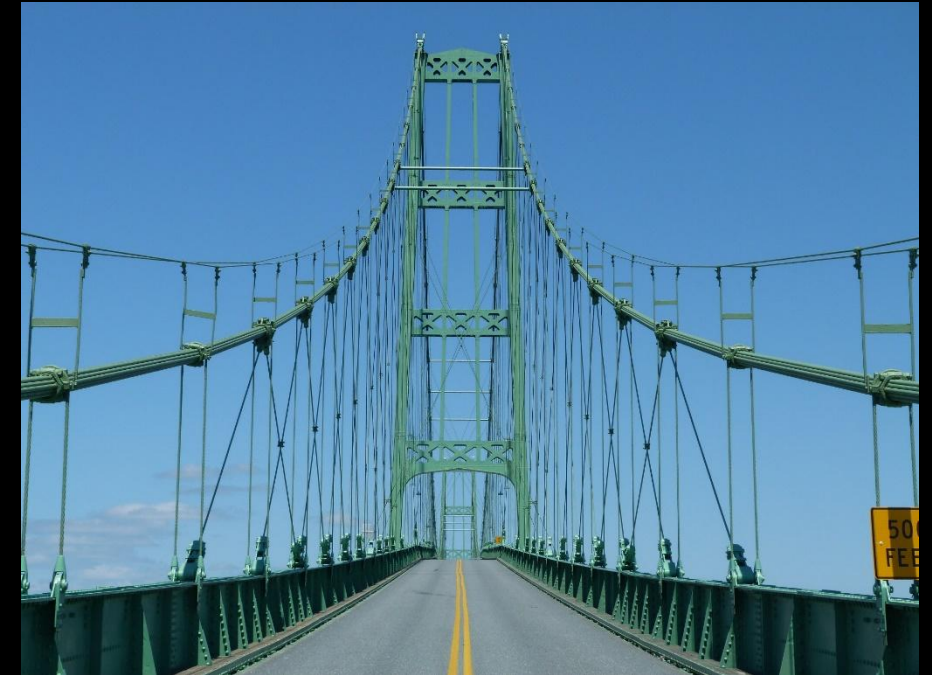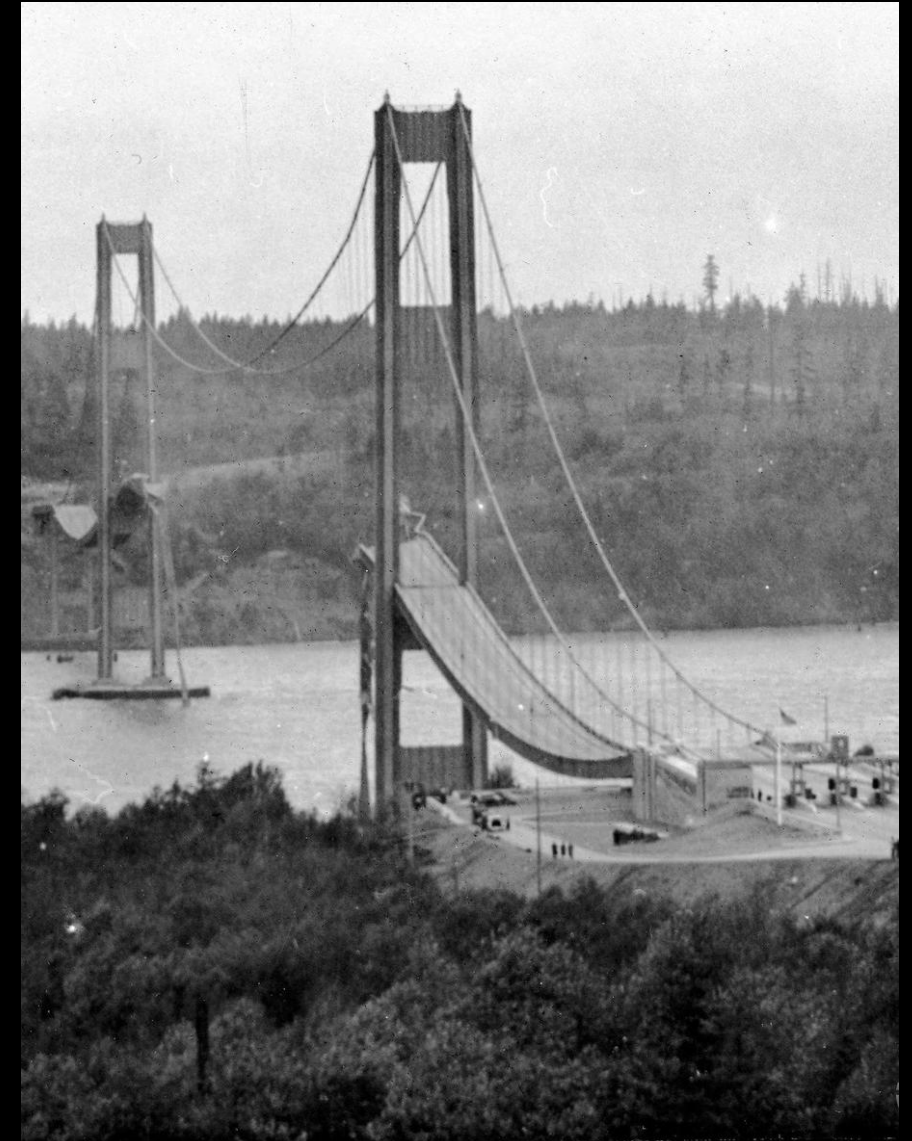
Cable-supported bridges – Common aspects: Historical perspective

- On November 7, 1940, the unimaginable happened: The Tacoma Narrows Bridge (span 853 m), designed by Leon Moisseiff, collapsed after oscillating in steady wind with a velocity of merely ca. 68 km/h.

- Moisseiff was one of the leading suspension bridge designers of the time. He had extended the deflection theory for lateral load, i.e. wind, and used it in his Tacoma Narrows design (see notes).

- Therefore, the bridge was extremely slender not only vertically ($h/l = 1/355$, $\approx$ George Washington Bridge with one deck), but also transversally ($b/l = 1/72$, compared to $b/l = 1/47$ in the Golden Gate Bridge and $b/l = 1/33$ in the George Washington Bridge).

- The Bridge had experienced large vertical oscillations under modest wind already during construction. Frederick B. Farquharson at the University of Washington had therefore carried out wind tunnel tests already in 1939. He recommended several measures, but most of them failed. Finally, the installation of aerodynamic fairings along the deck was decided, but the bridge collapsed less than a week later – leaving the question open if these fairings would have helped.

- The collapse was investigated by a commission including Othmar Ammann and Theodore von Kármán. Prof. Jakob Ackeret carried out wind tunnel experiments in this context at ETH Zurich.

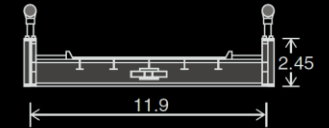# Cable-supported bridges – Common aspects: Historical perspective

- Some highschool physics textbooks erroneously use the Tacoma failure as example for resonance. This would imply a periodic excitation by an external force (such as vortex shedding or buffeting).

- However, the bridge collapsed due to torsional flutter ("torsional galloping" in older textbooks), see section *wind-induced oscillations*:
  - → self-exciting divergent aeroelastic phenomenon, where aerodynamic forces on the bridge deck couple with its motion
  - → if the energy input by aerodynamic forces per cycle is larger than that dissipated by the bridge's damping, the amplitude of oscillations grows
  - → if continued for some time, this leads to collapse

- Flutter is related to "resonance" insofar as in coupled flutter, a coupling of aerodynamic forces and deck motion occurs if the relevant vertical and torsional eigenfrequencies (nearly) coincide.

- The collapse marked a turning point in bridge design, particularly for cable-supported bridges:
  - → Aerodynamic effects, which had received little attention before, became a major concern in long-span bridge design on that very day
  - → Today, wind tunnel testing on long-span and/or slender bridges is common, and computational fluid mechanics is increasingly used.

Cable-supported bridges – Common aspects: Historical perspective

- The Tacoma Narrows bridge was rebuilt in 1950, with a much deeper and wider stiffening girder, ($h/l = 1/87$ vs. $1/355$, $b/l = 1/46$ vs. $1/72$, truss box girder with high torsional stiffness vs. open cross-section).

- The towers had suffered severe damage, being deflected almost 4 m towards the shore after collapse of the main span. Only the cable anchorages, tower pedestals and foundations could be re-used. The steel (cables, deck, towers) was sold as scrap.

- In 2007, a second bridge was added, with equal span.

Cross-section of collapsed bridge (1940)

Cross-section of rebuilt bridge (1950)
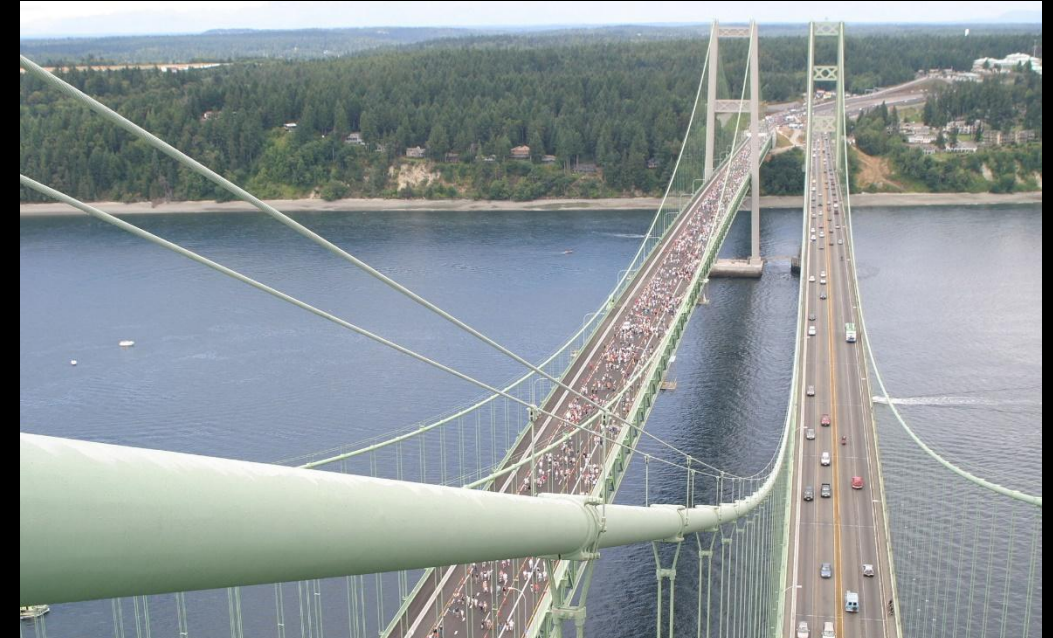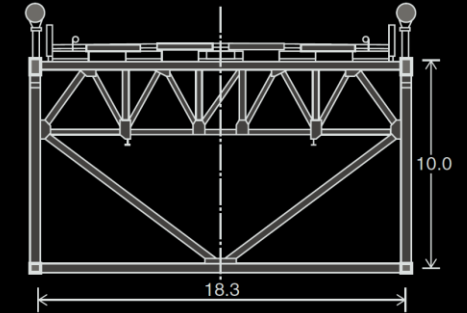
Cable-supported bridges – Common aspects: Historical perspective

- The Verrazzano Narrows Bridge was the last bridge designed by Othmar H. Ammann (1964, span 1298 m, longest until 1981, h/l = 1/170).

- The bridge is named after Giovanni da Verrazzano, Italian explorer who discovered the entrance to the Hudson River in 1524. It was misspelled ("Verrazano") until 2018, when the name of the bridge was officially changed under Governor Andrew Cuomo.

- Like all suspension bridges built after the Tacoma Narrows bridge collapse, the Verrazzano Narrows bridge was subjected to scale-model tests in a wind tunnel and has a torsionally stiff cross-section to avoid flutter: The box truss section (depth 7.30 m between top and bottom chord axis) was provided from the beginning, though the bridge initially carried only one deck (unlike in the George Washington Bridge).

- Seasonal contractions and expansions of the suspension cables cause a seasonal variation of the deck elevation at midspan of 3.60 m.

Cable-supported bridges – Common aspects: Historical perspective

- In the Severn Bridge (1966, main span 978 m), the designers of Freeman, Fox & Partners introduced two revolutionary concepts:

  → an aerodynamic, slender, closed steel box-girder cross-section (streamlined "airfoil"), providing the torsional stiffness required to prevent flutter at much smaller drag forces than present in truss box girders (optimised based on wind tunnel tests)

  → slightly inclined hangers to increase stiffness and energy absorption under vertical displacements and thereby increasing the damping.

- As a result, an extremely slender and elegant bridge could be built (h/l = 1/326) without oscillation problems.

- Streamlined box girder cross-sections have been used in many subsequent cable-supported bridges (typically with an orthotropic steel deck); the inclined hangers were repeated in the Humber Bridge.

- Since 2018, the Second Severn Bridge is operative, about 6 km downstream of the First Severn Bridge (cable-stayed bridge, main span 456 m).
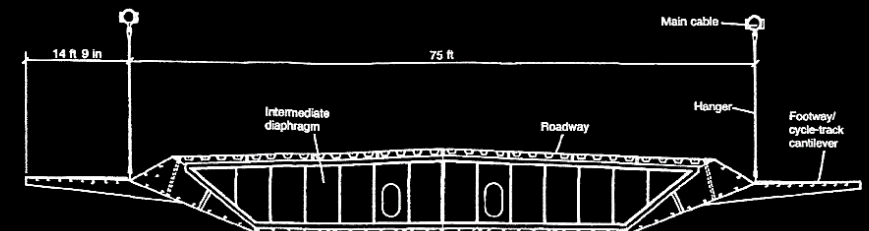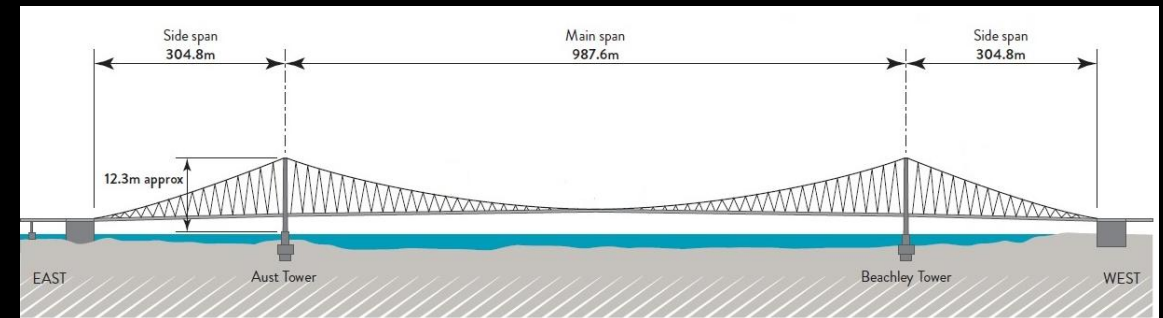
Cable-supported bridges – Common aspects: Historical perspective

- In the Humber Bridge (1991, main span 1410 m, record until 1998, h/l = 1/313), Freeman, Fox & Partners again used a streamlined steel box girder with orthotropic steel deck, as well as the slightly inclined hangers.
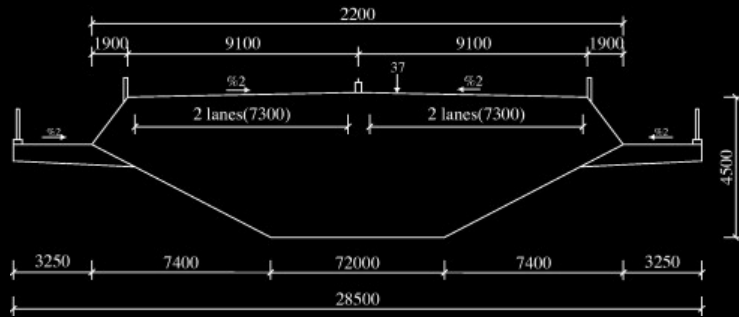
Cable-supported bridges – Common aspects: Historical perspective

- The Storebælt East Bridge (1998, main span 1624 m, h/l = 1/380), designed by a team led by COWI, has conventional vertical hangers.

- The very slender steel box girder, again with orthotropic deck, is equipped with guide vanes in the main span (photo below, bottom edges) to enhance aerodynamic stability.

- The box girder is uncoated inside (corrosion protection by dehumidification).
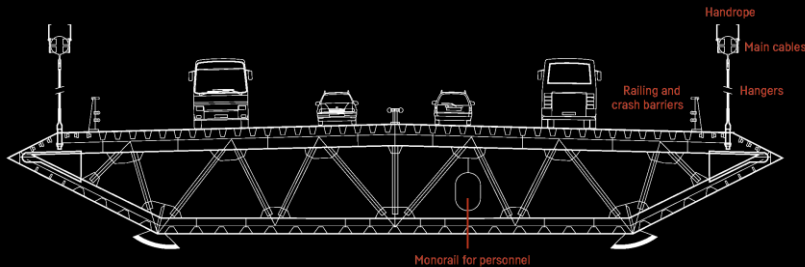
Cable-supported bridges – Common aspects: Historical perspective

- The Akashi-Kaikyo Bridge (1998, main span 1990 m) was the longest span bridge in service worldwide for more than three decades. It was designed by Satoshi Kashima at the Japan Bridge Engineering Centre

- It was designed for very high wind speed (286 km/h) and earthquakes (magnitude 8.5).

- Other than in the recent European long-span suspension bridges, its cross-section is a steel truss box girder, which is considerably less slender ($h/l = 1/136$) than in the Severn (1/326), Humber (1/313) and Storebaelt (1/380) bridges, but provides aerodynamic stability at very high wind velocities.

14.00

35.50
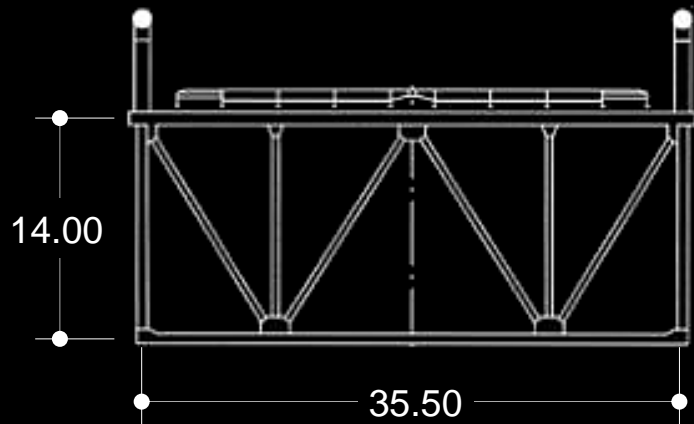
Cable-supported bridges – Common aspects: Historical perspective

- The two main cables, with a diameter of 1.12 m, were fabricated using prefabricated parallel wire strands (PPWS)

- Each main cable consists of 290 PPWS with 127 wires Ø5.23 mm, totalling 36'830 wires per cable (see *Cable Types* section).

Note: The main cables of major suspension bridges were previously produced by air spinning, as invented by John Roebling in the Niagara Falls Bridge in 1855 (see there and *Cable Types* section).

Cable-supported bridges – Common aspects: Historical perspective

- The Çanakkale Bridge, crossing the Dardanelles Strait with a main span of 2023 m, is the longest span bridge since its commissioning in 2022. Designers are Pyunghwa (South Korea, basic design) and COWI (Denmark, detailed design).

- Currently, 90 suspension bridges with spans above 700 m exist worldwide (Wikipedia, June 2023). Out of these, 41 are located in China.

- Despite the tremendous evolution of cable-stayed bridges towards longer spans (see following slides), many suspension bridges are currently under construction, primarily in China (28 of the 29 currently under construction).

Suspension bridges with main span ≥ 600 m
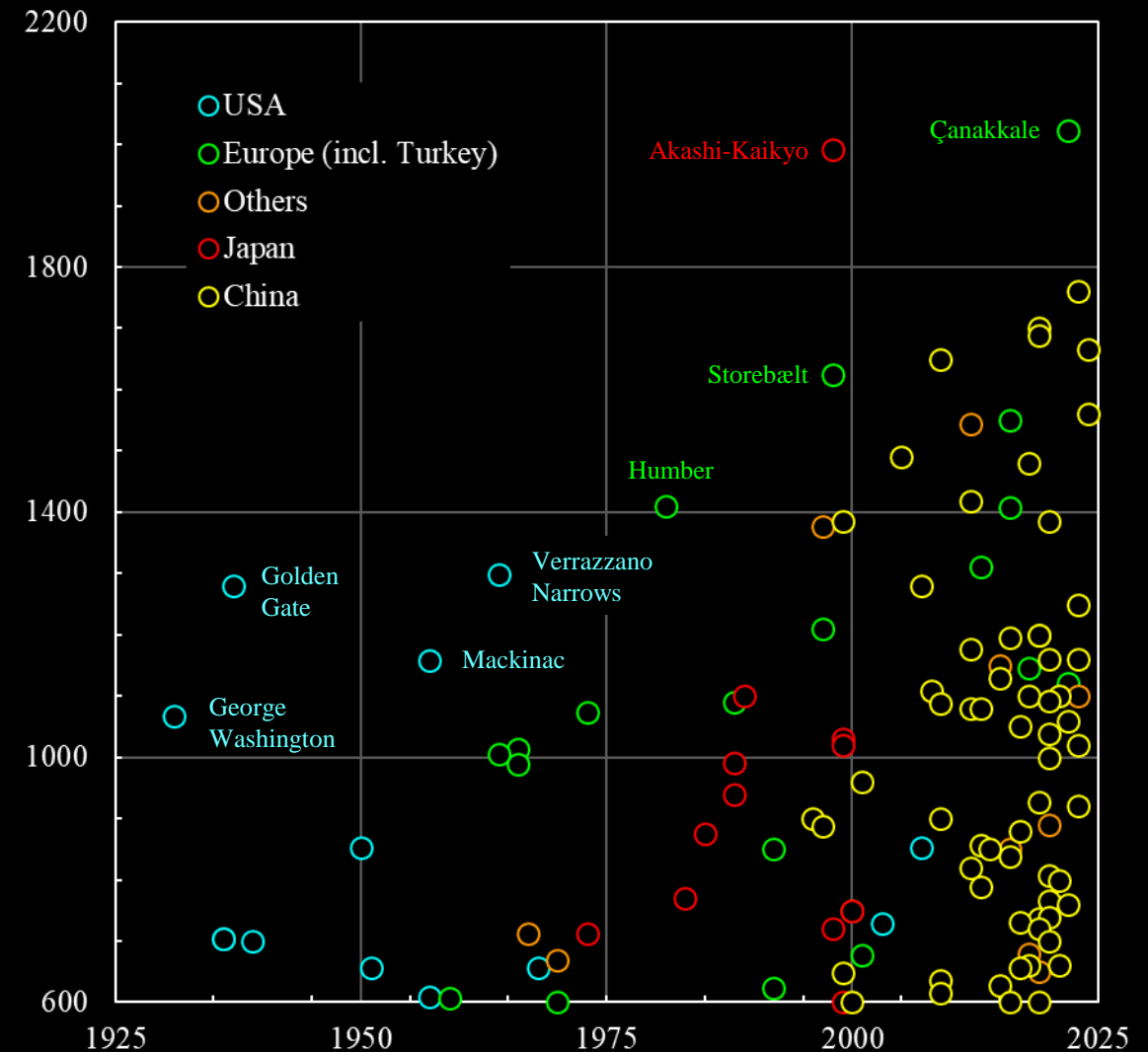
Cable-supported bridges – Common aspects: Historical perspective

- While suspension bridges are still the most economical solution for very long spans, cable-stayed bridges are increasingly being considered for longer spans as well.

- This is illustrated by the fact that since 1990, 67 cable-stayed bridges with spans above 500 m have been built, (47 in China), and a further 29 are currently under construction, mainly in China (Wikipedia, April 2020).

- The Changtai Yangtse Bridge connecting Taixing and Changzhou in China will be the longest span cable-stayed bridge from its commissioning (2024, main span 1'176 m, designed by the China Railway Major Bridge Reconnaissance and Design Institute (BRDI).

Cable-stayed bridges with main span ≥ 500 m

Cable-supported bridges – Common aspects: Historical perspective

- Hybrid cable systems, such as in the third Bosporus crossing designed by Michel Virlogeux and Jean-Francois Klein (2016, span 1'408 m) are viable alternatives for long spans:
  - → combination the structural efficiency of (relatively short and steep) stay cables near pylons and suspension system at midspan
  - → efficient and fast erection (stayed cantilevering from pylons can start before, and continue while suspension cables are being installed).

Cable-supported bridges – Common aspects: Historical perspective

- Hybrid cable systems, such as in the third Bosporus crossing designed by Michel Virlogeux and Jean-Francois Klein (2016, span 1'408 m) are viable alternatives for long spans:
  - → combination the structural efficiency of (relatively short and steep) stay cables near pylons and suspension system at midspan
  - → efficient and fast erection (stayed cantilevering from pylons can start before, and continue while suspension cables are being installed)

Cable-supported bridges – Common aspects: Historical perspective

- So far, the historical perspective has focused on suspension bridges (including the Roeblings' stayed suspension bridges).

- It is completed in the following by highlighting some major steps in the development of cable-stayed bridges.

- Among the first major cable-stayed bridges were the Albert bridge in London (1873, span 122 m) and the Stefanik Bridge in Prague (1868-1949, span 100 m), both designed by Rowland Ordish.

- Similar as John Roebling, Ordish used a combination of stays and suspension system (rods), but the stays carried most of the load in his designs.

Cable-supported bridges – Common aspects: Historical perspective

- A similar, hybrid solution with predominant stay action was used e.g. by Albert Gisclard in the Pont de Cassagne (1908, main span 158 m).

Cable-supported bridges – Common aspects: Historical perspective

- The following bridges are often referred to as the first "modern" cable stayed bridges:

  → Concrete: Pont de Donzère-Mondragon (Albert Caquot, 1952, span 81 m, concrete deck girder)

  → Steel: Strömsund Bridge (Franz Dischinger, 1956, span 183 m, steel girders with orthotropic steel deck)

Cable-supported bridges – Common aspects: Historical perspective

- In the first cable-stayed bridges, few massive stays (in many cases even only one stay per span) were used. In German, such bridges are commonly referred to as "Zügelgurtbrücken".

- Using single stays facilitated analysis and design, as the stays could be treated as "flexible supports" (replacing a pier)

- A pioneer of this typology was Riccardo Morandi, who designed several similar bridges like the Lake Maracaibo Bridge (1962, 5 main spans @ 235 m, total length 8.7 km. built in record time, stays exchanged due to corrosion in 1982).

- To increase the stiffness of the stays, Morandi later replaced the bare cables by prestressed concrete ties, which greatly increased their structural efficiency in SLS.

- In addition, the concrete protects the prestressing steel from corrosion until a critical chloride level is reached (e.g. due to deicing salts, airborne sea salt or industrial flue gases).

- Morandi's concept of prestressed concrete ties was adopted by many other designers due to its high efficiency, see bottom example (Donaubrücke Metten, 1981, span 145 m).

Cable-supported bridges – Common aspects: Historical perspective

- Riccardo Morandi had used prestressed concrete ties in a number of his bridges, among which the Viadotto del Polcevera in Genova (1967, main spans 208 m).

- In this bridge, the prestressed concrete ties were roughly 5 times stiffer than the bare steel.

- Despite that severe corrosion of all stays was detected (primarily due to airborne salt and industrial flue gases, Morandi warned the authorities in 1979), only one pylon was strengthened in 1993, installing modern, controllable and replaceable stays.

- In 2018, the bridge collapsed at another pylon. Failure was most likely caused by localised corrosion of a stay near the top anchorage (favoured by improper grouting, see frame bridges). Some investigations attribute it to other causes, including fatigue.

- Independently of the true cause, single stay bridges obviously lack robustness. Therefore, modern cable-stayed bridges are designed such that failure of a single cable will not cause collapse.

- When judging Morandi's design, it must be kept in mind that robustness was not a design goal at the time (not only in bridges: for example, cars did not have dual brake circuits in the 1960s).

Cable-supported bridges – Common aspects: Historical perspective

- The Theodor Heuss Brücke (1958, span: 260 m) and the (Rhein-)Kniebrücke (1969, span 319 m), both located in Düsseldorf and designed by Fritz Leonhardt, underline the leading role of German engineers in the development of cable-stayed bridges.

- Both bridges share a harp arrangement of the stays, in the case of the Kniebrücke combined with anchor piers at all back stays, enabling a very slender deck girder in the main span.

Cable-supported bridges – Common aspects: Historical perspective

- One of the first cable-stayed bridges with multiple number of stays was the Rheinbrücke Bonn Nord (1967, span 280 m), designed by Hellmut Homberg.

- This was also among the few early cable-stayed bridges with only one suspension plane, requiring a high torsional stiffness of the deck girder.

Cable-supported bridges – Common aspects: Historical perspective

- The Puente de Rande, designed by Fabrizio de Miranda and Florencio del Pozo (1978, widened in 2011, span 401 m, second longest span at time of erection) was another early multi-stay cable-stayed bridge.

- The Barrios de Luna bridge (1983, span 440 m) is an early example of a bridge with closely spaced cables, enabling a very slender deck girder.

- The designers Carlos Fernández Casado and Javier Manterola took advantage of computing power to analyse the highly statically indeterminate system.

Cable-supported bridges – Common aspects: Historical perspective

- Cable-stayed bridges are the most economical solution today for long spans (~300…1000 m) due to their efficient construction

- If designed with care, they are also aesthetically attractive, such as e.g. the main span of the Ponte Vasco da Gama (1998, span 420 m, total length 17.2 km)

Cable-supported bridges – Common aspects: Historical perspective

- With the Pont de Normandie (1994, span 856 m), designed by Michel Virlogeux, the span range of cable-stayed bridges was greatly increased.

- The Stonecutters Bridge (2009, span 1018 m), designed by Arup, COWI and Buckland & Taylor, was the first cable-stayed bridge with a span exceeding a kilometre.

- Clearly, with such long spans, aerodynamic effects are as important in cable-stayed bridges as in suspension bridges.

- The progress of cable-stayed bridges towards longer spans and more slender decks clearly benefitted from the experiences with aerodynamic effects in long-span suspension bridges. For example, the twin deck of the Stonecutter's bridge was chosen primarily for aerodynamic reasons.
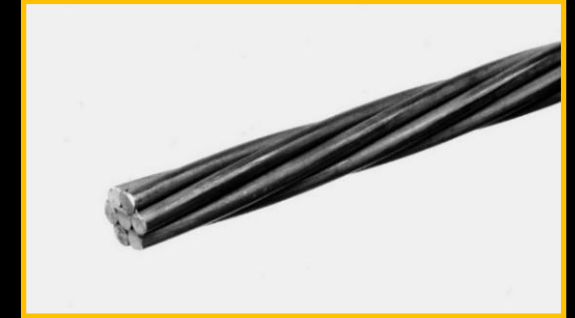
Cable-supported bridges

Common aspects – Cable types

Cable-supported bridges – Common aspects: Cable types

- Cables in modern cable-supported bridges mostly consist of
  - → high-strength steel wires (commonly cylindrical)
  - → f_{pk} = 1770…1860 MPa (as in post-tensioning strands)
  - → Ø5.0… 5.5 mm in suspension bridges
  - → Ø7 mm in stay cables (parallel wire strands).

- Several wires are often shop-assembled to form prefabricated strands.

- The simplest form of strands are seven-wire strands, as used for post-tensioning tendons. The same strands may be used for cable-supported structures:
  - → 7 wires Ø5 mm, nominal diameter 15 mm = 0.6"-strand, A_p = 150 mm² (140 mm² in older strands)
  - → moderate reduction of stiffness compared to the straight wire (Ep ≈ 195 GPa)

- Note however that standard strands will not generally pass the fatigue and ductility tests required for stay cables (elevated demand, performance generally controlled by anchorages).

Seven-wire strand

Stress-strain relationships
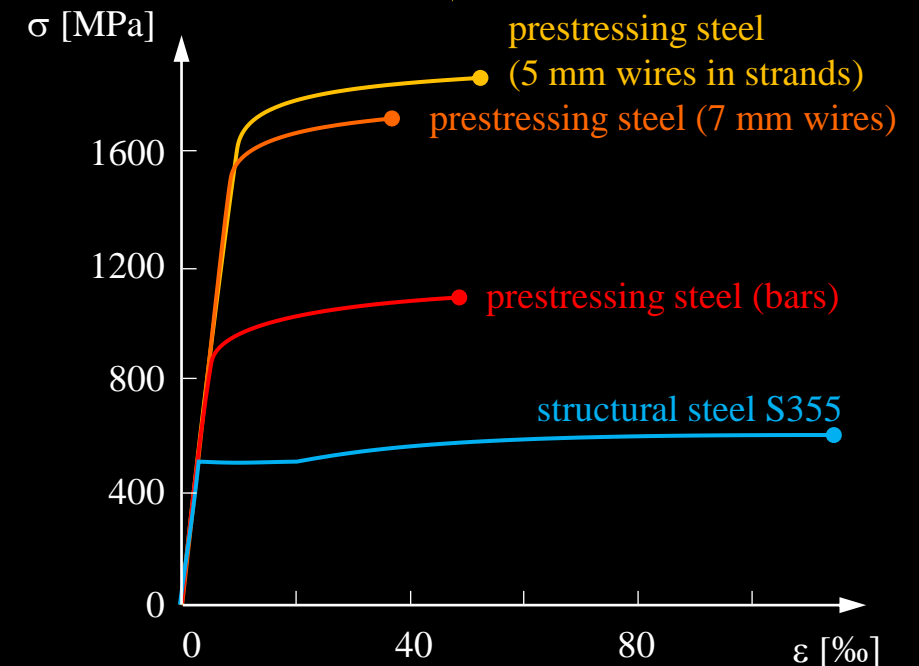
Cable-supported bridges – Common aspects: Cable types

- Multi-wire helical bridge strands ("spiral strands", offene Spiralseile) consist of
  - → successive layers of cylindrical wires
  - → spinning in alternating direction around a straight core
  - → ca. 10% reduction of ultimate load due to twisting
  - → more pronounced stiffness reduction than in 7-wire-strands ($E \approx 160$ GPa, nominal modulus, referred to steel cross-section)
  - → wires are often galvanized for corrosion protection

- Helical strands are compacted at first loading
  - → irreversible elongation at first loading
  - → pre-stretching common (characteristic design load +10…20%) to ensure elastic behaviour in service
  - → no need to wrap or apply bands to hold the wires together

Multi-helical bridge strand
(spiral strand)

[Fatzer.com]

Lillebaelt Bridge multi-helical strand exhibit

[Gimsing 2012]
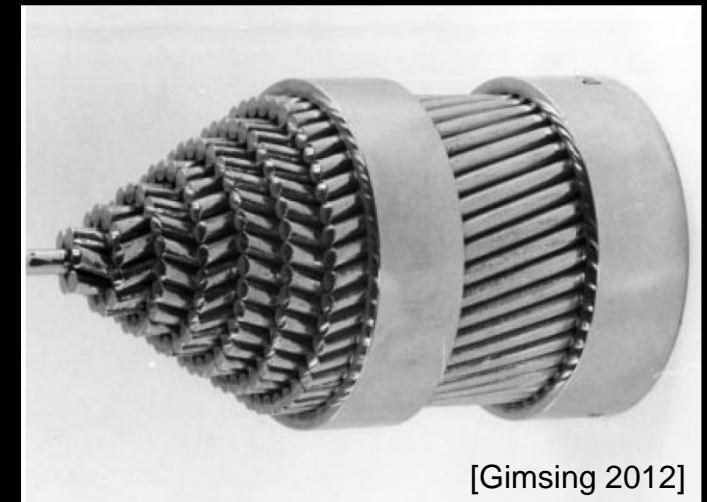
Cable-supported bridges – Common aspects: Cable types

- **Locked coil strands** (vollverschlossene Spiralseile) consist of two types of twisted wire:

  → **core = helical strand**, surrounded by outer layers = **Z-shaped, interlocking wires** spinning in alternating directions around the helical strand core (→ subject to irreversible elongation at first loading)

  → **tight surface, small void ratio** (only ca. 10%), reduced sensitivity to transverse pressure (saddles, anchorages)

  → slightly **lower strength of wires** (f_{pk} = 1370…1570 MPa), additional 10% reduction of ultimate load due to twisting

  → moderate stiffness reduction ($E_{eq} \approx$ 180 GPa)

  → usually **galvanized, combined only with surface coating** (little extra weight)

  → always manufactured in **full length and cross-section** (Ø40…180 mm), **including sockets**, delivered pre-stretched to site on reels

  → main use:
  … single, large-diameter locked coil strands: stay cables
  … multiple smaller diameter locked coil strands as bundle (for suspension bridges and stay cables, obsolete)

Locked coil strand

[Fatzer.com]

Locked coil strand section
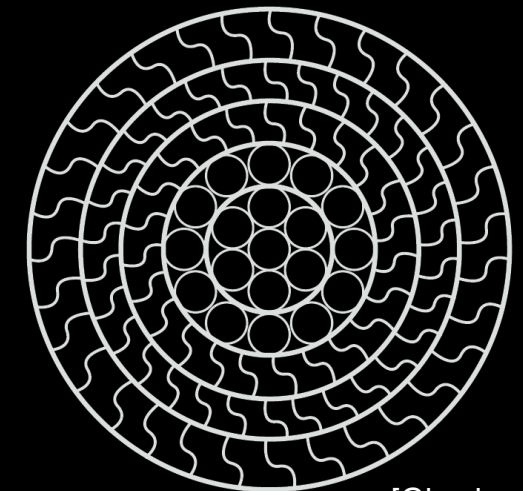
[Gimsing 2012]

Cable-supported bridges – Common aspects: Cable types

- Parallel-wire main cables, consisting of a large number of individual wires, have been used since the early days of suspension bridges.

- Until the 1960s, the main cables of all major suspension bridges (including George Washington Bridge, Golden Gate Bridge, …) were fabricated on site by the air-spinning method:

  → wires are drawn across the spans one by one (later several at a time) by spinning wheels, travelling between end anchorages

  → after a certain number of wires is installed, they are bundled to hexagonal strands (to minimise voids when assembling them)

  → all strand bundles are finally compressed into a dense packed cylinder (using a travelling hydraulic press) and wrapped with wires

- This process is simple, but weather sensitive, time consuming and very labour intense. In smaller suspension bridges, rather than individual wires, prefabricated strands were therefore hauled from one end anchorage to the other already in early bridges. In such cases, until the 1960s, helical strands were used (reasons see next slide), with the related disadvantages (higher void ratio, smaller stiffness, initial elongation requiring pre-stretching).

Cable-supported bridges – Common aspects: Cable types

- Pre-fabricated parallel-wire strands PPWS (Paralleldrahtkabel)
 - → require neither reducing strength nor stiffness compared to the individual wires, which is clearly an advantage over helical strands, but they
  - → were not used until the 1960s due to concerns about reeling (curving the undistorted section of a large parallel wire strand causes high stresses in the inner- and outermost wires)

- However, tests in the 1960s showed that parallel wire strands rotate when reeled (thus avoiding the excessive stresses).

- Since then, PPWS cables have largely replaced helical and locked-coil cables in short and medium span, as well as air-spun parallel wire cables in large span suspension bridges.

- Since long cables are required, the number of wires per strand is limited by transport and erection capacities. In recent suspension bridges, PPWS with up to 127 wires Ø5 mm were used, assembling the main cables from a large number of PPWS (figure: Strand reel Akashi-Kaikyo bridge, weight 85 t for a 4 km long 127-wire strand; 290 strands form each of the two main cables).

- The PPWS are hexagonal as the air-spun strands.

Prefabricated parallel wire strands

(parts of a main cable)

KANMONKYU BRIDGE STRAND
(91 Ø5.04)

AKASHI KAIKYO BRIDGE STRAND
(127 Ø5.23)
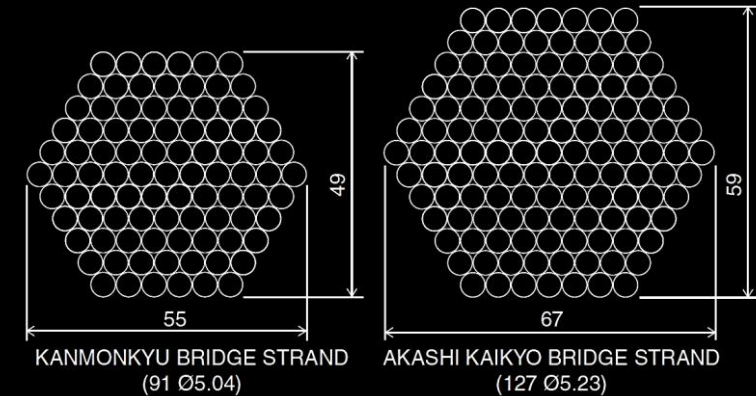
[Gimsing 2012]

Strand reel
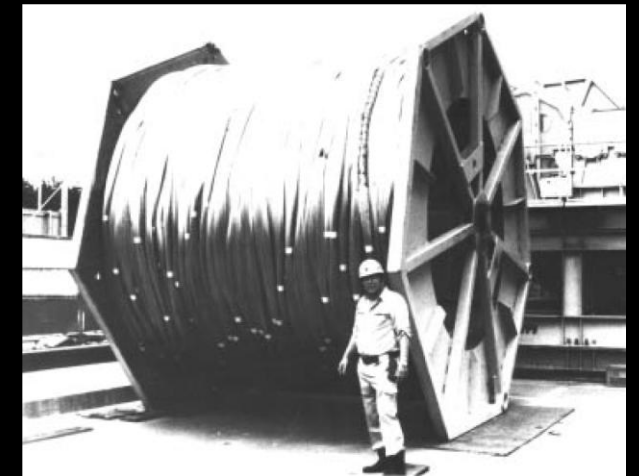
[Gimsing 2012]

Cable-supported bridges – Common aspects: Cable types

Parallel wire cable

(Golden Gate Bridge, one of two suspension cables, *air-spun strands*)
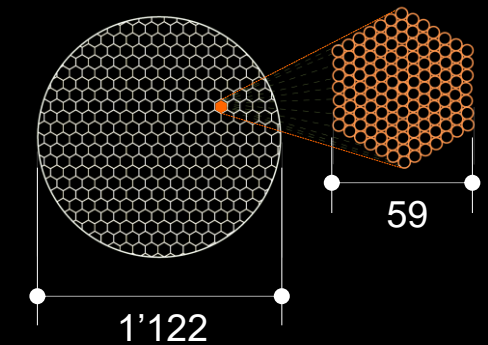

Cable detail (note outermost wires deformed by compaction)

61 strands @ 452 wires Ø5 mm

(27'572 wires per cable)

4.33 t/m = 42.5 kN/m

PPWS cable

(Akashi-Kaikyo Bridge, one of two suspension cables, *prefabricated strands*)

Cable and strand dimensions [mm]

290 strands @ 127 wires Ø5 mm
(36'830 wires per cable)

6.33 t/m = 62 kN/m

Cable-supported bridges – Common aspects: Cable types

- Larger parallel wire strands (up to 499 wires Ø7mm could be produced according to suppliers) are used for stay cables (top figure: largest stay cable of Zarate-Brazo Largo Bridges in Argentina (337 Ø7 mm wires)

- Perfectly parallel wire strands need to be held together
    - → wrapping by a spiral cable was usual in early cable-stayed bridges using parallel wire strands
    - → additional PE tube with corrosion inhibitor in void
    - → disadvantage: large diameter (wind loads) and higher dead load

- Since the 1990s, "New parallel wire strands", developed in Japan, are being used (bottom figure). In these, the wire bundle is slightly twisted
    - → self-consolidating under tension (no need for wrapping)
    - → easier (un)reeling
    - → improved corrosion protection (cover extruded directly on wire bundle)

Prefabricated parallel wire strands

(stay cable)

[Gimsing 2012]

HDPE cover
filament tape
wires Ø7 mm

[Gimsing 2012]
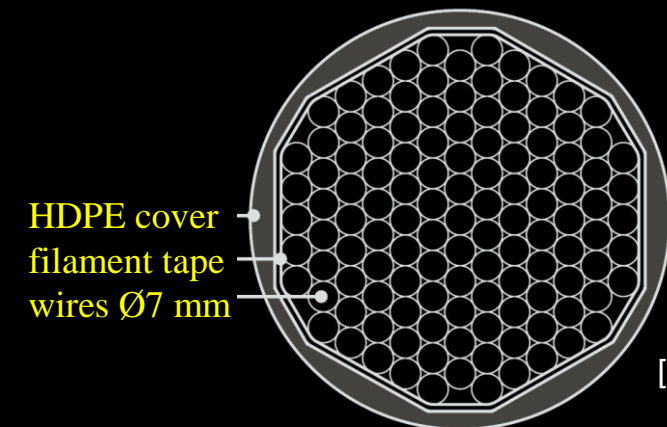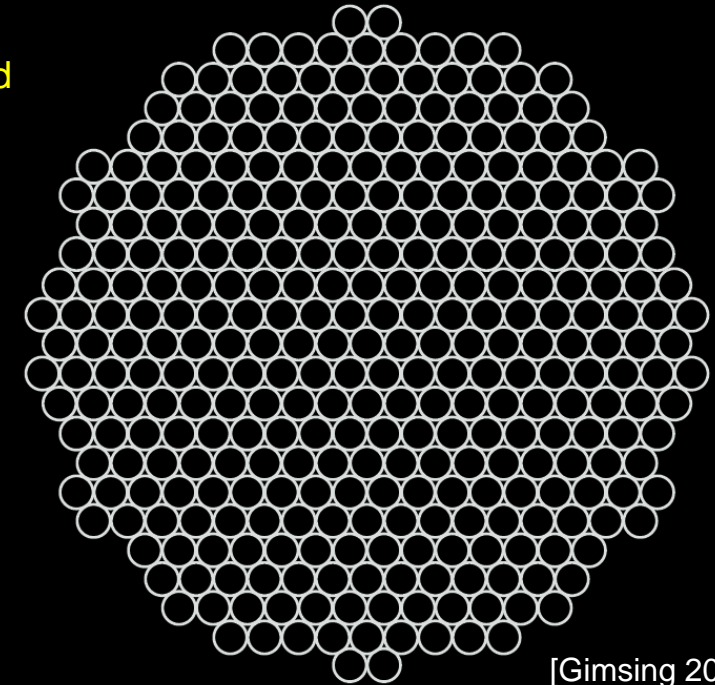
Cable-supported bridges – Common aspects: Cable types

- **Parallel strand stay cables** consisting of 7-wire strands (up to 127 strands per cable according to suppliers) are often an economical solution today.
  - → usually installed and stressed one by one ('Isotension method'), small stressing equipment sufficient
  - → commonly made of galvanized wires today
  - → frequently each strand is protected by an extruded HDPE sheath (bottom figure)

- When using galvanized strands with individual HDPE sheaths
  - → no further corrosion protection is often provided
  - → but the stays need to be held together every 30-40 m to avoid individual oscillations of the strands
  - → cylindrical pipes are often provided to reduce drag (wind load on cables)
  - → relatively large void ratio, requiring larger diameters

- Alternatively, one may dispense of HDPE sheathing (reduced diameter), but dehumidification of the HDPE tube is then required for corrosion protection.

Parallel strand cables
(7-wire strands)

95
37 NOS. SEVEN-WIRE STRANDS

121
61 NOS. SEVEN-WIRE STRANDS

[Gimsing 2012]

147
91 NOS. SEVEN-WIRE STRANDS

Strand detail

HDPE sheath

[tensa.nl]

galvanized wire
Ø7 mm

wax filling

Cable-supported bridges – Common aspects: Cable types

air spinning method

round wires Ø5…7 mm

Z-shaped wires

prefabricated parallel strand method

parallel-wire strands

helical strands (spiral strands)

mantle

core

locked-coil strands

multi-wire helical strands

7-wire helical strands

suspension bridge main cables

stay cables / hangers

parallel wire cables (long span)

locked coil / helical strands (medium span)

parallel-wire

parallel-strand

multi-wire strand

locked-coil

Cable-supported bridges – Common aspects: Cable types

air spinning method

round wires Ø5…7 mm

Z-shaped wires

prefabricated parallel strand method

parallel-wire strands

helical strands (spiral strands)

mantle

core

locked-coil strands

multi-wire helical strands

7-wire helical strands

suspension bridge main cables

stay cables / hangers

parallel wire cables (long span)

parallel-wire (stay cables)

parallel-strand (stay cables)

locked coil / helical strands (medium span)

multi-wire strand

locked-coil (susp./stay cables)

Cable-supported bridges – Common aspects: Cable types

- **Modern parallel strand stay cables, including anchors,** are high-tech, durable components (example see illustration)
- Using "wedge-only" anchoring, individual strands can be controlled and replaced if required (check fatigue resistance)

Compatible with modern construction methods
Compact anchorages fully prefabricated in workshop, no anchorage component assembly on the deck, single strand installation with light equipment, easy force monitoring and adjustment.

Full encapsulation
Each strand separately protected inside the anchorage.

Increased corrosion protection
Factory-applied individual protection treatment, up to 100 years design life in the most aggressive environments.

Economical
Faster installation and erection cycles. Reduced maintenance.

Increased stay anchorage protection
Deviator placed in the guide pipe povides an additional level of protection by filtering cable bending stresses before they reach the anchorage.

Versatile
Designed to receive in the future vibration damping systems (friction dampers) if necessary.

High fatigue resistance
200 MPa with an upper load of 45% of the stay capacity over 2×10^6 load cycles; excellent ultimate resistance after fatigue testing (min. 95% of the specified stay capacity).

Replaceable strands
Ability to remove and to replace individual strands on demand.
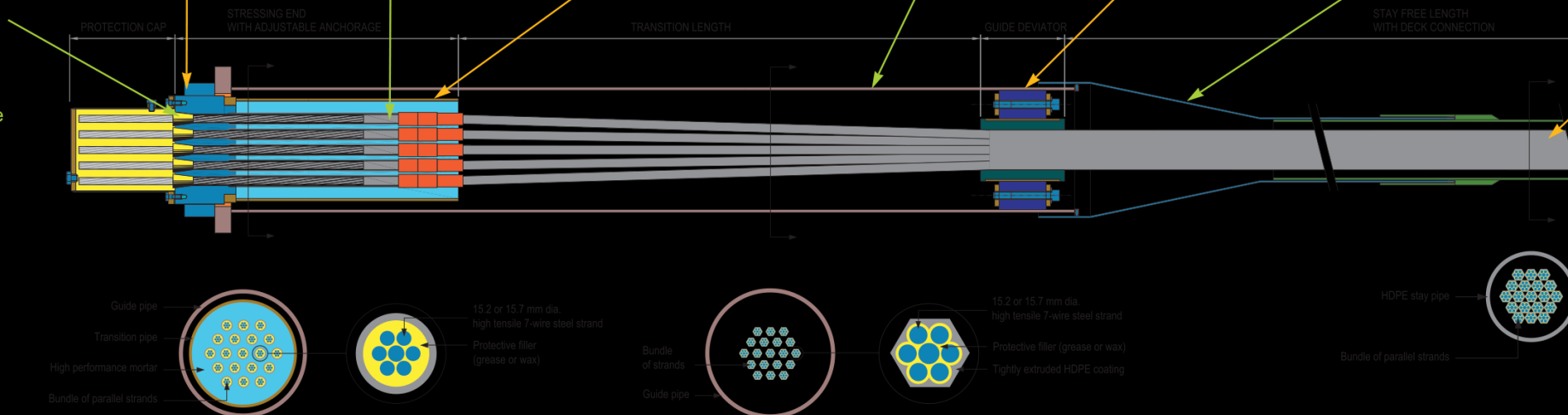
[VSL Stay Cable System 2000]

Cable-supported bridges

Common aspects – Static analysis of cables
General cable behaviour

Cable-supported bridges – Common aspects: Laterally loaded cables

Cable-supported bridges differ significantly from girders:

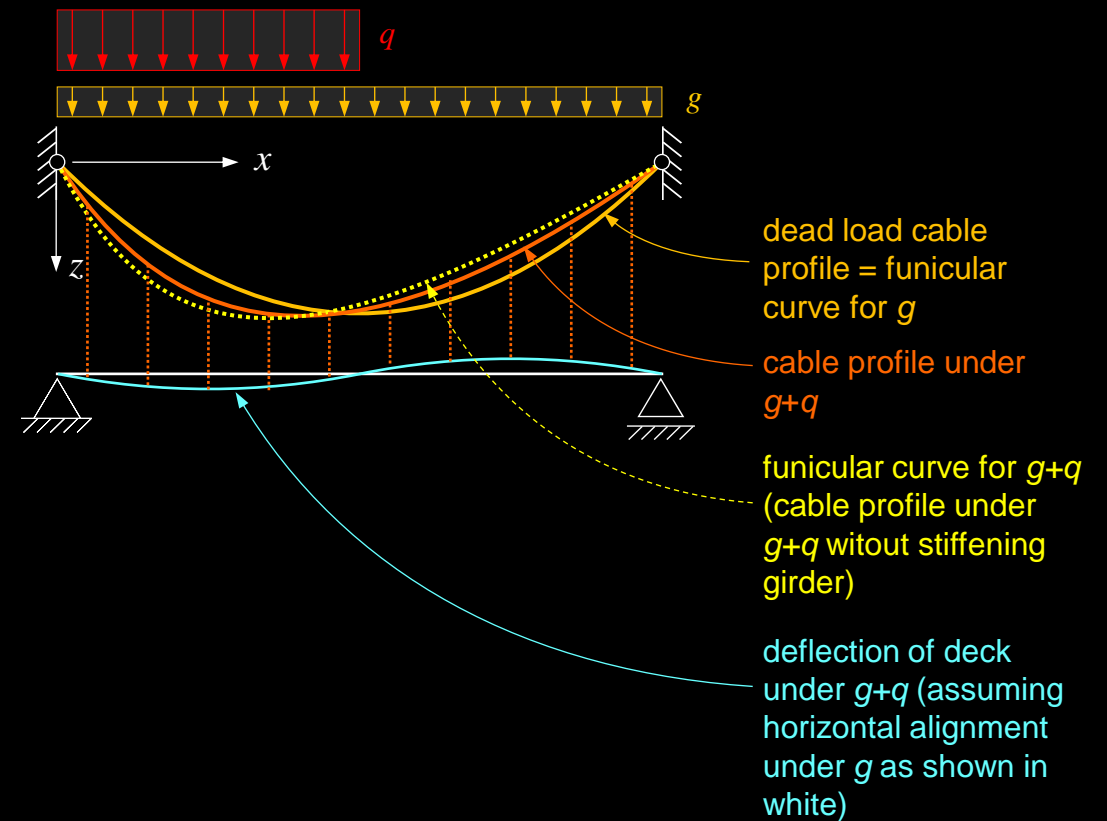- Girders as main structural component typically
  - → require a relatively high amount of material
  - → directly support the bridge deck
  - → are supported directly on piers
  - → cause only vertical reactions under vertical loads
  - → extend over the length of the obstacle to be crossed

- Cables as main load-carrying element typically
  - → require small quantities of structural material
  - → require secondary elements (hangers) to transfer the deck loads to the cables
  - → require supports (towers or pylons) much higher than the deck level
  - → extend far beyond the obstacle to be crossed
  - → require heavy anchor blocks to fix cables at their ends

- In spite of their high structural efficiency, cable supported bridges are therefore only advantageous if material consumption – and saving weight – is essential
  - → Cable-supported bridges are economical only for long spans

Cable-supported bridges – Common aspects: General cable behaviour

- While cables are very stiff under funicular loads (loads for which the cable's initial geometry is funicular, commonly dead load), they are considerably more flexible than girders under non-funicular load configurations.

- Hence, in the design of cable-supported structures, deformations are more of a concern than strength.

- In the detailed analysis and design of cable-supported bridges, numerical methods are used today, accounting for nonlinearities caused by large displacements, for the final layout as well as erection stages.

- If common cable configurations are used (reasonably two-dimensional cable planes), the initial geometry of the cable system may be determined using the same numerical methods, or the approximations for preliminary design outlined on the following slides.

- For complex, three-dimensional cable configurations, specialised form-finding tools may be used.

Cable profiles under non-symmetric load

dead load cable profile = funicular curve for g

cable profile under $g+q$

funicular curve for $g+q$ (cable profile under $g+q$ witout stiffening girder)

deflection of deck under $g+q$ (assuming horizontal alignment under g as shown in white)

Cable-supported bridges – Common aspects: General cable behaviour

- The cable geometry under a given load can be determined iteratively, using the cable equation. This is outlined here following the lines of Marti, Theory of Structures (2012).

- Since large deformations occur, the equilibrium conditions must be formulated for the deformed system (using linear statics, a cable with $EI \rightarrow 0$ can only resist loads for which its initial geometry is funicular).

- Consider a flexible cable with constant axial stiffness but $EI = 0$ spanning between points O and A (left figure). The cable has an initial length L, and carries a vertical line load $q(x)$ (including its self-weight).

- The cable equation is obtained formulating equilibrium of the deformed system (right figure and equations).

- The additional terms $L\alpha_T\Delta_T$ and $L\sigma_0/E$ account for possible thermal strain and cable prestress, constant along the cable length.

Static system of cable and cable element
(adapted from Marti, 2012; α = secant inclination due to anchorage height difference)
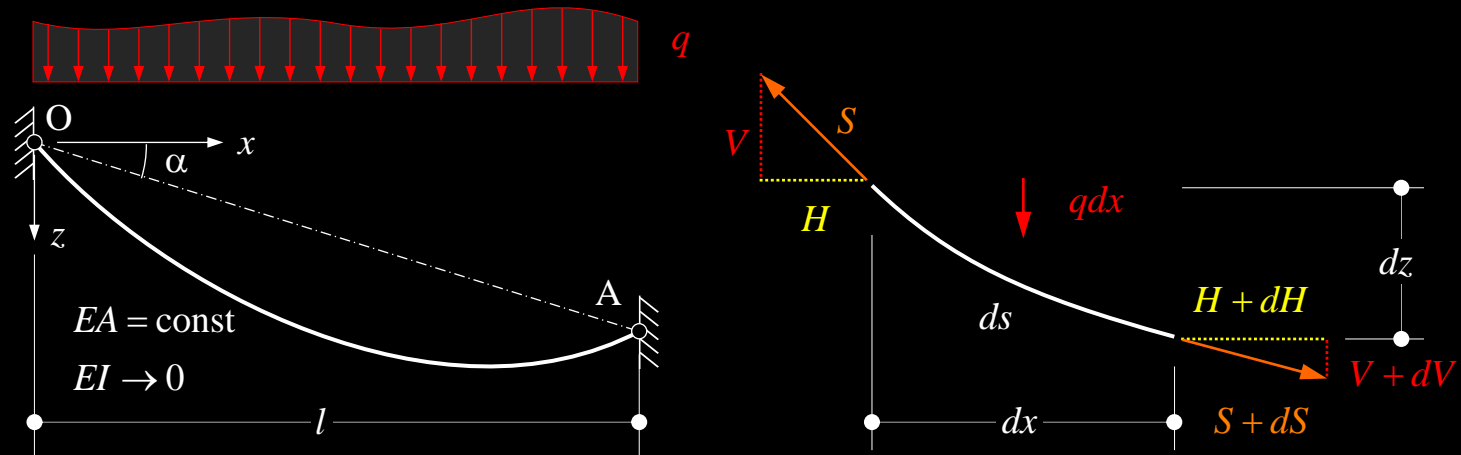
geometry: (a) $ds = \sqrt{dx^2 + dz^2} = dx\sqrt{1 + z'^2}$ $\{$with $z' = dz/dx\}$

equilibrium:
(b) $\Sigma F_x = dH = 0$
(c) $\Sigma F_z = qdx + dV = 0$
(d) $\Sigma M_y = Hdz - Vdx = 0$
$\rightarrow$
$\begin{cases} H = \text{const} & \{\text{directly from (b)}\} \\ V = Hz' & \{\text{rewrite (d), with } z' = dz/dx\} \\ -Hz'' = q & \{\text{differentiate (d), insert (c)}\} \end{cases}$

cable force: (e) $S = \sqrt{H^2 + V^2} = H\sqrt{1 + z'^2}$ $\{$since $V = Hz'$, see above$\}$

deformed cable length: $\int_o^l \sqrt{1 + z'^2}\,dx = L\left(1 + \alpha_T\Delta T - \frac{\sigma_0}{E}\right) + \int_o^l \frac{S\sqrt{1 + z'^2}}{EA}\,dx$ ("cable equation")

(initial length L changes due to elastic strains S/EA, thermal strains $\alpha_T\Delta T$ and prestress σ_0)

Cable-supported bridges – Common aspects: General cable behaviour

- Using (e) and the equivalent shear force $\bar{V}$ and bending moment $\bar{M}$ in a simply supported beam subjected to q as reference (bottom figures), the rightmost term of the cable equation and the cable geometry can be expressed as:

$$\int_o^l \frac{S\sqrt{1+z'^2}}{EA}\,dx = \frac{H}{EA}\int_o^l \left(1+z'^2\right)dx = \frac{Hl}{EA} + \frac{H}{EA}\int_o^l \left(\tan\alpha + \frac{\bar{V}}{H}\right)^2 dx$$

$$z = x\tan\alpha + \frac{\bar{M}}{H} \qquad z' = \tan\alpha + \frac{\bar{V}}{H} \qquad z'' = -\frac{q}{H}$$

- For a given initial cable length and load, the cable geometry can be determined by (i) assuming a value of *H*; (ii) determining *z* and *z'* from the relationships above and (iii) iterating until the cable equation is satisfied, i.e.:

$$\int_o^l \sqrt{1+z'^2}\,dx = L\left(1 + \alpha_T \Delta T - \frac{\sigma_0}{E}\right) + \frac{Hl}{EA} + \frac{H}{EA}\int_o^l \left(\tan\alpha + \frac{\bar{V}}{H}\right)^2 dx$$

(note that q and hence $\bar{V}$ and $\bar{M}$ need to be adjusted to account for the cable self-weight unless this is negligible)

- In design, *L* is usually not given, but needs to be determined to achieve a certain sag = *z* at midspan → vary *L* or σ_0 until desired sag is obtained (and the cable equation satisfied).

Equivalent stress resultants for simply supported beam (adapted from Marti, 2012)
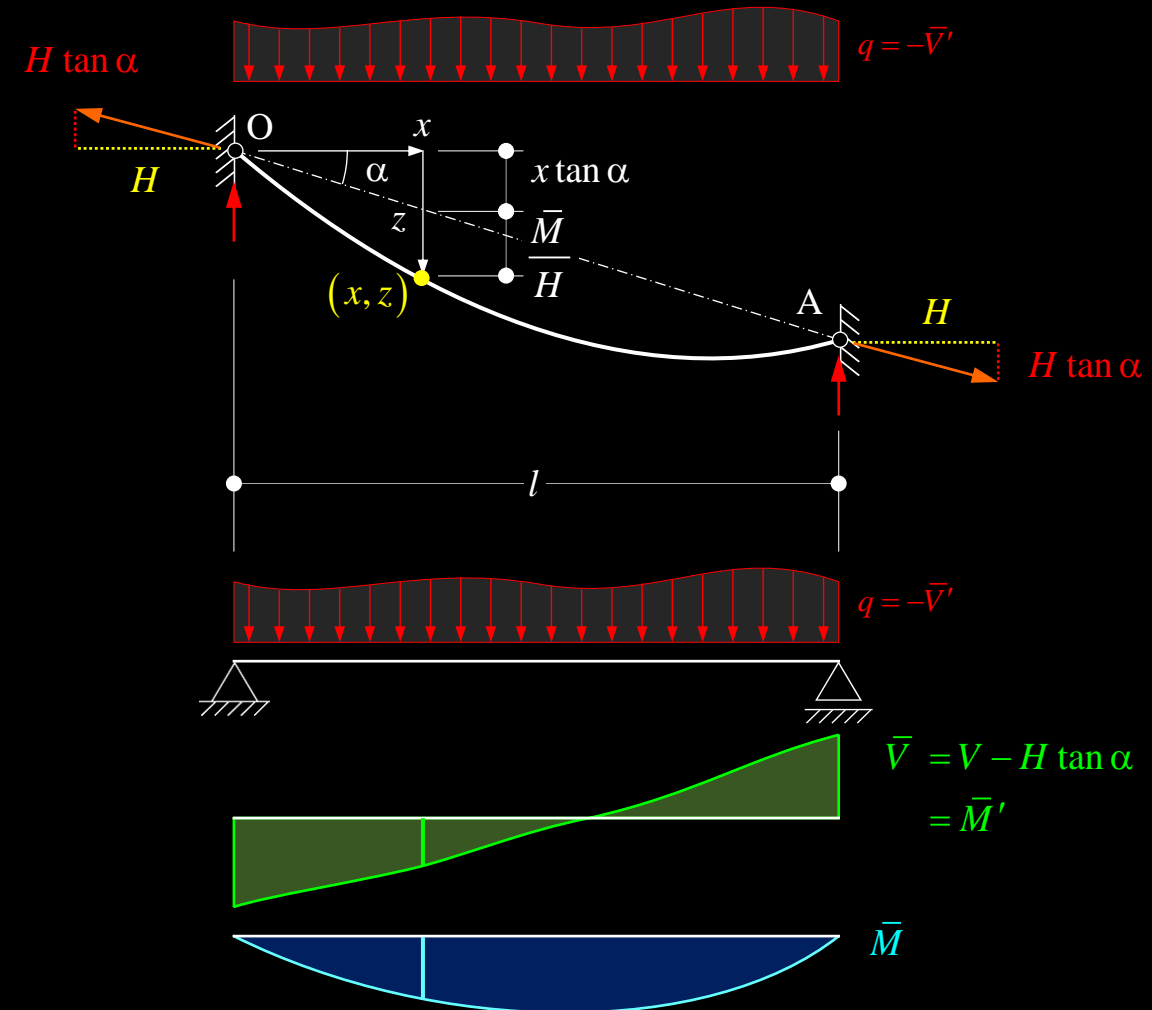
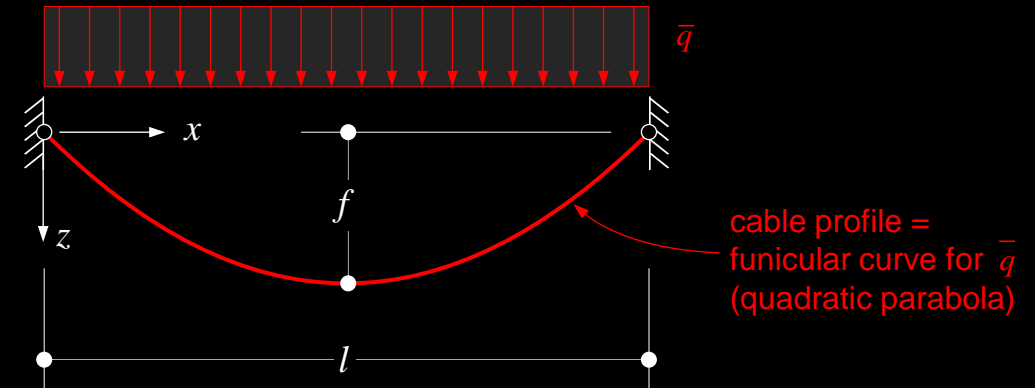# Cable-supported bridges – Common aspects: General cable behaviour

- For detailed design, numerical procedures (implemented in commercial software programs, such as e.g. Larsa 4D, Sofistik or Midas) are used.

- In preliminary design, and to determine the initial geometry in the numerical model, a uniformly distributed load (total loads span divided by span length) may be assumed.

- Under uniform load, the cable geometry is a quadratic parabola, and the integrals in the cable equation can be expressed analytically (see Marti, Theory of Structures), i.e., the length of the deformed cable under a load $\bar{q}$ is:

$$\frac{l}{2}\left[\sqrt{1+\beta^2}+\frac{\ln\left(\beta+\sqrt{1+\beta^2}\right)}{\beta}\right]=L\left(1+\alpha_T\Delta T-\frac{\sigma_0}{E}\right)+\frac{\bar{q}l^2}{2EA\cdot\beta}\left(1+\frac{\beta^2}{3}\right)$$

where $\beta=\dfrac{4f}{l}$ and $\dfrac{l}{2}\left[\sqrt{1+\beta^2}+\dfrac{\ln\left(\beta+\sqrt{1+\beta^2}\right)}{\beta}\right]\approx l\left(1+\dfrac{\beta^2}{6}-\dfrac{\beta^4}{40}\right)$

- Starting from a desired geometry (e,g. assuming $f \rightarrow \beta$ under dead load g), the initial cable length L is obtained. Knowing L, the sag f under any load q (or temperature difference) is determined by solving the equation for β.

Horizontal cable under uniform load

cable profile = funicular curve for $\bar{q}$ (quadratic parabola)

auxiliary parameter (sag/span): $\beta=\dfrac{4f}{l}$

hor. component of cable force: $H=\dfrac{\bar{q}l^2}{8f}$

maximum cable force: $S=H\sqrt{1+\beta^2}$

cable elongation ($\Delta T=0, \sigma_0=0$): $\Delta L=\dfrac{\bar{q}l^2}{2EA\cdot\beta}\left(1+\dfrac{\beta^2}{3}\right)=\dfrac{Hl}{EA}\left(1+\dfrac{\beta^2}{3}\right)$

Cable-supported bridges

Common aspects – Static analysis of Cables
Laterally (usually vertically) loaded cables

Cable-supported bridges – Common aspects: Laterally loaded cables

- On this and the following slides, the behaviour of suspension bridges (resp. their main cables) is investigated following the example used by Gimsing (see notes for source).

- The example is based on the following basic parameters:
  - span $l = 1'000$ m, $f_g/l = 0.1$ (100 m sag under g)
  - dead load $g = 220$ kN/m, traffic load $q = 80$ kN/m
  - cable cross-section $A = 0.56$ m^2 (14'551 wires Ø7 mm) (cable weight = 44.0 kN/m ≈ 20% of g, not negligible!)

- Solving the cable equation for $\beta_g = 0.4$ (dead load geometry, no thermal strain nor prestress), the initial cable length L is:
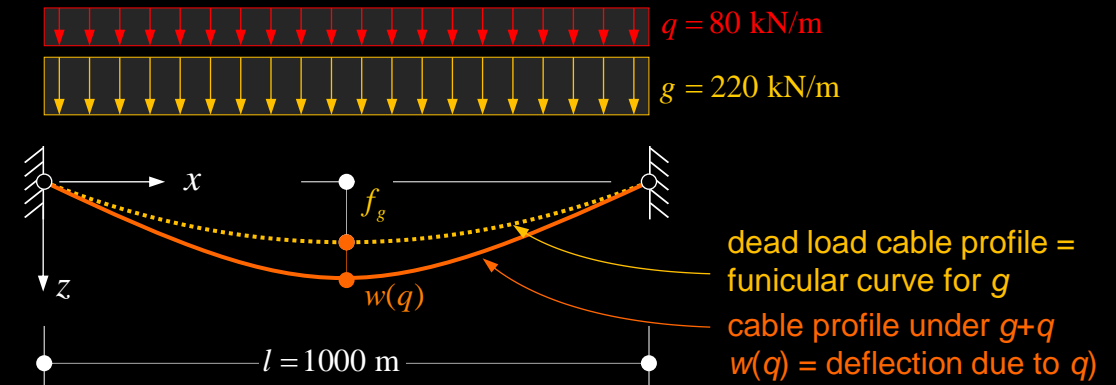
$$\frac{l}{2}\left[\sqrt{1+\beta_g^2} + \frac{\ln\left(\beta_g + \sqrt{1+\beta_g^2}\right)}{\beta_g}\right] = L + \frac{gl^2}{2EA \cdot \beta_g}\left(1 + \frac{\beta_g^2}{3}\right) \rightarrow L = 1023.474 \text{ m}$$

- The full load geometry is obtained by solving for β_{g+q} :

$$\frac{l}{2}\left[\sqrt{1+\beta_{g+q}^2} + \frac{\ln\left(\beta_{g+q} + \sqrt{1+\beta_{g+q}^2}\right)}{\beta_{g+q}}\right] = L + \frac{(g+q)l^2}{2EA \cdot \beta_{g+q}}\left(1 + \frac{\beta_{g+q}^2}{3}\right)$$

$$\rightarrow \beta_{g+q} = 0.4069, \quad f_{g+q} = \frac{\beta_{g+q}l}{4} = 101.726 \text{ m}, \quad w(q) = 101.726 - 100 = 1.726 \text{ m}$$

Deflection under traffic load acting over varying width b (adapted from Gimsing 2012)

Dead load ($g = 220$ kN/m, chosen $\rightarrow f_g = 100$ m):

$$\beta_g = \frac{4f_g}{l} = 0.4000 \qquad H_g = \frac{gl^2}{8f_g} = 275 \text{ MN}$$

$$S_g = H_g\sqrt{1+\beta_g^2} = 296 \text{ MN} \quad \sigma_g = \frac{S_g}{A_c} = 491 \text{ MPa}$$

Full load ($g + q = 300$ kN/m, cable equation $\rightarrow f_{g+q} = 101.726$ m):

$$\beta_{g+q} = \frac{4f_{g+q}}{l} = 0.4069 \qquad H_{g+q} = \frac{(g+q)l^2}{8f_{g+q}} = 368 \text{ MN}$$

$$S_{g+q} = H_{g+q}\sqrt{1+\beta_{g+q}^2} = 398 \text{ MN} \quad \sigma_{g+q} = \frac{S_{g+q}}{A_c} = 711 \text{ MPa}$$

Cable-supported bridges – Common aspects: Laterally loaded cables

- This slide compares the midspan deflection due to traffic load over the central part of the main span, over a varying portion *b* of the span *l*:

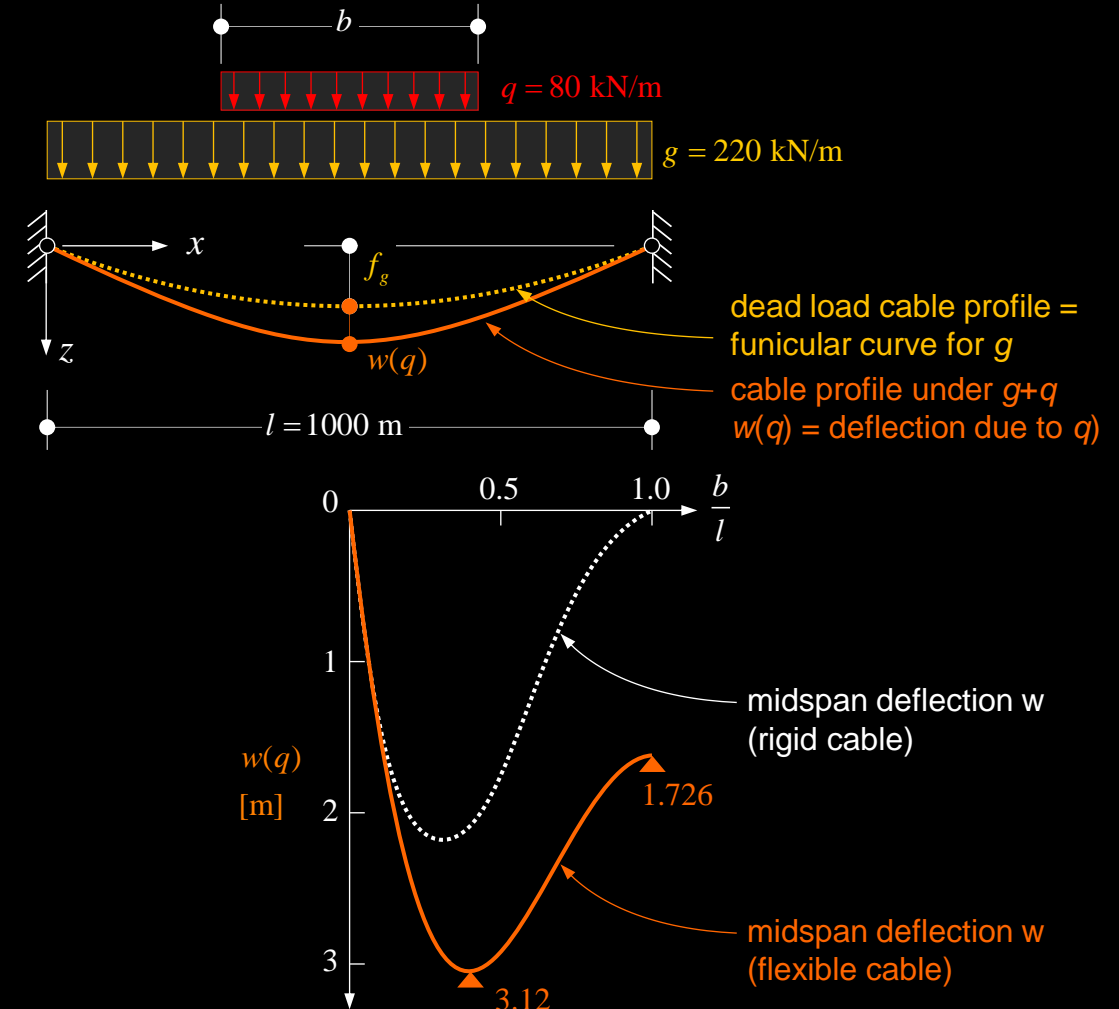 → the midspan deflection under traffic load over the full span is 1.726 m, fully due to cable elongation.

  the same deflection is obtained for only ca. 10% loaded length

  → under partial length loading, the cable deflects more, with a maximum deflection of 3.12 m for a loaded length of about 40% of the span

  → only about 1/3 of the maximum deflection is due to cable elongation for 40% loaded length. The remaining deflection is due to the change of cable geometry.
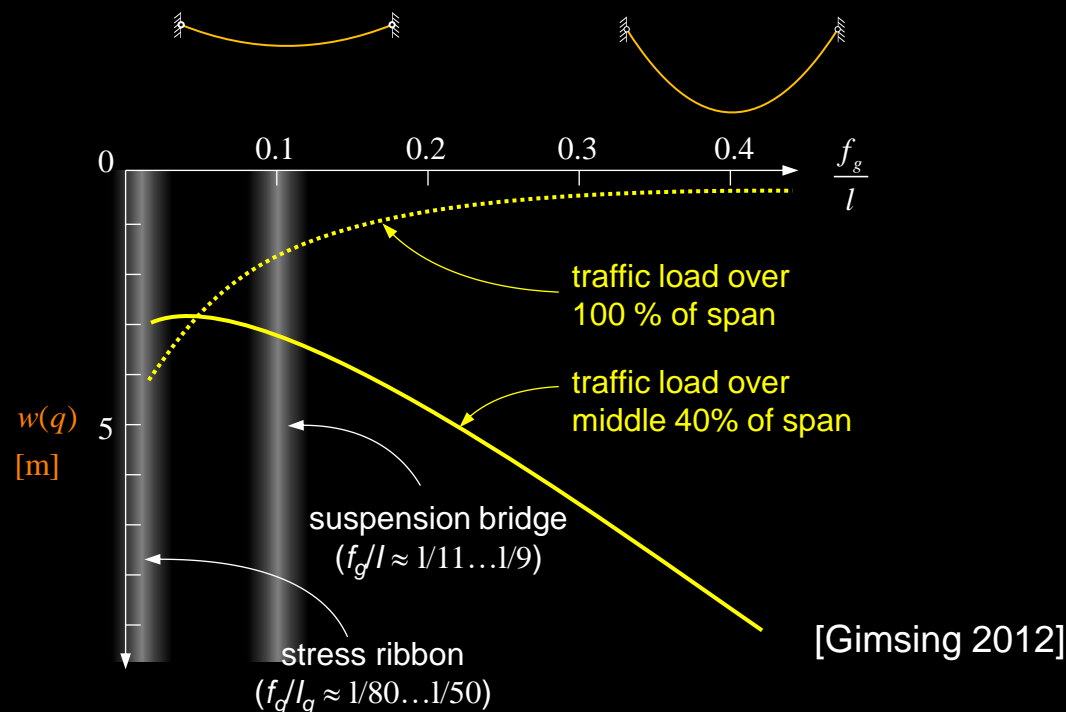
  note that under uniform load (traffic load over the full span), deflections of a rigid cable are zero.

Deflection under traffic load acting over varying width *b* (adapted from Gimsing 2012)

$q = 80 \text{ kN/m}$

$g = 220 \text{ kN/m}$

f_g

$w(q)$

$l = 1000 \text{ m}$

dead load cable profile = funicular curve for *g*

cable profile under *g+q* $w(q)$ = deflection due to *q*

$\frac{b}{l}$

$w(q)$ [m]

midspan deflection w (rigid cable)

1.726

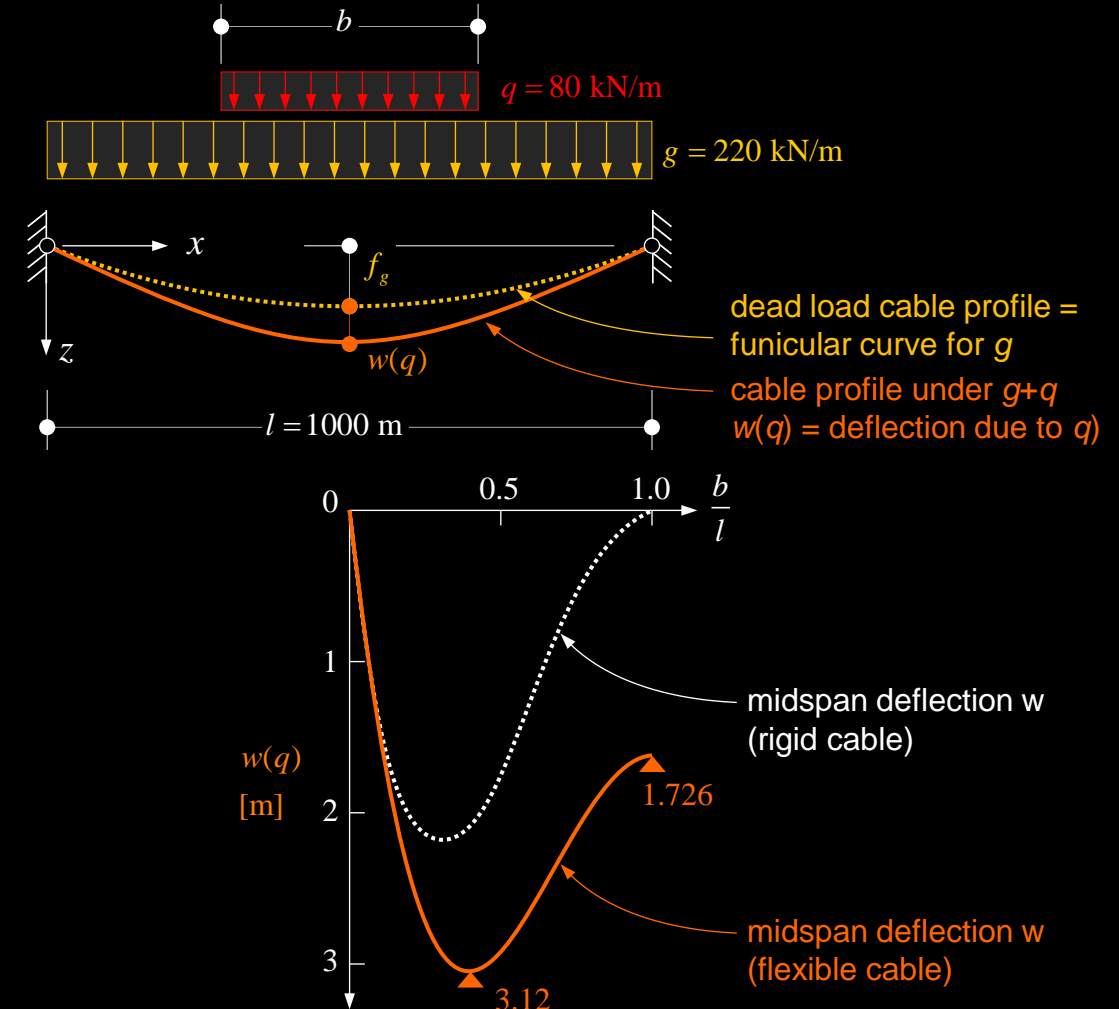midspan deflection w (flexible cable)

3.12

Cable-supported bridges – Common aspects: Laterally loaded cables

- As illustrated on the previous slide, starting from the fully loaded span, the midspan deflection increases if traffic loads in the outer parts are removed

- This effect, which is the opposite of what is observed in a simply supported beam, is more pronounced in slack cables (high sag/span ratio f_g/l) than in taut ones, see figure below (cable area adjusted to account for f_g/l):
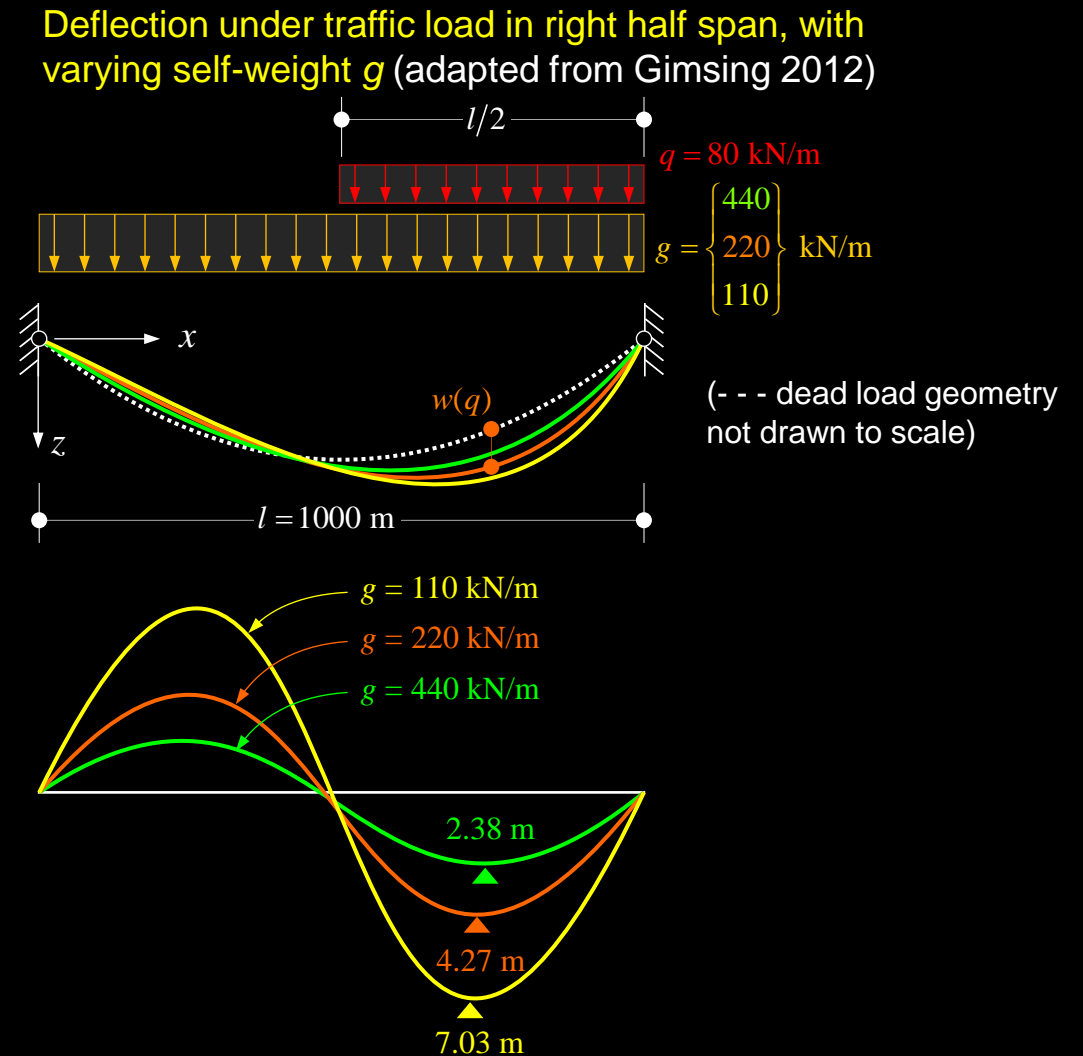
Deflection under traffic load acting over varying width b (adapted from Gimsing 2012)

$q = 80$ kN/m

$g = 220$ kN/m

dead load cable profile = funicular curve for g

cable profile under $g+q$
$w(q)$ = deflection due to q

$l = 1000$ m

traffic load over 100 % of span

traffic load over middle 40% of span

suspension bridge $(f_g/l \approx 1/11…1/9)$

stress ribbon $(f_g/l_g \approx 1/80…1/50)$

[Gimsing 2012]

midspan deflection w (rigid cable)

midspan deflection w (flexible cable)

1.726

3.12

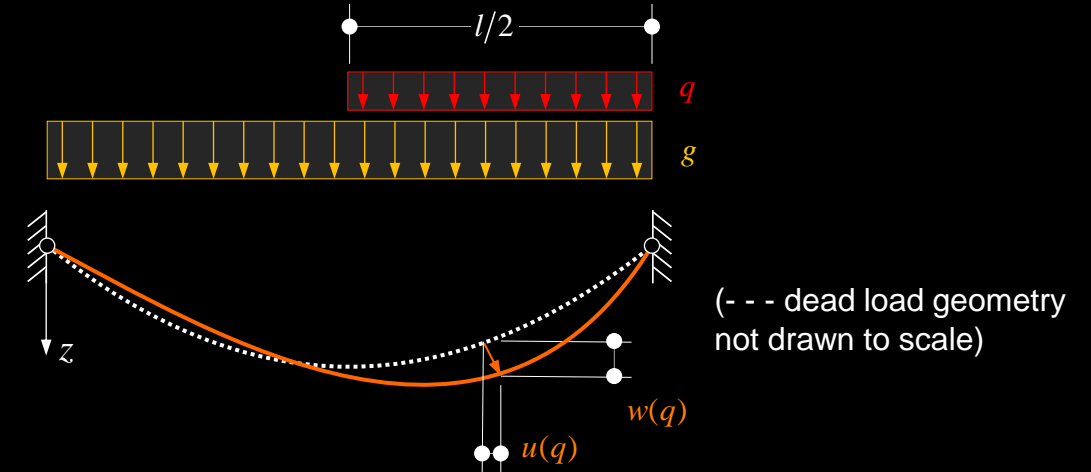# Cable-supported bridges – Common aspects: Laterally loaded cables

- The tension force in the cable (due to uniform load) has a stiffening effect on the deformations caused by traffic loads (the deviation from funicular load caused by the traffic load decreases with higher dead load).

- This is illustrated on this slide considering traffic load on one half of the span, and varying the dead load (same / double / half the value of previous slides):
  - → the maximum deflection under traffic load is significantly affected by the dead load
  - → modern lightweight suspension bridges (steel box girders with orthotropic steel deck) deflect much more under traffic loads than old suspension bridges with heavy steel trusses and concrete decks due to their reduced weight
  - → The bending stiffness of girders, neglected here, does not alter this conclusion, see next slides.
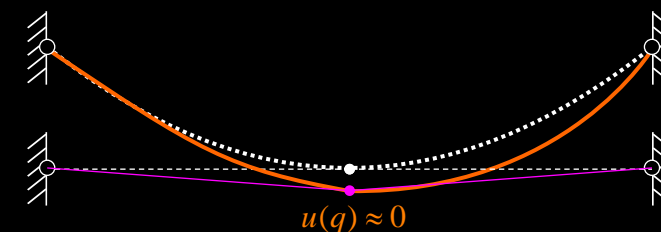
Deflection under traffic load in right half span, with varying self-weight g (adapted from Gimsing 2012)

$q = 80 \text{ kN/m}$

$g = \begin{Bmatrix} 440 \\ 220 \\ 110 \end{Bmatrix} \text{ kN/m}$

$l/2$

x

z

$w(q)$

$l = 1000 \text{ m}$

(- - - dead load geometry not drawn to scale)

$g = 110 \text{ kN/m}$
$g = 220 \text{ kN/m}$
$g = 440 \text{ kN/m}$

2.38 m

4.27 m

7.03 m

Cable-supported bridges – Common aspects: **Laterally loaded cables**

- Under non-symmetrical load, the points on the cable between its ends shift to the side with higher load (upper figure).

- This can be prevented, for example, by providing a prestressed guy cable (lower figure), which is connected to the middle of the main cable, see Marti (2012).

- The guy cable will cause a slight kink in the main cable at the connection, and a significantly stiffer behaviour

- In suspension bridges, a connection of suspension cables and deck girder is often used to achieve this effect.

- So far, a single span with rigid supports has been assumed. On the following slides, the effect of several spans is investigated.

Deflection under traffic load in right half span

$l/2$

q

g

(- - - dead load geometry
not drawn to scale)

z

$w(q)$

$u(q)$

Deflection under traffic load in right half span with guy cable (see Marti 2012)

$u(q) \approx 0$

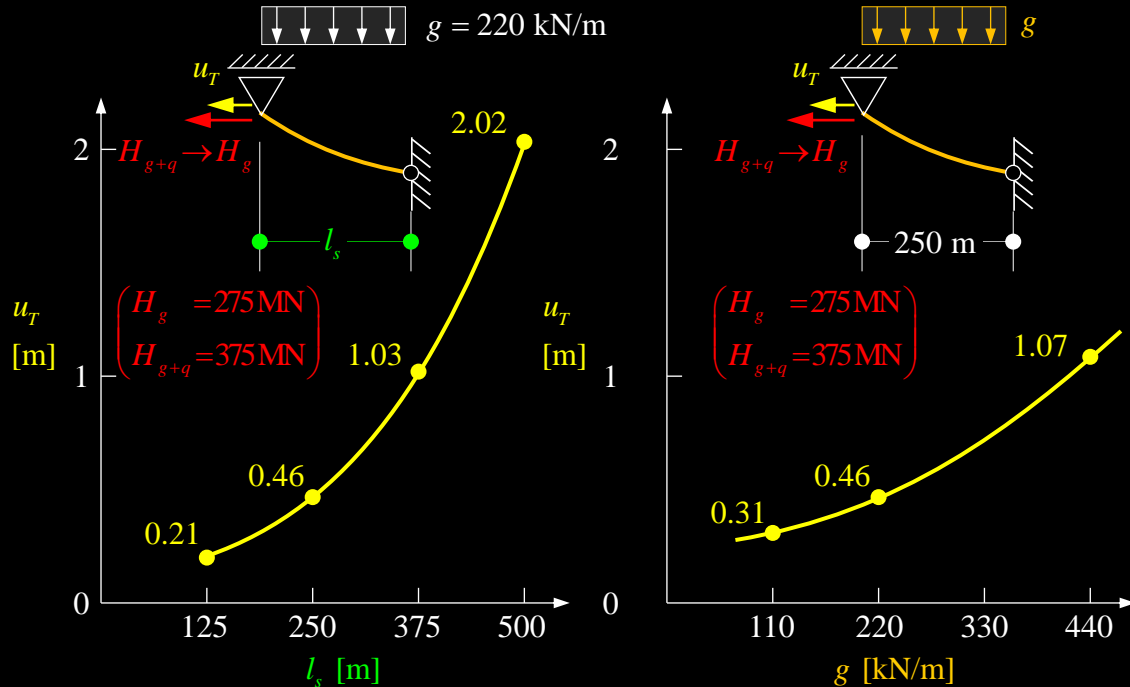# Cable-supported bridges – Common aspects: Laterally loaded cables

- The deformations of suspension bridges are significantly affected by the span layout. This is illustrated following (once again) an example given by Gimsing [Gimsing 2012].

- The figure compares the deflections of two three-span cables with spans of 500+1000+500 m and 250+1000+250 m, respectively, due to traffic load in the main span (other parameters as previous slides).

  → midspan deflection in bridge with short side span is only ca. 40% of that with long side span (in a continuous beam, the midspan deflection would only decrease by ca. 20% if the side span is halved)

  → strong influence of side span length primarily caused by horizontal displacements u_T of the tower tops (almost four times larger for long side span)

  → horizontal displacements of the tower tops are primarily caused by sag reduction of the cables in the end spans (and not the elongation of the cable), see following slide.

Deflection under traffic load in main span, with varying side span length (adapted from Gimsing 2012)
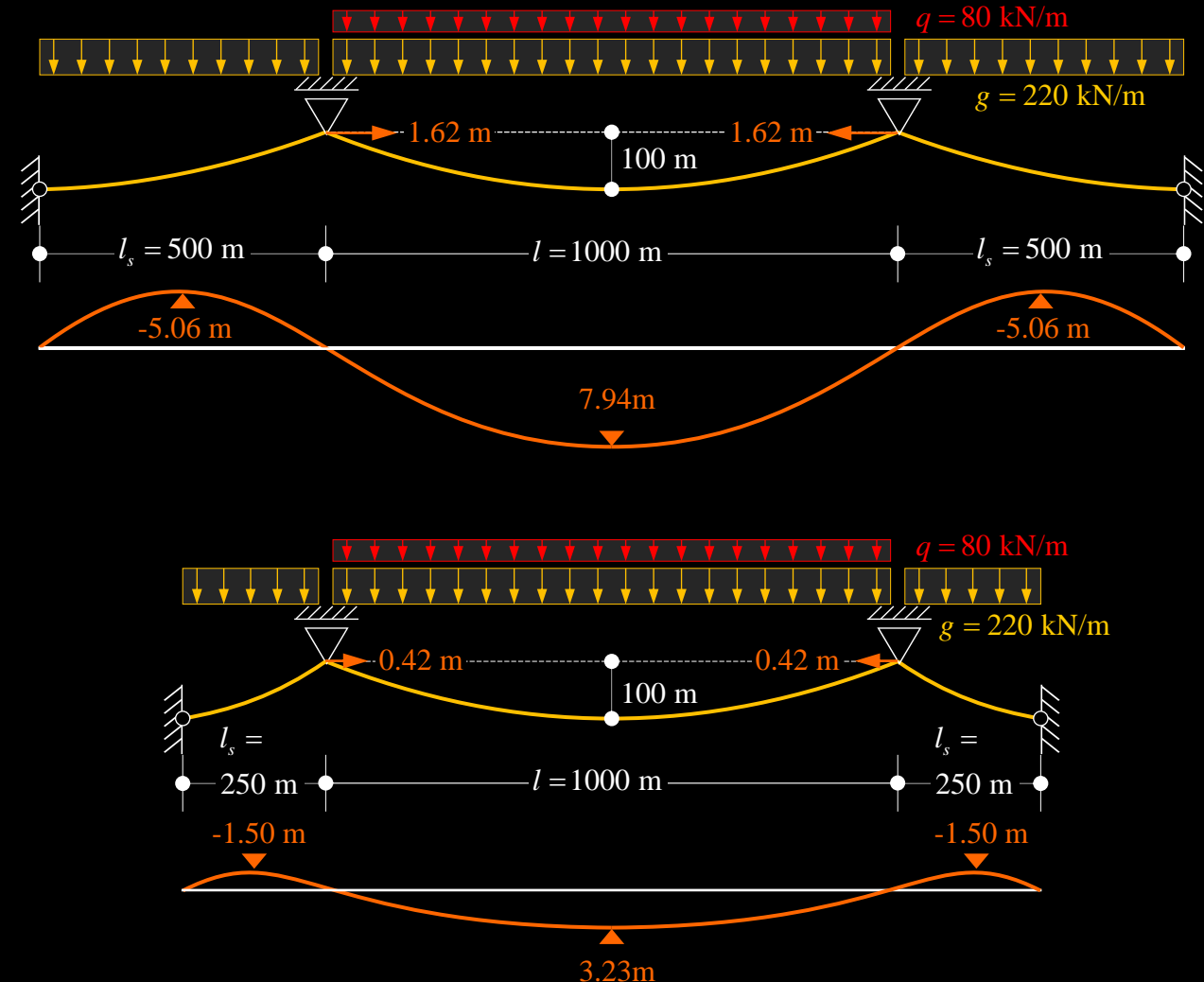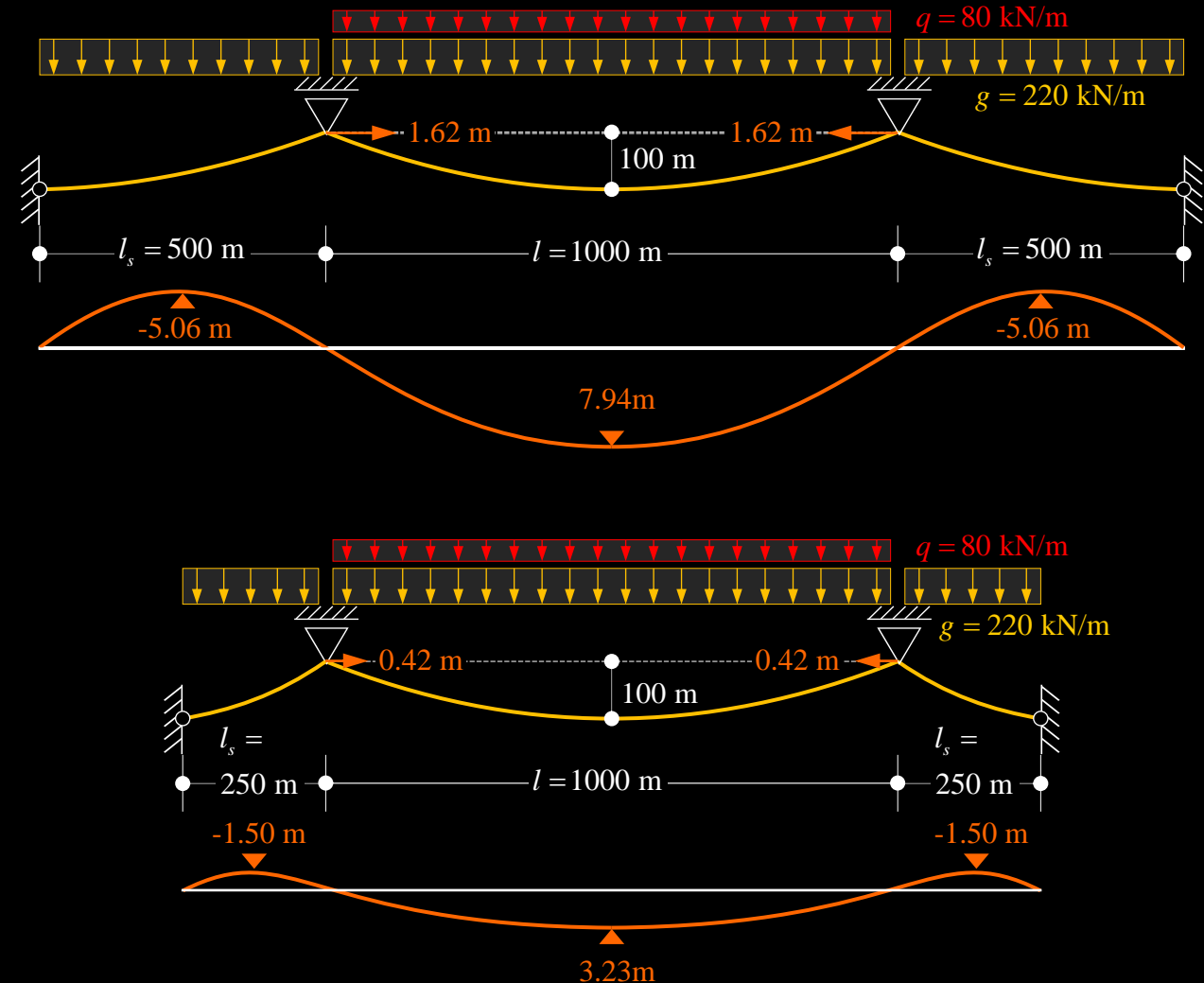
Cable-supported bridges – Common aspects: Laterally loaded cables

- Horizontal displacements of the tower tops are
  - → **smaller with short side spans** since the cable is initially tauter in the side spans (smaller sag required at same cable force and dead load)
  - → **larger for higher dead load** since the cable is initially slacker in the side spans (larger sag required at same cable force and span)
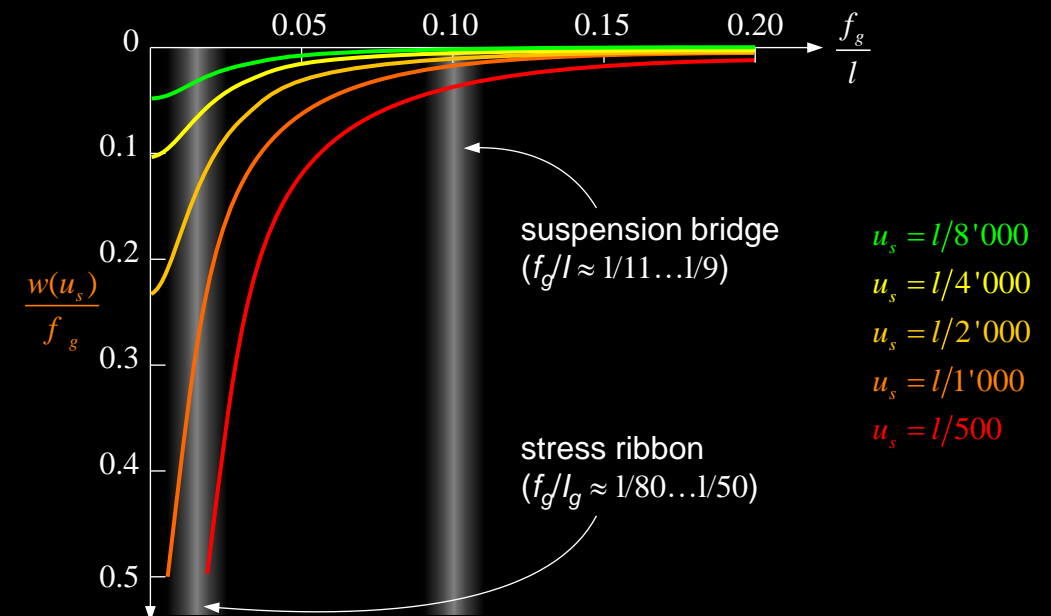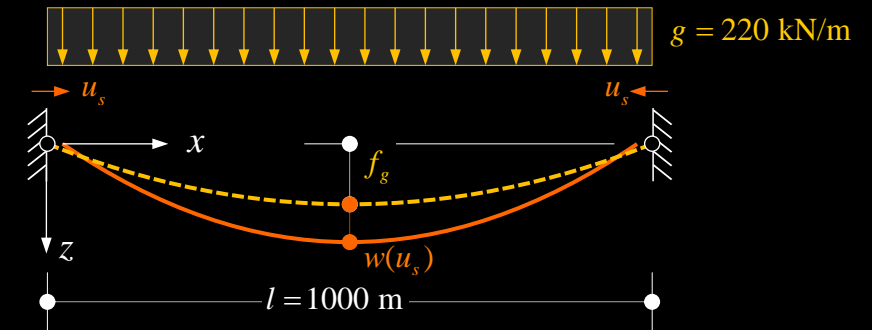

Deflection under traffic load in main span, with varying side span length (adapted from Gimsing 2012)

Cable-supported bridges – Common aspects: Laterally loaded cables

- The sensitivity of cables to horizontal displacements of the supports increases with reduced sag:
  - → Under equal support displacements, taut cables deflect much more than slack cables
  - → Effect particularly relevant in stress-ribbons (see section on stress ribbon bridges)

- Strains imposed to the cables (temperature, creep and shrinkage in stress-ribbons) have a similar effect as horizontal support displacements.

Deflection due to horizontal support displacements

$g = 220$ kN/m

u_s u_s

x

f_g

z

$w(u_s)$

$l = 1000$ m

$\dfrac{w(u_s)}{f_g}$

$\dfrac{f_g}{l}$

suspension bridge
($f_g/l \approx 1/11 \ldots 1/9$)

stress ribbon
($f_g/l_g \approx 1/80 \ldots 1/50$)

$u_s = l/8'000$

$u_s = l/4'000$

$u_s = l/2'000$

$u_s = l/1'000$

$u_s = l/500$

Cable-supported bridges – Common aspects: **Laterally loaded cables**

- So far, it has not only been assumed that the cable acts as a rope without bending stiffness, but the stiffening effect of the deck girder has been neglected.

- This is justified in preliminary design, as illustrated by this slide comparing the deflections for the cable alone with those of suspension bridges with two different stiffening girder layouts:

  → differences negligible for traffic load over entire main span

  → differences small for traffic load over half the main span

Comparison of deflections under traffic load
(adapted from Gimsing 2012)

——— cable alone
——— suspension bridge, stiffening girder simply supported (*)
——— suspension bridge, stiffening girder continuous (*)

(*) inertia of a modern 3 m deep steel box girder
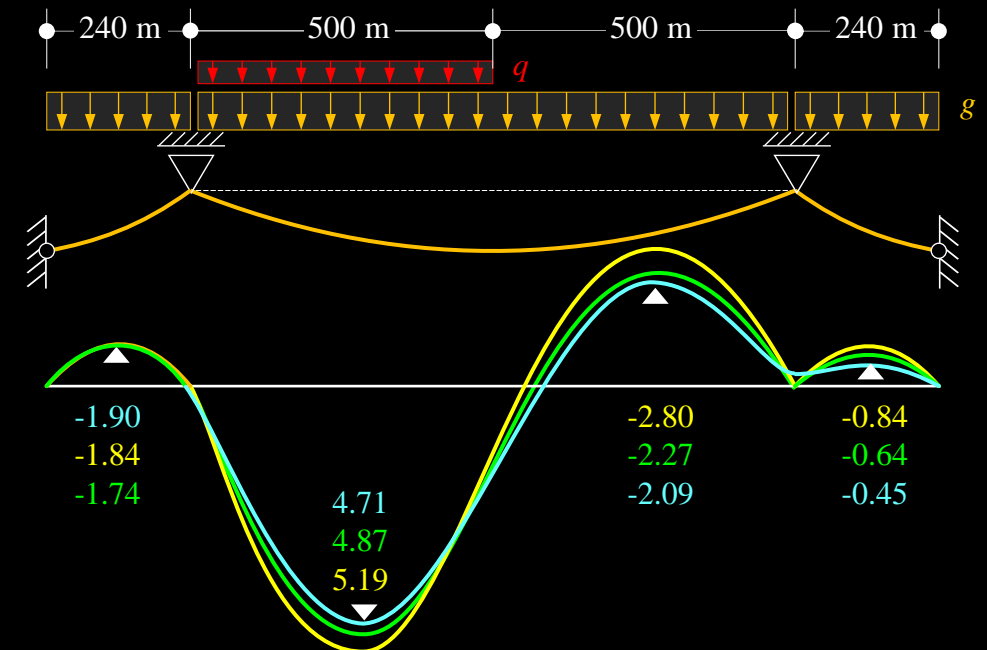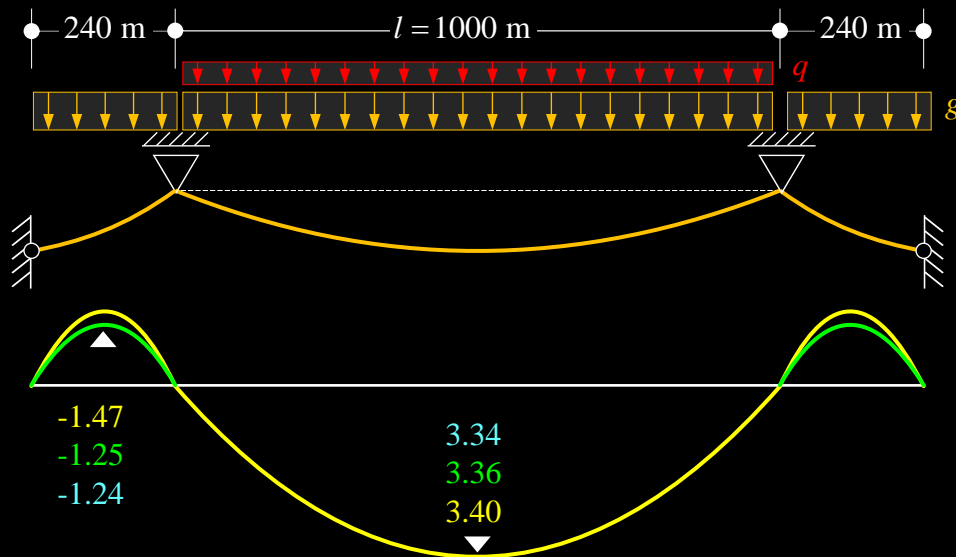
Cable-supported bridges

Common aspects – Static analysis of Cables

Axial stiffness of laterally loaded cables

Cable-supported bridges – Axial stiffness of laterally loaded cables

- The axial stiffness of laterally loaded cables is highly relevant in cable-supported structures, as illustrated on the previous slides.

- It is particularly important for long stay cables, whose axial stiffness – which directly affects the vertical displacements of the bridge girder – is reduced by the sag (photo).

- If a horizontal cable without lateral load ($q_0 = 0$) is subjected to an increase dH of the horizontal force H (figure), its end support B will displace to the right by:

$$du = dH \cdot \frac{l}{EA}$$

  A lateral load $q_0 > 0$ on the cable causes a sag, $q_0 l^2/(8H)$, and the displacement of support B due to dH for $q_0 > 0$ can be approximated using the cable equation (see Marti, 2012):

$$du = dH\left(\frac{l}{EA} + \frac{q_0^2 l^3}{12H^3} \right)$$

- Comparing the two results, the axial stiffness of the laterally loaded cable, idealised as straight cable with the chord length can be expressed using an idealised modulus of elasticity:

$$E_i = \frac{E}{1 + \frac{q_0^2 l^2}{12H^3} EA} \qquad \rightarrow du = dH \cdot \frac{l}{E_i A}$$
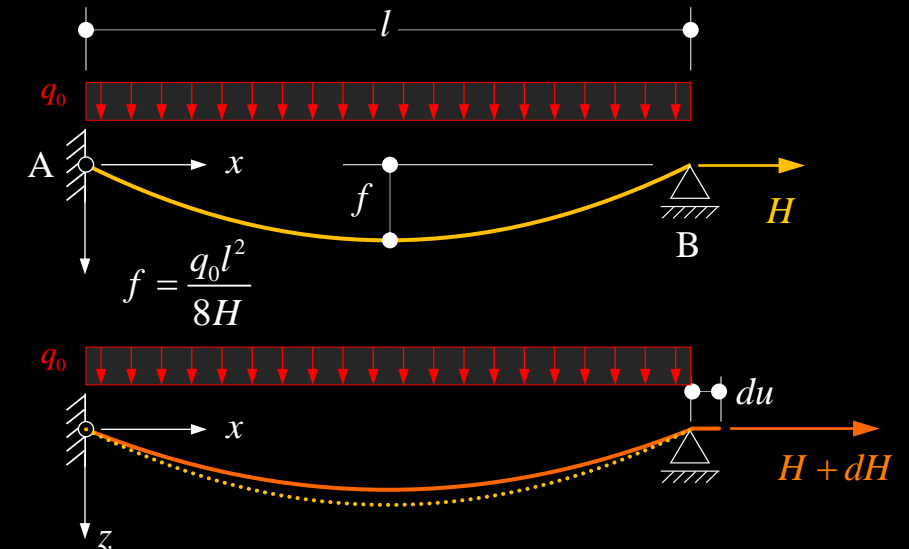
Cable-supported bridges – Axial stiffness of laterally loaded cables

- Similarly, for a cable at an angle α to the horizontal with a total weight G, one gets (see Marti, 2012), with S = force in direction of cable chord:

$$E_i = \frac{E}{1 + \dfrac{G^2 \cos^2 \alpha}{12 S^3} EA} \qquad \rightarrow ds = dS \cdot \frac{l}{E_i A}$$

known as *Ernst* Equation (see notes for source and further information).

- Using the specific weight γ of the cable (total cable weight / steel volume), the idealised modulus of elasticity can be rewritten:

$$G \approx \gamma \cdot A \cdot l, \quad \sigma = \frac{S}{A} \qquad \rightarrow E_i = \frac{E}{1 + \dfrac{\gamma^2 a^2}{12\sigma^3} E}; \qquad \frac{1}{E_i} = \frac{1}{E} + \frac{\gamma^2 a^2}{12\sigma^3}$$

- As seen from the plot on the right, the axial stiffness is significantly reduced in long cables, even if they are taut (high stress levels)

- The idealised modulus of elasticity above is valid at one specific stress level (tangent modulus). For more refined analyses, the following approximate secant stiffness between two stress levels can be used:

$$E_{sec} = \frac{E}{1 + \dfrac{\gamma^2 a^2}{24}\left(\dfrac{\sigma_1 + \sigma_2}{\sigma_1^2 \cdot \sigma_2^2}\right) E}; \quad \frac{1}{E_{sec}} = \frac{1}{E} + \frac{\gamma^2 a^2}{24}\left(\frac{\sigma_1 + \sigma_2}{\sigma_1^2 \cdot \sigma_2^2}\right)$$
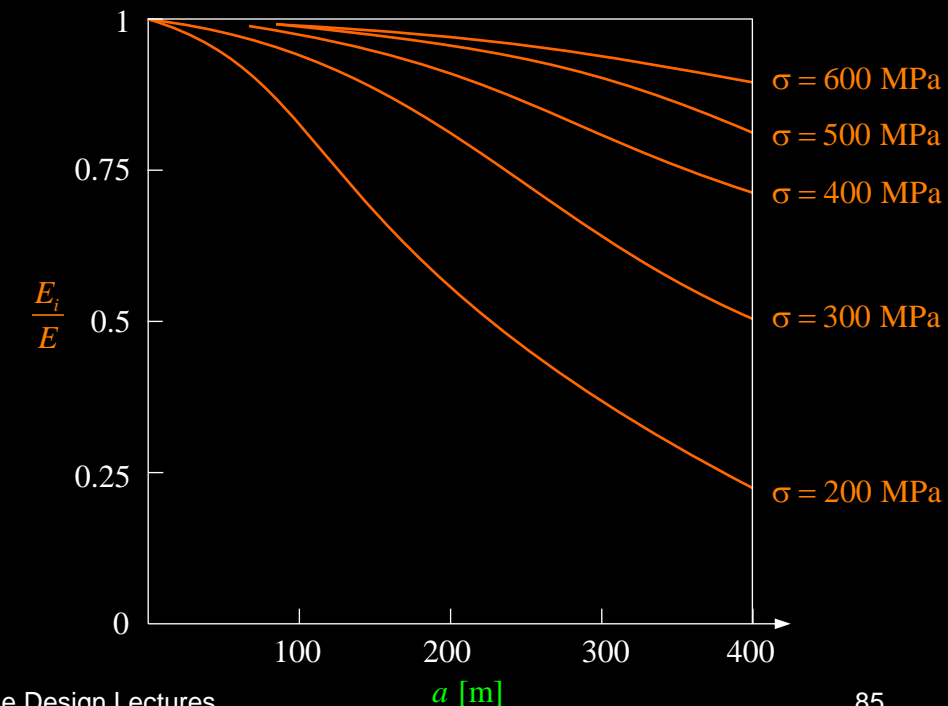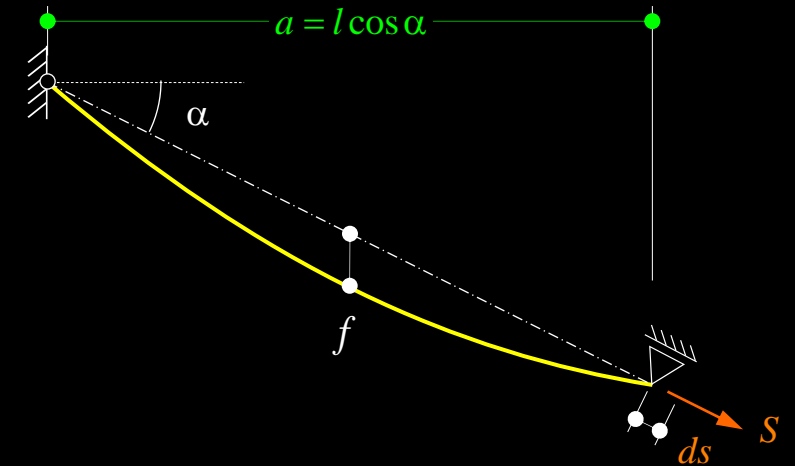
Cable-supported bridges – Axial stiffness of laterally loaded cables

- As seen from the plot on the previous slide, the reduction of the idealised modulus of elasticity is pronounced for long cables working at a low stress.

- In bridges, the vertical (rather than axial) stiffness of the stays is of primary interest. Considering a single stay cable inclined at an angle α, the cable force due to a load Q and the resulting cable elongation are

$$S = \frac{Q}{\sin \alpha} \qquad ds = \frac{Q}{\sin \alpha} \cdot \frac{l}{E_i A}$$

and assuming that the deck girder is axially rigid, the vertical displacement (using e.g. the Williot diagram) corresponds to

$$w = \frac{ds}{\sin \alpha} = \frac{Q}{\sin^2 \alpha} \cdot \frac{l}{E_i A}$$

- Hence, the vertical stiffness of the stay is

$$k_z = \frac{Q}{w} = \frac{E_i A}{l} \sin^2 \alpha = E_i A \cdot \frac{h^2}{l^3} \qquad \left(\frac{h}{l} = \sin \alpha \right)$$

- As the longest stays are typically also the flattest, their vertical stiffness is thus strongly reduced by the combined effect of sag (E_i), and inclination.

- The equations still neglect the difference between chord direction and cable inclination at the bottom anchorage, which is relevant for very low stress and large sag (erection), see notes on previous slide for details.
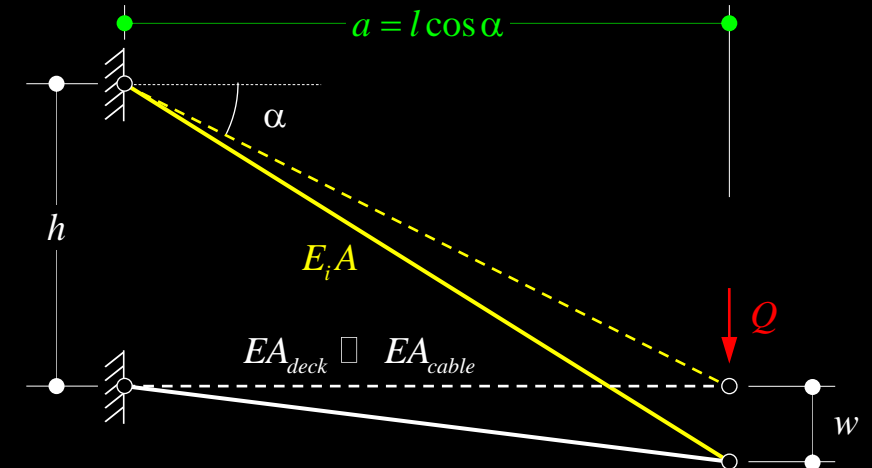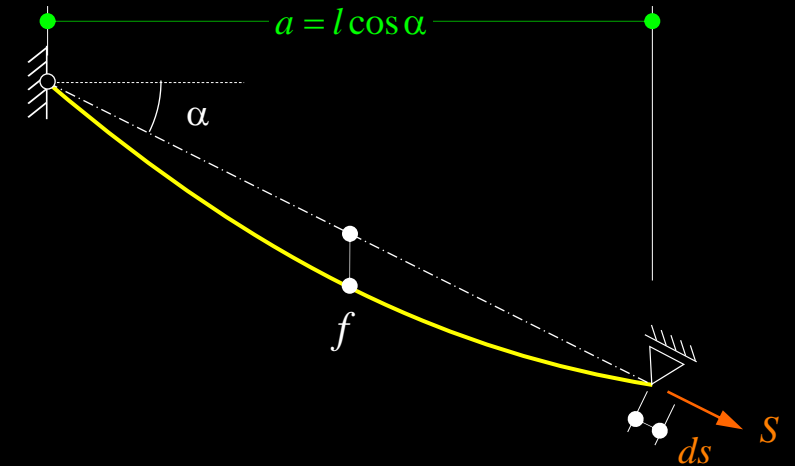
Cable-supported bridges

Common aspects – Static analysis of Cables

Combined cable-type and bending response

Cable-supported bridges – Common aspects: **Bending of cables**

- When analysing the global structural behaviour of cable-supported bridges, it is usually sufficient to neglect the bending stiffness of the cables – even in the case of stress-ribbons with a relatively stiff cross-section (see section on stress-ribbons).

- However, local bending of the cables (resp. stress ribbons) needs to be considered to verify
  - → fatigue stresses, particularly for stay cables
  - → serviceability of stress ribbons (crack widths, durability)

- The behaviour of stress-ribbons can be analysed by accounting for the combined cable-type and bending response. As outlined by Marti (Theory of Structures, 2013, Chapter 18.9), the differential equation

$$EIw'''' - \left(H + \Delta H\right)w'' = q - g\,\frac{\Delta H}{H} \qquad \left(H = H(g), \Delta H = \Delta H(q)\right)$$

with the solution

$$w = c_1 + c_2 x + c_3 \cosh(\lambda x) + c_4 \sinh(\lambda x) + w_{part} \qquad \left(\lambda = \frac{H + \Delta H}{EI}\right)$$

covers the entire spectrum from a pure bending response only ($\lambda = 0$), to a pure cable-type response ($\lambda \to \infty$). Note that it has been assumed in the derivation of the differential equation that the dead load g is carried by cable tension alone.

Stress-ribbon geometry used for illustrations on next slides (typical stress-ribbon footbridge)

Elevation

Cross-section

$EA_c^I = 21$ GN
$EI_c^I = 137$ MNm^2
$EA_p = 4$ GN
$EI_p = 1$ MNm^2
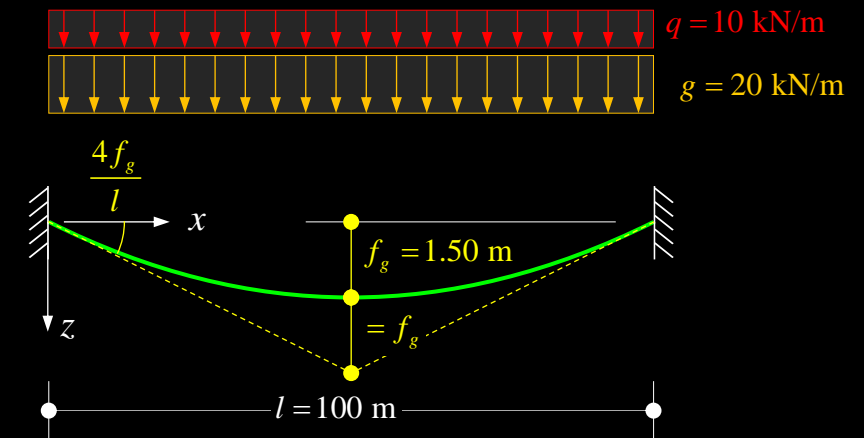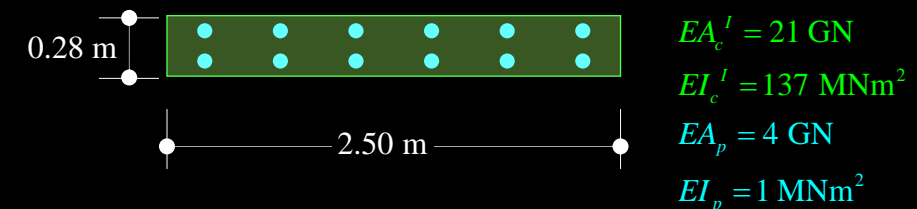
Cable-supported bridges – Common aspects: **Bending of cables**

- In cables – particularly stay cables and stress-ribbons – bending moments are caused by sag variations (due to load, imposed strains or dynamic effects), since the end anchorages are commonly fixed, rather than hinged.
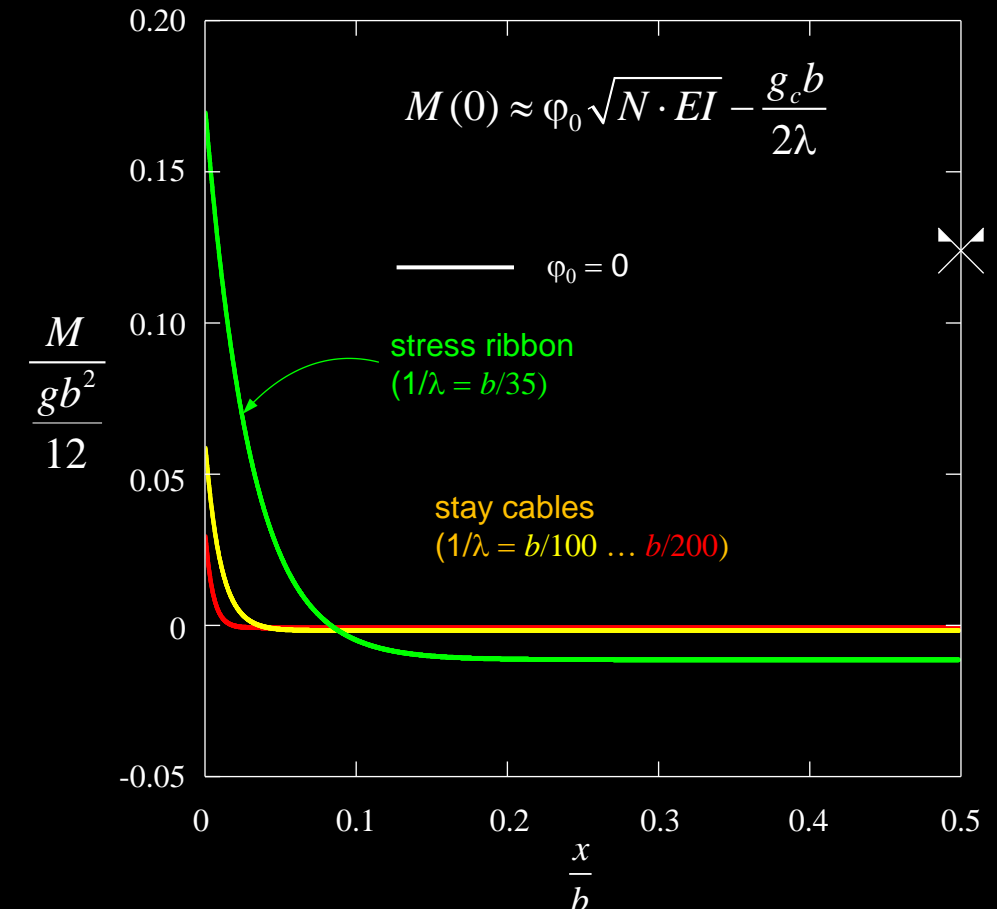
- Solving the differential equation given on the previous slide, one gets the following expression for the bending moments (Marti 2012, 19.9.2.2):

$$M(x) = \frac{g_c}{\lambda^2} + \left(\varphi_0 - \frac{g_c b}{2N}\right)\sqrt{N \cdot EI} \cdot \frac{\cosh\left[\lambda\left(\frac{b}{2} - x\right)\right]}{\sinh\left(\lambda\frac{b}{2}\right)} \quad \left(\lambda = \sqrt{\frac{N}{EI}}\right)$$

  where b = horizontal span and φ_0 = imposed end rotation of cable. The first term on the right side can usually be neglected.

- As illustrated in the figure for $\varphi_0 = 0$, the bending moments
  - $\rightarrow$ range from 5…20% of those in a clamped girder for $\varphi_0 = 0$
  - $\rightarrow$ are localised near the end anchorages (particularly for low bending stiffness, as is the case in stay cables)

- If the end rotation φ_0 is set to that of a hinged cable under dead load, as usual, variable loads and end rotations still cause bending moments.
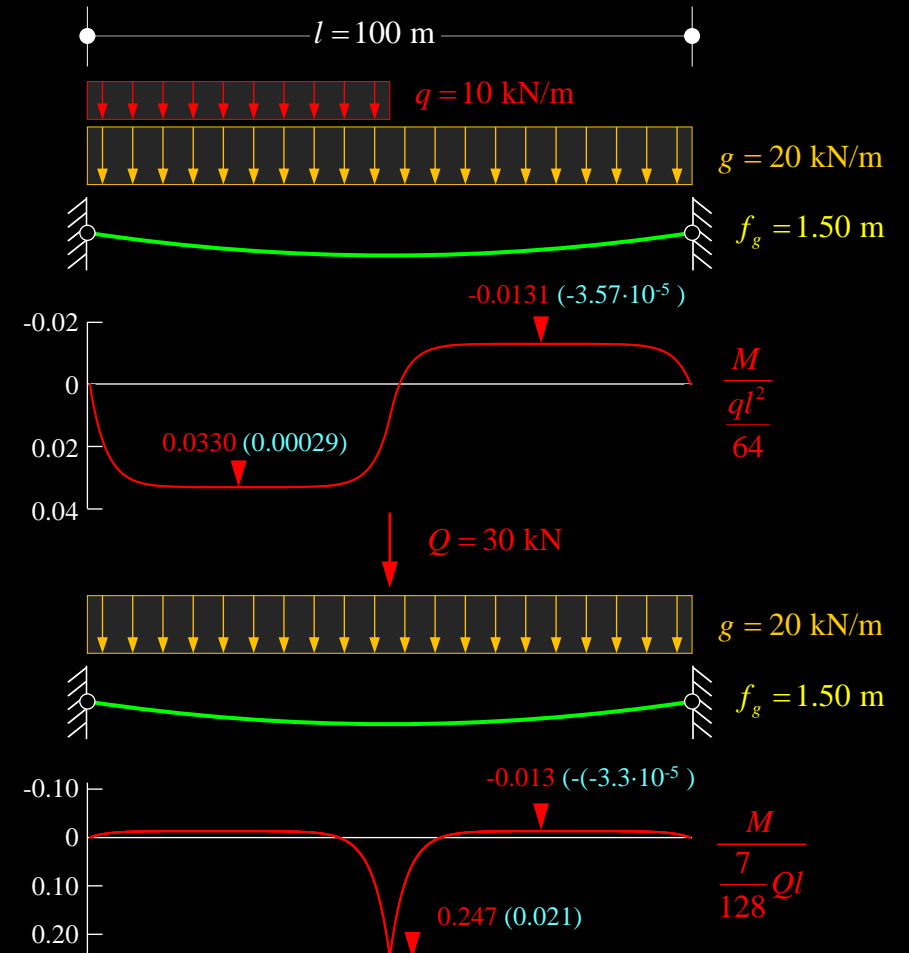
Bending moments due to dead load
(cable end rotation $\varphi_0 = 0$)

$$M(0) \approx \varphi_0 \sqrt{N \cdot EI} - \frac{g_c b}{2\lambda}$$

$\varphi_0 = 0$

stress ribbon
($1/\lambda = b/35$)

stay cables
($1/\lambda = b/100 \ldots b/200$)

Cable-supported bridges – Common aspects: **Bending of cables**

- In stress-ribbons, relevant bending moments are also caused by traffic loads. Analytical solutions are available e.g. for the cases shown on the right:
  - → asymmetric traffic load on half a span (Marti 2012, 18.9.3.2)
  - → concentrated load at midspan (Marti 2012, 18.9.3.3)

- The figures illustrate the bending moments for a typical stress-ribbon (cross-section see previous slides). It can be seen that the bending moments are 1-2 orders of magnitude smaller than in a beam of equal span, and also significantly smaller than in a two-hinged arch (where they would amount to $ql^2/64$ and $7Ql/128$, respectively). Due to the high slenderness of the stress ribbon, they are, however, still not negligible.

- The bending moments that would occur if only the cables were active (concrete as weight), whose values are indicated in brackets, are another order of magnitude smaller.

- For general loading, geometrically nonlinear analyses accounting for large deformations are required. Specialised software is recommended for such cases.

Bending moments under selected load configurations (normalised with M in a two-hinged arch under same load)

$l = 100$ m

$q = 10$ kN/m

$g = 20$ kN/m

$f_g = 1.50$ m

-0.0131 (-3.57·10⁻⁵)

0.0330 (0.00029)

$\dfrac{M}{\dfrac{ql^2}{64}}$

$Q = 30$ kN

$g = 20$ kN/m

$f_g = 1.50$ m

-0.013 (-(-3.3·10⁻⁵)

0.247 (0.021)

$\dfrac{M}{\dfrac{7}{128}Ql}$

Cable-supported bridges

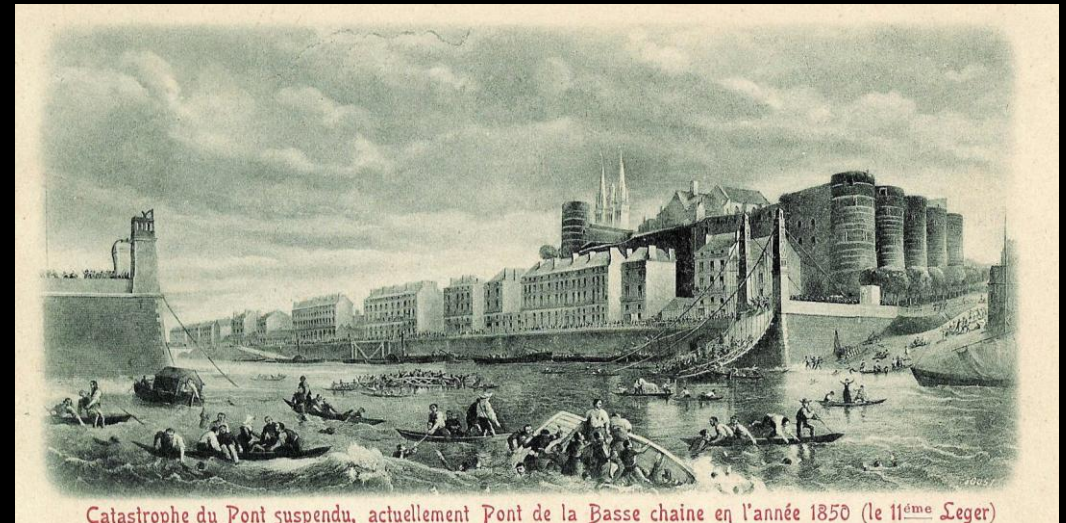Common aspects – Dynamic effects

Cable-supported bridges

Common aspects – Dynamic effects
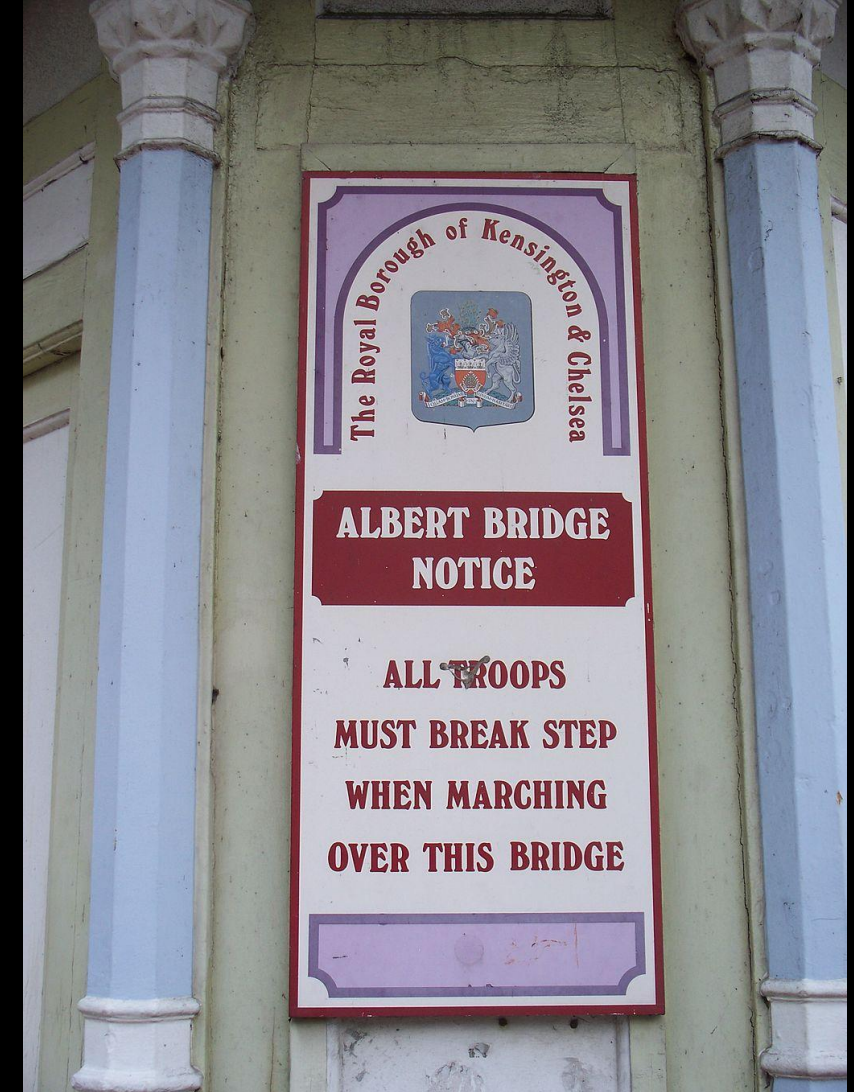Pedestrian-induced oscillations

Cable-supported bridges – Dynamic effects: Pedestrian-induced oscillations

- Many early suspension bridges suffered from excessive oscillations due to traffic or wind, and several unfortunately collapsed.

- For example, the following bridges collapsed due to oscillations caused by pedestrians:

  - According to some sources (Stiftung Deutsches Technikmuseum Berlin Historisches Archiv), the Saalebrücke in Nienburg (chain-stayed bridge, l = 80 m, Christian Gottfried Heinrich Bandhauer, 1825) collapsed due to rhythmic movements of the singing crowd on the bridge.

  - The Broughton chain suspension bridge (l = 44 m, S. Brown, 1826), collapsed in 1831 by a detachment of 74 soldiers marching in step. 20 soldiers were injured, six severely.

  - The Angers wire-cable suspension bridge (Pont de la Basse-Chaîne, l = 102 m, J. Chaley, 1838), presumably collapsed in 1850 by a combination of corrosion in anchor cables and resonance caused by a battalion of almost 800 soldiers crossing the bridge during a thunderstorm with strong wind (not walking in step, but involuntarily moving in tune, known as "lateral lock-in" today). 226 soldiers died.

75 ANGERS (M.-et-L.). — Ancien Pont suspendu de la Basse-Chaîne avant la Catastrophe du 16 avril 1850. — LL.

Catastrophe du Pont suspendu, actuellement Pont de la Basse chaine en l'année 1850 (le 11ème Léger)

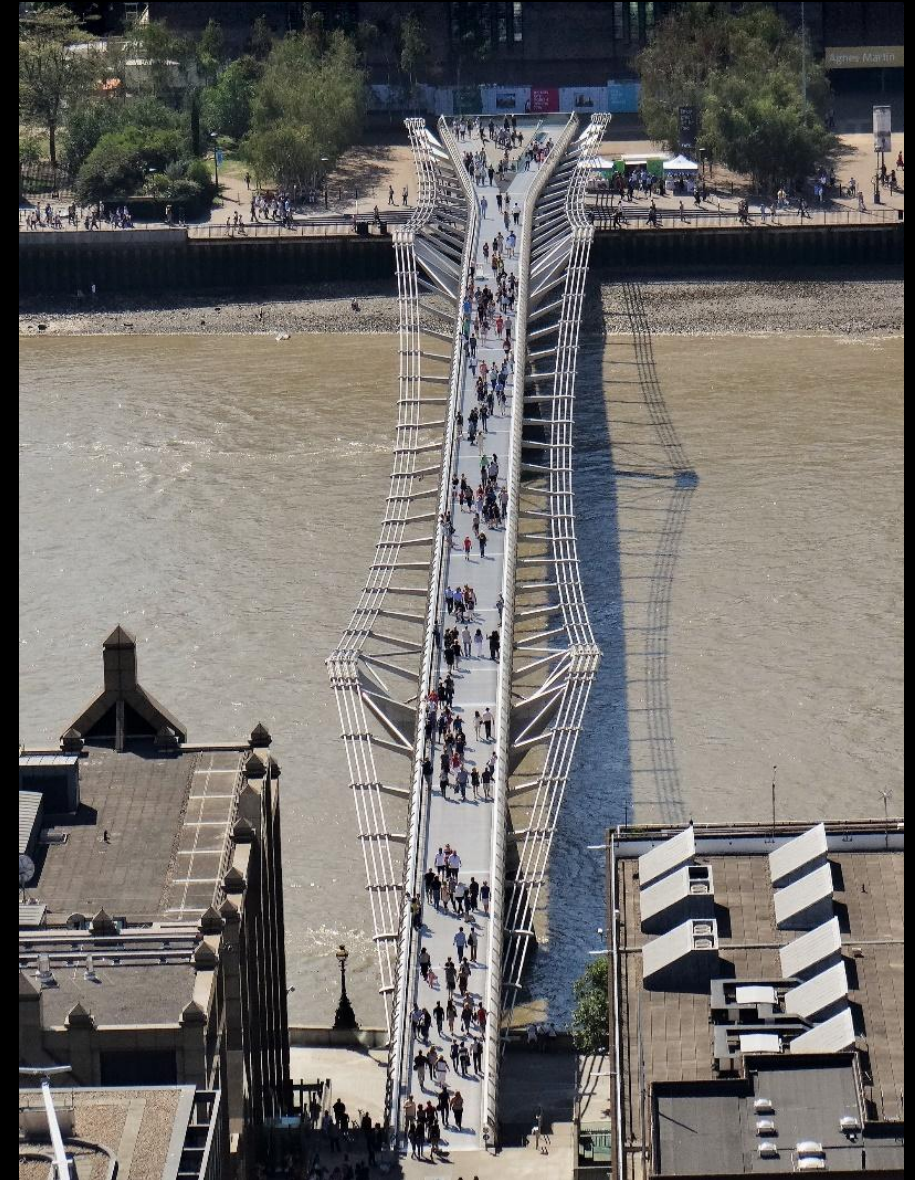# Cable-supported bridges – Dynamic effects: Pedestrian-induced oscillations

- Many lightweight bridges experience excessive oscillations under pedestrian load. Evidently, many people walking in step increase the amplitude of the vibrations.

- The Albert Bridge in London (1873) is one of many examples where troops are advised to break step to avoid problems. In Switzerland, the same rule holds e.g. for the pedestrian suspension bridge under the SBB Aarebrücke in Brugg, frequently used by soldiers in the nearby barracks.
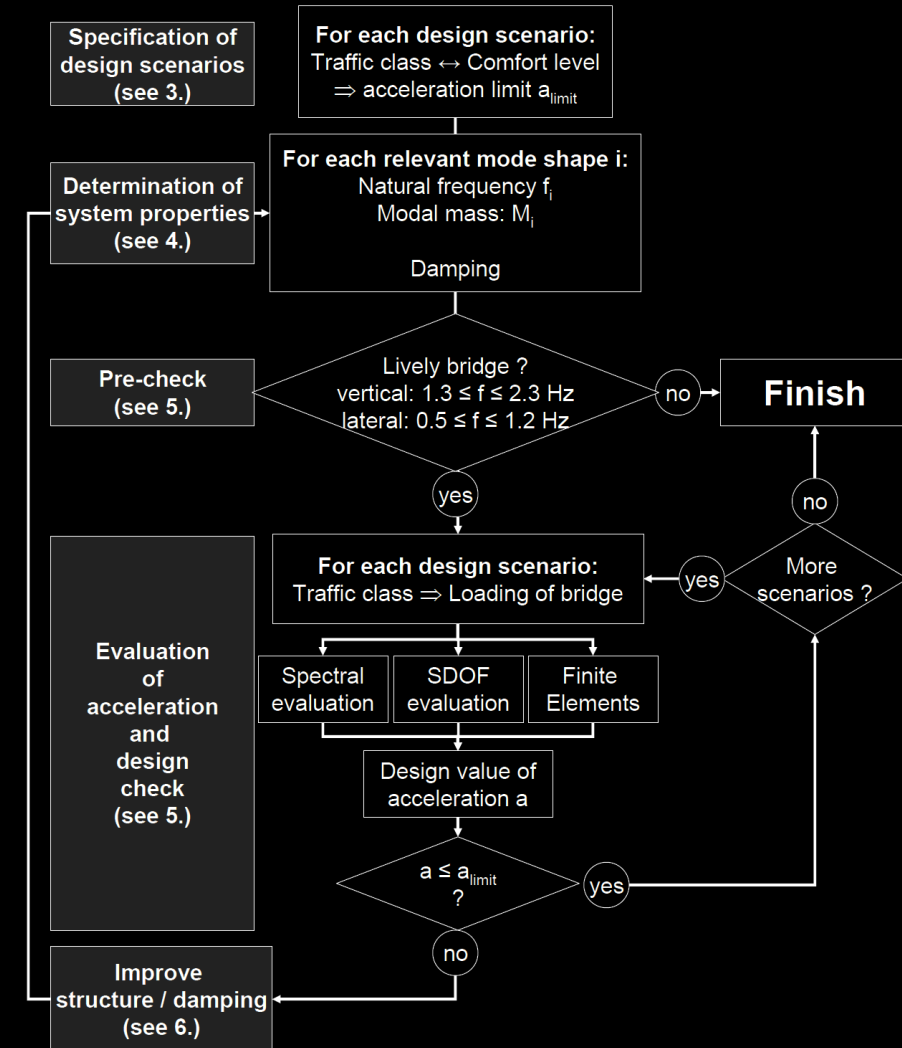
Cable-supported bridges – Dynamic effects: Pedestrian-induced oscillations

- Pedestrian-induced oscillations are not unique to cable-supported bridges, but may occur in any lightweight structure.

- Such oscillations, including lateral oscillations, were studied intensely by Prof. Hugo Bachmann at ETH Zurich in the 1980s. In a book published by IABSE 1987 (see notes), he had recommended to avoid the following frequency ranges in footbridges (or carry out detailed vibration analyses):
  - → vertical oscillations: 1.6…2.4 Hz   and 3.5…4.5 Hz
  - → lateral oscillations: 0.8…1.2 Hz   and 1.6 …2.4 Hz

- Bachmann had also already investigated the effect of the number of people simultaneously crossing a bridge (excitation, added mass), and their potential synchronisation with movements.

- Despite this knowledge, the Millennium Bridge in London (Arup / Foster Partners / A. Caro) was built in 2000 with the first two lateral eigenfrequencies in the critical range around 1 Hz (sources see notes).

- The bridge had to be evacuated at the opening due to severe lateral oscillations. The "wobbly bridge" was then retrofitted with 37 viscous dampers and 52 tuned mass dampers (cost: ca. 5 million pounds).

- The designers launched a research programme to study this problem, that "had not yet been incorporated into the relevant bridge design codes" (see notes).

Cable-supported bridges – Dynamic effects: Pedestrian-induced oscillations

- Current bridge design codes still primarily rely on frequency range recommendations similar to those of Bachmann, see e.g. SIA 260.

- Observing these recommendations, excessive oscillations due to pedestrian traffic are avoided, since the dominant eigenmodes of the bridge will have eigenfrequencies that differ sufficiently from the frequencies excited by pedestrians.

- These frequency ranges, particularly if higher natural frequencies are aimed at, are difficult to observe in footbridges (one might claim that any elegant footbridge is susceptible to oscillations).

- However, eigenfrequencies in the critical range need not necessarily cause problems, particularly if sufficient damping is provided – which is difficult to quantify in the design stage, though.

- Hence, as indicated in the figure (source see notes), if critical frequencies are present, it is recommended to
  - carry out dynamic analyses and (since damping is uncertain)
  - provide space for installing tuned mass dampers (Tilger) and/or viscous dampers in case oscillations should prove excessive

- For more details, see lecture *Structural Dynamics and Vibration Problems*

Cable-supported bridges – Dynamic effects: Pedestrian-induced oscillations

- Current bridge design codes still primarily rely on frequency range recommendations similar to those of Bachmann, see e.g. SIA 260.

- Observing these recommendations, excessive oscillations due to pedestrian traffic are avoided, since the dominant eigenmodes of the bridge will have eigenfrequencies that differ sufficiently from the frequencies excited by pedestrians.

- These frequency ranges, particularly if higher natural frequencies are aimed at, are difficult to observe in footbridges (one might claim that any elegant footbridge is susceptible to oscillations).

- However, eigenfrequencies in the critical range need not necessarily cause problems, particularly if sufficient damping is provided – which is difficult to quantify in the design stage, though.

- Hence, as indicated in the figure (source see notes), if critical frequencies are present, it is recommended to

  - carry out dynamic analyses and (since damping is uncertain)
  - provide space for installing tuned mass dampers (Tilger) and/or viscous dampers in case oscillations should prove excessive

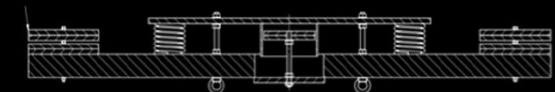- For more details, see lecture *Structural Dynamics and Vibration Problems*

Birskopfsteg Basel (zpf Ingenieure, oscillations already anticipated in design → 2 tuned mass dampers provided)

Very slender and elegant footbridge (h/l = 1/73)

Vertical Eigenfrequencies critical (0.9/2.9/3.9 Hz)

→ tuned mass dampers planned from beginning (located inside the steel box girder):

Cable-supported bridges

Common aspects – Dynamic effects
Wind-induced oscillations

Cable-supported bridges – Dynamic effects: Wind-induced oscillations

Introduction

- As outlined in the section "Historical Perspective", many early suspension bridges suffered from excessive oscillations also due to aerodynamic effects.

- The table on the right shows an overview of suspension bridges affected by wind-induced oscillation problems requiring stiffening measures in the best case, and leading to collapse in the worst.

- At the end of the 19th century, these problems were well known, due to the frequent problems with suspension bridges. John Roebling provided stays and stiff trusses in his suspension bridges (and retrofitted others) in order to prevent wind-induced oscillations.

- However, at the beginning of the 20th century, using the newly established deflection theory, the leading suspension bridge experts (Othmar Ammann, David Steinman, Leon Moisseiff, …) designed ever more slender suspension bridges.

Year	Bridge	Span	Incident
1818	Dryburgh Abbey Bridge	79	collapse
1821	Union Bridge	137	oscillations
1834	Lahnbrücke Nassau	75	collapse
1836	Brighton Chain Pier	78	collapse
1838	Montrose Bridge	131	collapse
1839	Menai Straits Bridge	176	partial failure
1852	Roche-Bernard Bridge	198	collapse
1854	Wheeling Bridge	310	collapse
1854	Queenston-Lewiston Bridge	259	collapse
1889	Niagra-Clifton Bridge	386	collapse
1895	Pont du Gottéron	151	partial failure
1937	Fyksesund Bridge	230	oscillations
1937	Golden Gate Bridge	1'280	oscillations
1938	Thousand Islands Bridge	240	oscillations
1939	Deer Isle Bridge Bridge	329	oscillations
1939	Bronx-Whitestone Bridge	701	oscillations?
1940	Tacoma Narrows Bridge	853	collapse

Cable-supported bridges – Dynamic effects: Wind-induced oscillations

Introduction

- Even before the Tacoma Narrows Bridge collapsed, severe wind-induced oscillations had been observed in several recently built, slender suspension bridges.

- Nonetheless, aerodynamic effects on bridges were only recognised and investigated in detail after the Tacoma Narrows Bridge collapse.

- Even if from today's perspective (see notes *), the mechanics of the failure were not fully understood at the time – aeroelasticity was a relatively new field of research even in aeronautics – the collapse marked a turning point in bridge design, particularly for cable-supported bridges:

  → Aerodynamic effects, which had received little attention before, became a major concern in long-span bridge design on that very day.

  → Today, wind tunnel testing for aerodynamic effects on long-span and/or slender bridges is common.

Cable-supported bridges – Dynamic effects: Wind-induced oscillations

Introduction

- Several slender suspension bridges from the 1930s were retrofitted after the Tacoma Narrows bridge collapse, based on the new knowledge. This and the next slides show a few examples.

- A lower deck bracing, forming a torsionally stiff truss girder, was installed in the Golden Gate Bridge (1937, span 1281 m), yet only in 1953. Comparing the slenderness with that of other bridges (particularly the Tacoma Narrows Bridge), an immediate stiffening indeed did not seem urgent:

Bridge	width/span	depth/span
Tacoma Narrows (collapsed)	1 / 72	1 / 350
Tacoma Narrows (rebuilt)	1 / 46	1 / 112
Golden Gate	1 / 47	1 / 168
George Washington, one deck	1 / 33	1 / 355
George Washington, two decks	1 / 33	1 / 120
Bronx-Whitestone	1 / 31	1 / 209

Cable-supported bridges – Dynamic effects: Wind-induced oscillations

Introduction

- The Bronx-Whitestone bridge (1939, span 701 m, right) was stiffened with stays and additional truss girders, reducing the slenderness to h/l = 1/91). In 2003, aerodynamic fairings were installed and the trusses removed, recovering the initial elegance.

- The Fyksesund Bridge (1937, span 230 m, bottom), was stiffened by bottom stays in 1945.

bottom stays
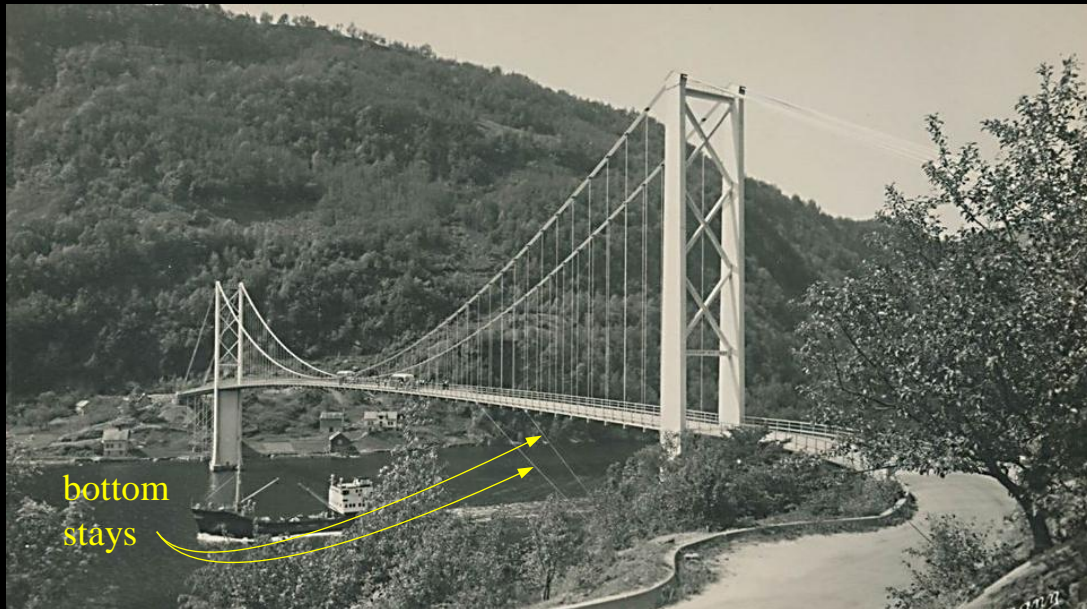
Cable-supported bridges – Dynamic effects: Wind-induced oscillations

Wind velocities and dynamic pressure

- Design of structures against wind load is based on a reference wind speed. SIA 261 uses the peak velocity, including gusts of a few seconds, measured 10 m above ground on a free field, with a return period of 50 years. Other codes are based on different reference values, and calculation of wind loads must not be mixed.

- Due to the surface roughness, the design wind speed varies depending on the terrain conditions and increases with the height above ground z, reaching a limit value at $z = 300\ldots500$ m).

- The dynamic pressure (Staudruck) q caused by a wind velocity u is:

$$q = \frac{\rho u^2}{2} \quad \left(\rho = \text{air density} \approx 1.2\, \frac{\text{kg}}{\text{m}^3} \right)$$

- For static analyses, only $q(u)$ is needed. For dynamic analyses – e.g. buffeting – the wind speed needs to be decomposed into
  $\rightarrow$ a time-constant mean wind speed u of constant direction
  $\rightarrow$ a superimposed, time variable turbulence part with horizontal, transverse and vertical components u_t v_t and w_t

- The turbulent components can be described in terms of turbulence intensity, integral length, and spectrum and are highly site-specific.

Characteristic values of dynamic pressure (SIA 261)
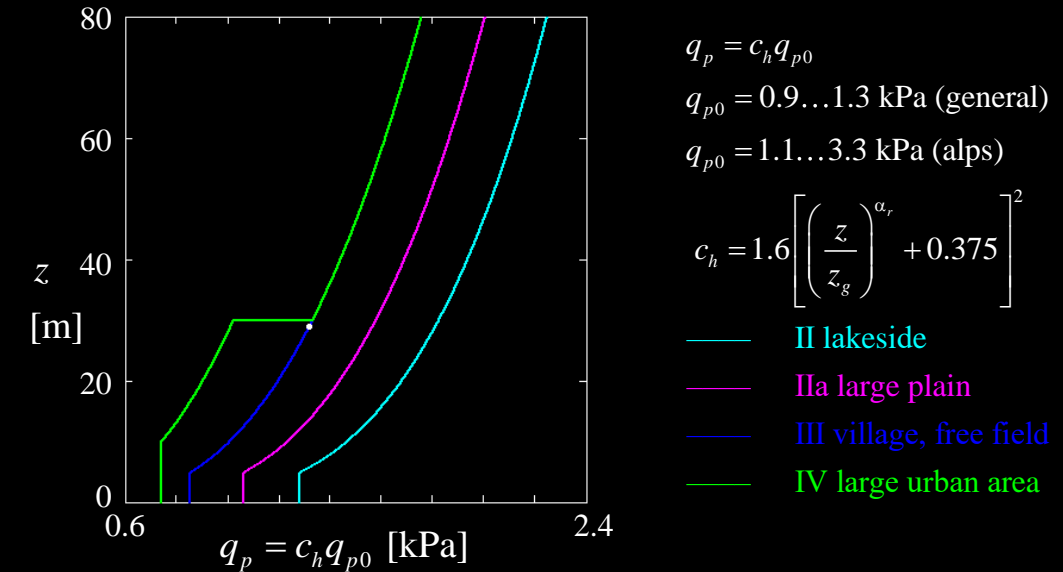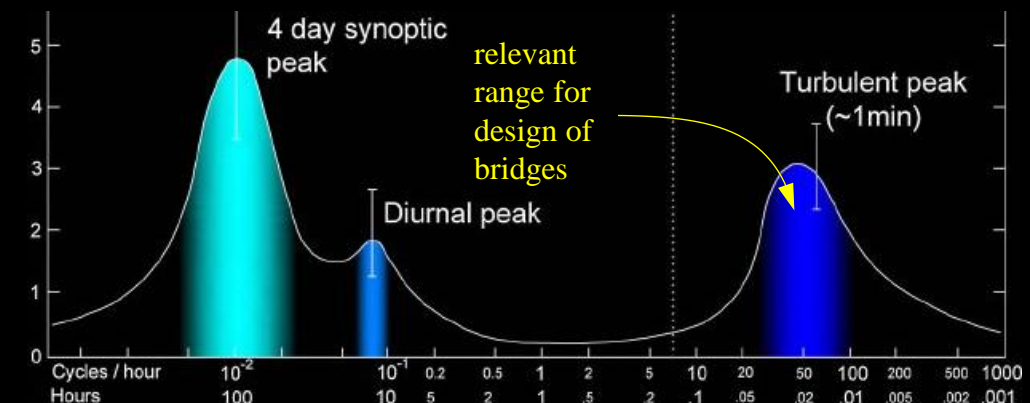
$$q_p = c_h q_{p0}$$
$$q_{p0} = 0.9\ldots1.3 \text{ kPa (general)}$$
$$q_{p0} = 1.1\ldots3.3 \text{ kPa (alps)}$$
$$c_h = 1.6\left[\left(\frac{z}{z_g}\right)^{\alpha_r} + 0.375\right]^2$$

— II lakeside
— IIa large plain
— III village, free field
— IV large urban area

Exemplary wind spectrum (power spectral density)

Cable-supported bridges – Dynamic effects: Wind-induced oscillations
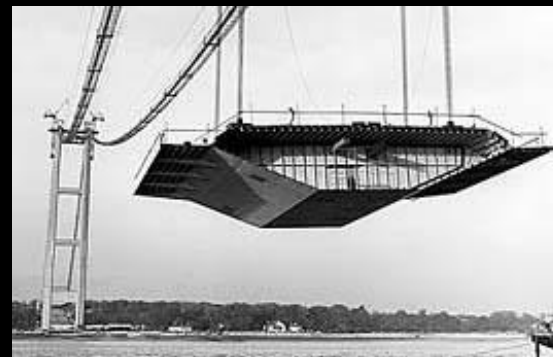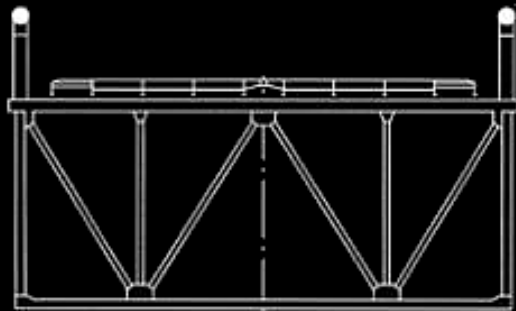
Aeroelasticity – Basic aspects

- Aerodynamic effects are relevant to tall, slender buildings and flexible long-span bridges.

- When studying these effects, the interaction of aerodynamic forces ($\rightarrow$ fluid dynamics) with the static and dynamic response ($\rightarrow$ structural mechanics) of the structure needs to be accounted for.

- This interaction is studied by aeroelasticity (Aeroelastik), a fundamental topic in aeronautical engineering.

- An in-depth treatment of aeroelasticity is beyond the scope of this lecture. In fact, even the most experienced designers of long-span bridges rely on specialised experts when designing for wind loads.

- However, some basic aspects are treated here to
  - $\rightarrow$ facilitate a basic understanding and awareness of potential problems caused by aerodynamic effects
  - $\rightarrow$ provide the common vocabulary required for communication with aerodynamic experts
  - $\rightarrow$ provide a basis for further study of this subject

Cable-supported bridges – Dynamic effects: Wind-induced oscillations
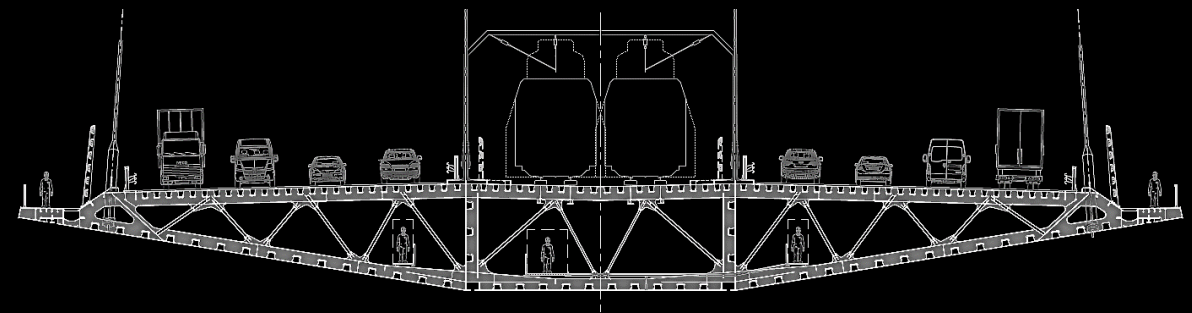
Aeroelasticity – Basic aspects

- Long-span bridge decks exposed to transverse wind can be analysed similarly to aircraft wings.

- This may be less obvious in the case of truss girders (bottom, Akashi-Kaikyo bridge cross-section), but is evident for streamlined modern bridge girders such as the deck of the Humber bridge (right).

Cable-supported bridges – Dynamic effects: Wind-induced oscillations

Aeroelasticity – Basic aspects

- Such streamlined girders (right: Third Bosporus Crossing) of modern long-span bridges indeed resemble airfoils (Tragflächen).

- Like the wings of an aircraft, bridge girders – as airfoils – may be damaged by torsional divergence and flutter, which are examined on the following slides.

- Further aerodynamic phenomena relevant to bridges, such as buffeting, vortex shedding and galloping are briefly outlined behind.

- Galloping is typical for bluff bodies (stumpfe Körper). Here, it has to be kept in mind that even streamlined bridge decks may become bluff by traffic on the bridge.

- Furthermore, other than in aircraft wings (where except in gliders, the air velocity is dominated by the cruise speed), wind on bridges is commonly turbulent and non-uniform in time and space.

Cable-supported bridges – Dynamic effects: Wind-induced oscillations

Aeroelasticity – Basic aspects

- The air flowing about an airfoil exerts stresses on its surface, that are nearly perpendicular to the surface (pressure >> friction).

- Integration of the stresses yields the following aerodynamic forces (per unit length) acting on the airfoil of width b ("chord length"):

  $f_D = c_D \cdot q \cdot b$ drag force (not referred to h as in structures)

  $f_L = c_L \cdot q \cdot b$ lift force

  $m_t = c_m \cdot q \cdot b^2$ aerodynamic moment (torque)

- Here, q is the dynamic pressure (Staudruck) corresponding to a turbulent airflow with uniform velocity u

  $$q = \frac{\rho u^2}{2} \quad \left(\rho = \text{air density} \approx 1.2 \, \frac{\text{kg}}{\text{m}^3} \right)$$

  and c_D, c_L and c_m are non-dimensional coefficients, depending on the angle of attack α, commonly determined from wind tunnel tests (see example in figure, for two different wing profiles).

- While aircraft wings are typically optimised to obtain high lift forces (resp. high lift/drag ratio), this is not desired in bridge girders.

Pressure (including friction) and resultant forces on an airfoil
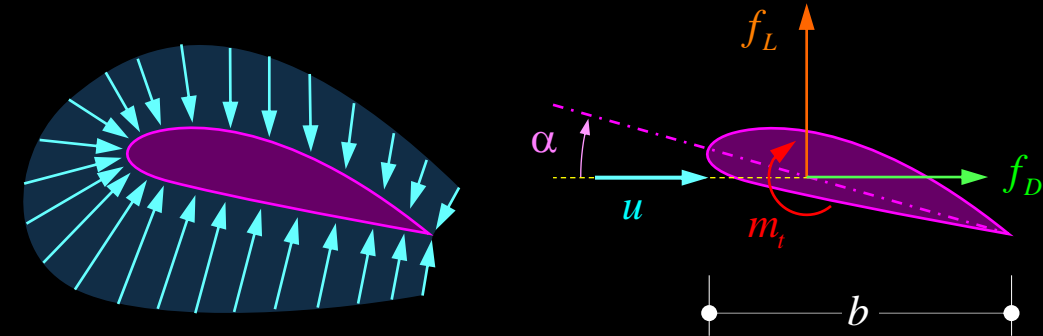
Lift and drag coefficients for standard wing profiles
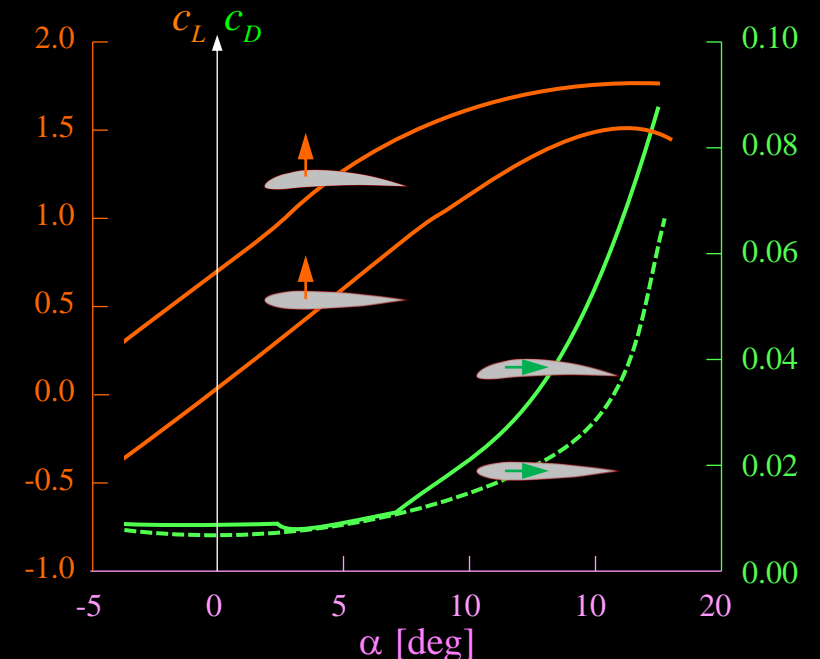
Cable-supported bridges – Dynamic effects: Wind-induced oscillations

Typical section model

- For a basic understanding of the phenomena of torsional divergence and flutter, only the aerodynamic lift force f_L and the aerodynamic torque m_t need to be considered, and it is sufficient to consider the simplified system of a "typical section":
  → flat plate rigid airfoil (width b) mounted on a stiff axis supported to the walls of a wind tunnel via springs representing the bending and torsional stiffness of the airfoil.

- The aerodynamic moment / torque (= coefficient c_m) depends on the position of the reference point. Commonly, the aerodynamic centre AC is chosen as reference (point about which the moment is independent of the angle of attack α) → $c_{m,AC}$ = constant.

- The total aerodynamic angle of attack α corresponds to an initial angle α_0 and the elastic twist of the axis α_e caused by the torque with respect to the shear centre. If the airfoil moves fast vertically (oscillation), α also depends on its velocity (relative velocity).

- With respect to the airfoil axis (shear centre) C, the resulting torque $m_{t,C}$ (all positive as shown in the figure) is

$$m_{t,C} = f_L \cdot e + m_{t,AC} = \left[c_L(\alpha) \cdot e + c_{m,AC} \right] \cdot b \cdot q$$

Typical section: Rigid, flat plate airfoil
(unit length section of an infinitely long wing)
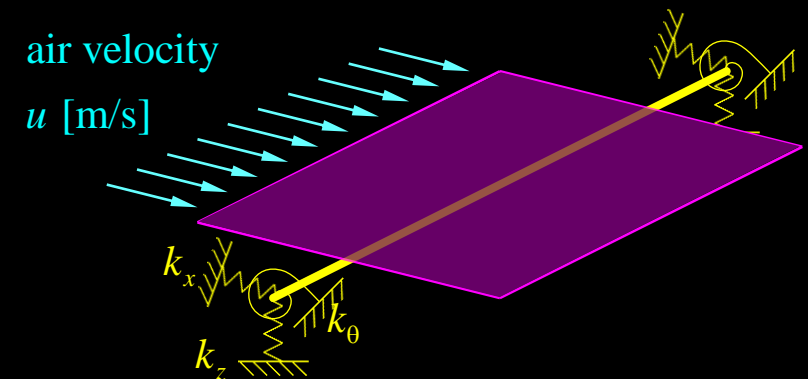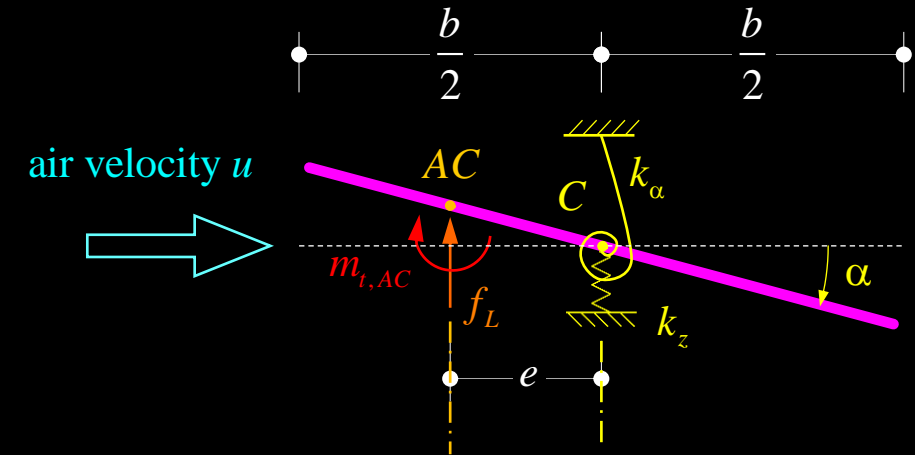
Cable-supported bridges – Dynamic effects: Wind-induced oscillations

Torsional divergence

- For a flat plate in two-dimensional incompressible subsonic flow, the lift coefficient and the position of AC are:

$$c_L = 2\pi \cdot \alpha \qquad e = \frac{b}{4}$$

and the resulting torque is thus:

$$m_{t,C} = \left(c_L \cdot e + c_{m,AC} \right) \cdot b \cdot q = \left(\pi\alpha b/2 + c_{m,AC} \right) \cdot b \cdot q$$

- This torque must be resisted by the torsional spring, i.e.

$$m_{t,C} = \left(\pi\alpha b/2 + c_{m,AC} \right) \cdot b \cdot q \overset{!}{=} k_\alpha \cdot \alpha_e$$

- Observing that $\alpha = \alpha_0 + \alpha_e$ and solving for the elastic twist α_e one gets:

$$\alpha_e = \frac{b \cdot q}{k_\alpha} \cdot \frac{\pi b \alpha_0 / 2 + c_{m,AC}}{1 - q\dfrac{\pi b^2}{2k_\alpha}}$$

- The elastic twist of the airfoil becomes infinite when the denominator is zero, i.e., for a dynamic pressure and corresponding wind speed

$$q\frac{\pi b^2}{2k_\alpha} = 1 \;\rightarrow\; q = \frac{2k_\alpha}{\pi b^2} = \frac{\rho u^2}{2} \qquad \rightarrow u_D = \frac{2}{b}\sqrt{\frac{k_\alpha}{\pi\rho}}$$

Typical section: Rigid, flat plate airfoil
(unit length section of an infinitely long wing)
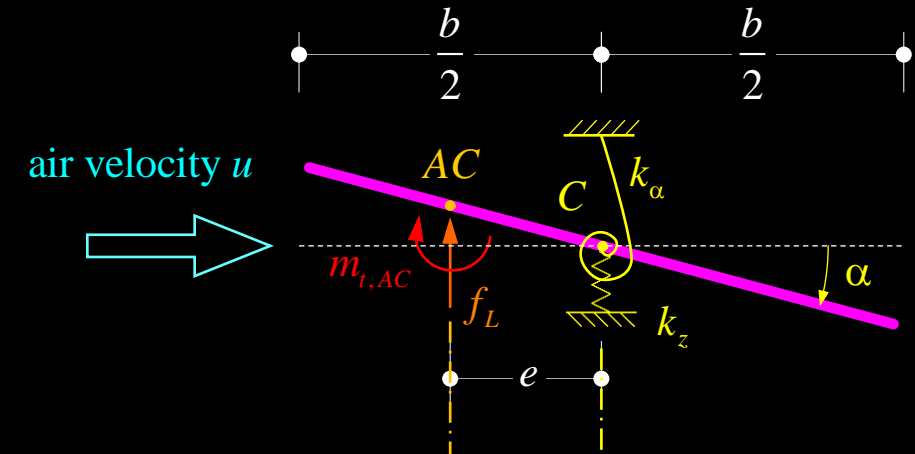
Wind tunnel test of a bridge section at NTNU

Cable-supported bridges – Dynamic effects: Wind-induced oscillations

Torsional divergence

- Hence, at the wind speed u_D, the flat plate airfoil would fail in torsion. This phenomenon is referred to as torsional divergence.

- For a general airfoil, the lift coefficient c_L differs from $2\pi\alpha$ and is not linear in α (and the distance e varies with α). Hence, the theoretical value of u_D derived above – that can be determined without wind tunnel testing – is of little use in design.

- However, for small variations of α, it may be approximated by the first order Taylor series

$$c_L = c_{L0} + \frac{\delta c_L}{\delta \alpha} \cdot \alpha$$

which yields the applied torque

$$m_{t,C} = c_{L0} \cdot b \cdot q \cdot e + \frac{\delta c_L}{\delta \alpha}\left(\alpha_0 + \alpha_e\right) \cdot b \cdot q \cdot e + c_{m,AC} \cdot b \cdot q \overset{!}{=} k_\alpha \cdot \alpha_e$$

and the elastic twist and critical wind speed (obtained by setting the denominator in the first equation equal to zero)

$$\alpha_e = \frac{b \cdot q}{k_\alpha} \cdot \frac{e\left(c_{L0} + \frac{\delta c_L}{\delta \alpha}\alpha_0\right) + c_{m,AC}}{1 - q \cdot \frac{\delta c_L}{\delta \alpha} \cdot \frac{be}{k_\alpha}} \qquad \rightarrow u_D = \sqrt{\frac{2k_\alpha}{\frac{\delta c_L}{\delta \alpha} \cdot \rho be}}$$

Typical section: Rigid, flat plate airfoil
(unit length section of an infinitely long wing)
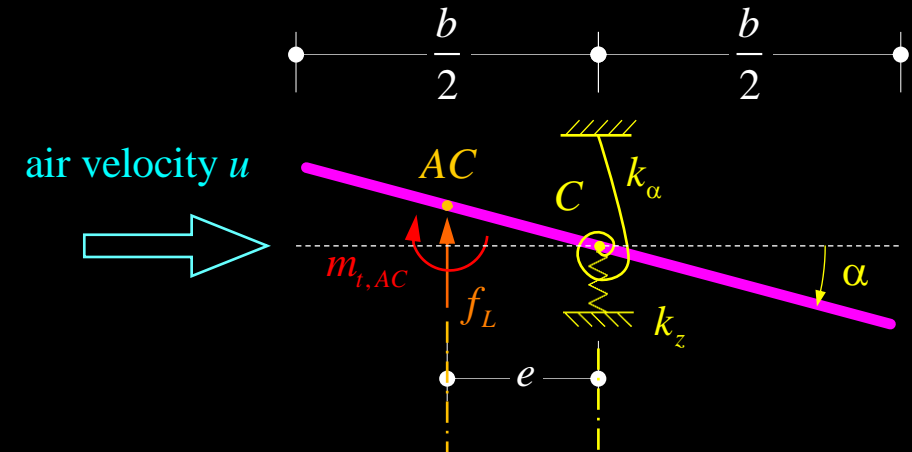
Wind tunnel test of a bridge section at NTNU

Cable-supported bridges – Dynamic effects: Wind-induced oscillations

Torsional divergence

- The distance e cannot directly be obtained from wind tunnel tests, since the coefficient $c_{m,AC}$ is unknown.

- In bridge aeroelasticity, the total aerodynamic moment coefficient c_t referred to the bridge axis (combining the above values and determined from wind tunnel tests) is thus commonly used

$$m_{t,C} = qb^2 c_t(\alpha) = \frac{\rho u^2}{2} b^2 c_t(\alpha)$$

- Using again the first-order Taylor series, and setting the denominator of the resulting equation for the elastic twist equal to zero, one gets the critical wind speed u_d for torsional divergence

$$m_{t,C} = \frac{\rho u^2}{2} b^2 \left(c_{t0} + \alpha \frac{\delta c_t}{\delta \alpha} \right) = k_\alpha \cdot \alpha_e$$

$$\rightarrow \alpha_e = \frac{\rho u^2}{2} \frac{b^2}{k_\alpha} \frac{c_{t0} + \alpha_0 \dfrac{\delta c_t}{\delta \alpha}}{1 - \dfrac{\rho u^2}{2} \dfrac{b^2}{k_\alpha} \dfrac{\delta c_t}{\delta \alpha}} \rightarrow u_D = \sqrt{\frac{2k_\alpha}{\rho b^2 \dfrac{\delta c_t}{\delta \alpha}}}$$

- Using plots of the coefficient c_t (and its derivative) determined from wind tunnel tests, the critical wind speed u_D can be determined.

Exemplary aerodynamic moment coefficient and derivative (including traffic effect [Pospisil et al., see notes])
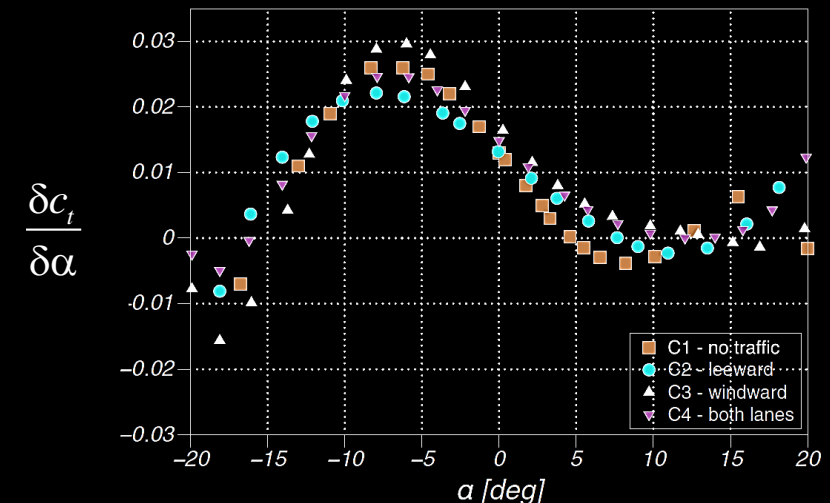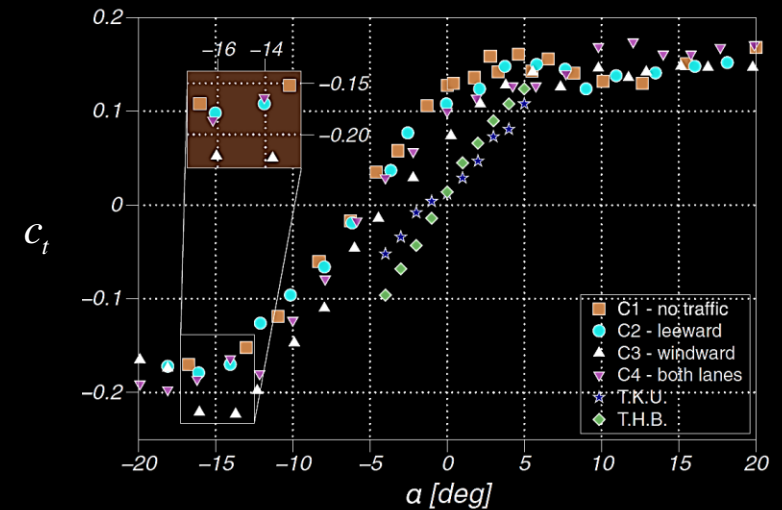
Cable-supported bridges – Dynamic effects: Wind-induced oscillations
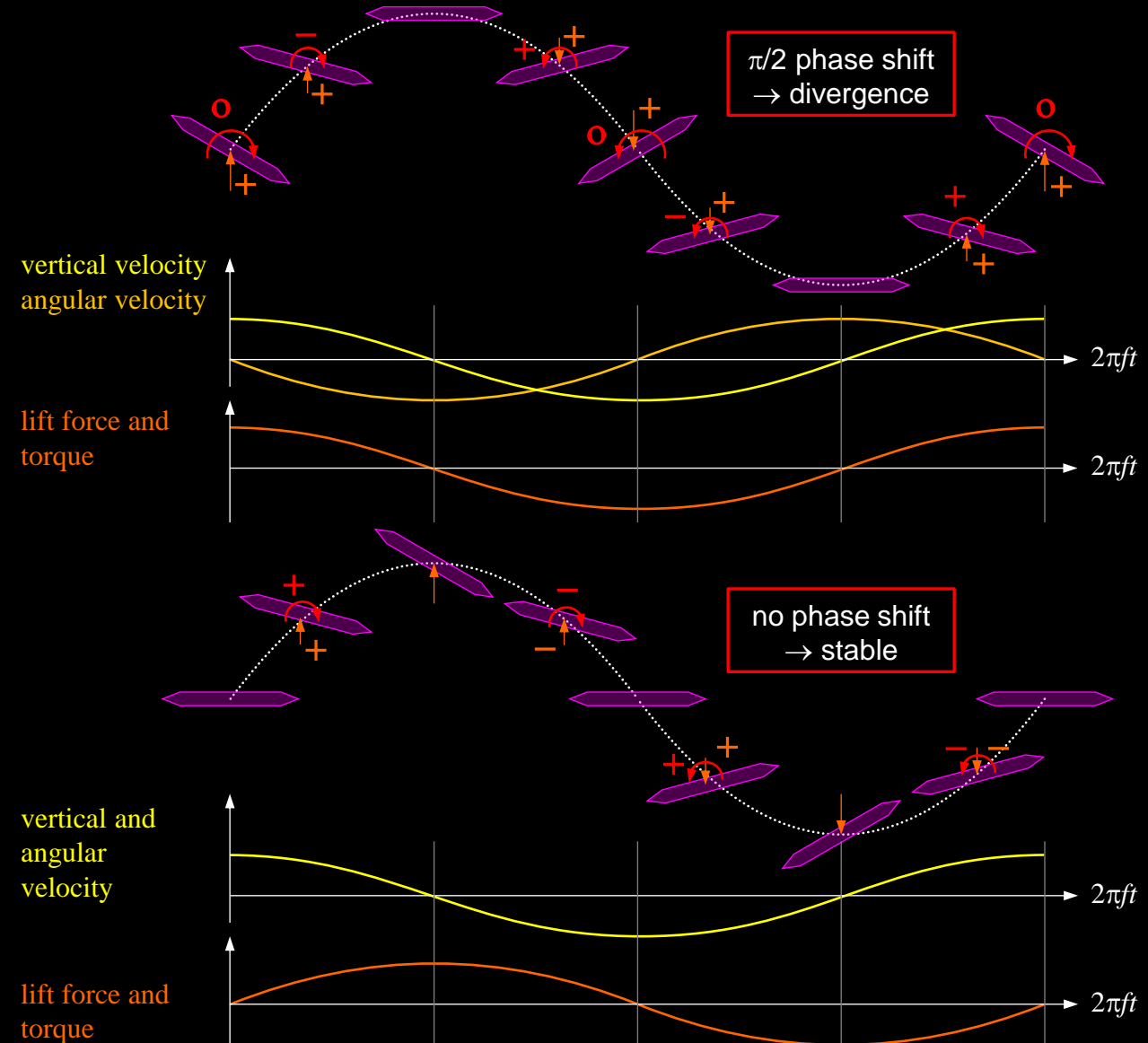
Coupled flutter

- Torsional divergence is usually not critical in bridges. However, the critical wind speed for torsional divergence u_D is useful for the analysis of coupled flutter as well.

- Coupled flutter, a divergent aeroelastic instability phenomenon occurring at the flutter velocity $u_f < u_D$, has the following characteristics:
  - simultaneous vertical and torsional harmonic oscillation
  - coupling of vertical and torsional oscillations due to nearly coinciding eigenfrequencies f_v and f_t
  - energy accumulation and, eventually, collapse

- The phenomenon of flutter is known in bridge engineering since the prominent Tacoma Narrows Bridge collapse by torsional flutter in 1940 (see section *historical perspective*).

Cable-supported bridges – Dynamic effects: Wind-induced oscillations

Coupled flutter

- Other than torsional or vertical flutter, coupled flutter (also referred to as "classic flutter") can be understood – in a simplified manner – by considering the energy balance of a bridge deck subjected to simultaneous vertical and torsional oscillations with equal frequency (figures).

- Energy is fed into the system when the signs of
  - vertical velocity and lift force
  - angular velocity and torque

  coincide; for opposite signs, energy is extracted.

- For a phase shift of $\pi/2$ (upper figure):
  - the work done by the aerodynamic torque cancels out
  - the work done by the lift force is always positive
  - $\rightarrow$ energy is accumulated in every cycle
  - $\rightarrow$ amplitude of oscillations increases correspondingly
  - $\rightarrow$ flutter instability

- Without a phase shift, the work done by lift force as well as torque cancel out (lower figures) $\rightarrow$ no instability

Cable-supported bridges – Dynamic effects: Wind-induced oscillations

Coupled flutter

- The torsional eigenfrequency f_t of cable-supported bridges with two cable planes is commonly larger than their vertical eigenfrequency f_v (see figure; for A-shaped pylons with inclined cable planes, the torsional frequency is even higher).

- However, the equivalent torsional stiffness, and hence f_t, is reduced by the aerostatic pressure, which increases with air velocity.

- For a flat plate airfoil, this leads to the flutter velocity

$$u_f = u_D \sqrt{1 - \frac{f_v^2}{f_t^2}} \leq u_D$$

where u_d = is critical wind speed for torsional divergence.

- The above equation is strongly simplified and neglects the dynamic nature of wind loads. A better approximation is given by Selberg's semi-empirical equation:
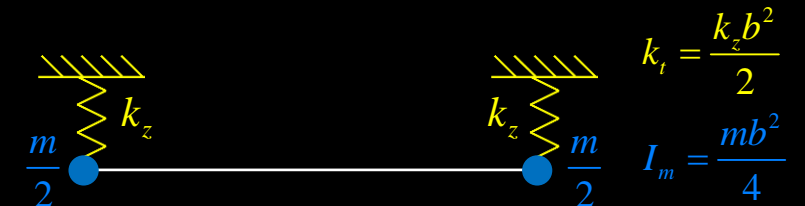
$$u_f = 0.52 u_D \sqrt{\left(1 - \frac{f_v^2}{f_t^2}\right) \cdot b \cdot \sqrt{\frac{m}{I_m}}} \leq u_D$$

where m is the mass of the girder per unit length and I_m is the corresponding mass moment of inertia (see figure).

Ratios of vertical and torsional eigenfrequencies for Bridges with two cable planes at their edges

$$k_t = \frac{k_z b^2}{2}$$

$$I_m = \frac{mb^2}{12}$$
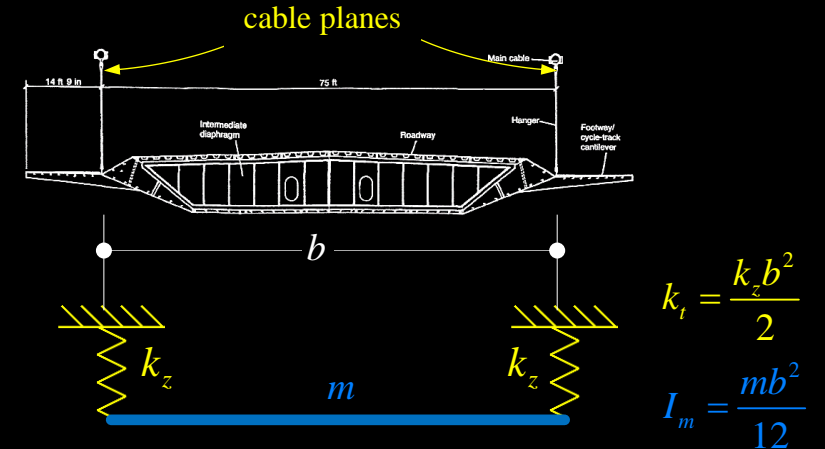
$$f_v = \frac{1}{2\pi}\sqrt{\frac{2k_z}{m}}, \quad f_t = \frac{1}{2\pi}\sqrt{\frac{k_t}{I_m}} = \frac{1}{2\pi}\sqrt{\frac{6k_z}{m}} \rightarrow \frac{f_t}{f_z} = \sqrt{3}$$

$$k_t = \frac{k_z b^2}{2}$$

$$I_m = \frac{mb^2}{4}$$

$$f_v = \frac{1}{2\pi}\sqrt{\frac{2k_z}{m}}, \quad f_t = \frac{1}{2\pi}\sqrt{\frac{k_t}{I_m}} = \frac{1}{2\pi}\sqrt{\frac{2k_z}{m}} \rightarrow \frac{f_t}{f_z} = 1$$

Cable-supported bridges – Dynamic effects: Wind-induced oscillations

Coupled flutter

- Selberg's simple equation is useful for first estimations of the flutter velocity as long as f_t/f_v > 1.5. As illustrated in the figure, the approximation is much better for the streamlined girder ("airfoil") than the bluff variants.

- A more realistic semi-empirical approximation of the critical flutter velocity of a bridge girder, originally proposed by Scanlan and Tomko (see notes for sources) is possible based on the formulation of the equations of motion of a two-dimensional section of a symmetrical bridge deck with linear viscous damping and restoring forces:

$$m\ddot{h} + d_h\dot{h} + k_h h = L_h$$
$$I_m\ddot{\alpha} + d_\alpha\dot{\alpha} + k_\alpha\alpha = M_\alpha$$
$$m\ddot{p} + d_p\dot{p} + k_p p = D_p$$

- In the above equations, "d" is been used for the viscous damping coefficients and k for the stiffnesses, to distinguish from aerodynamic coefficients. For the remaining notation (common in aeroelastic analysis of bridges), see figure.

-

Comparison of critical wind speed determined in wind tunnel tests and flutter velocity according to Selberg
[variants for Lillebaelt bridge, taken from Gimsing 2012)

U_{cr}/U_f = 0.43

U_{cr}/U_f = 0.62

U_{cr}/U_f = 0.91

U_{cr}/U_f = 0.77
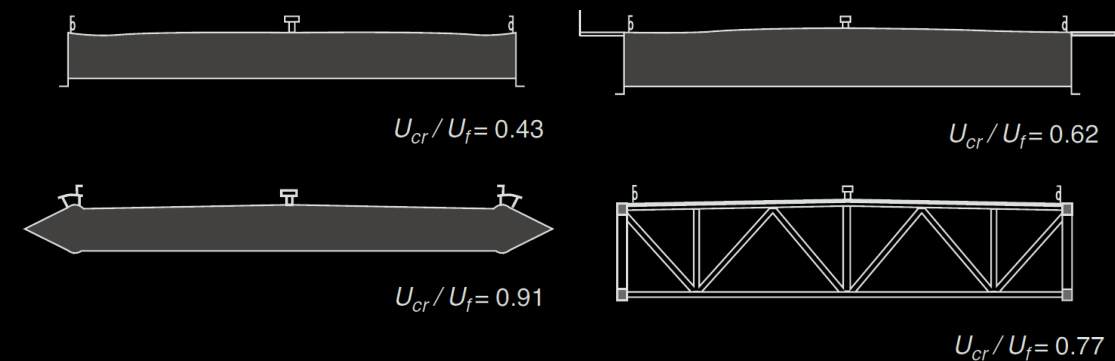
Two-dimensional bridge deck section – notation
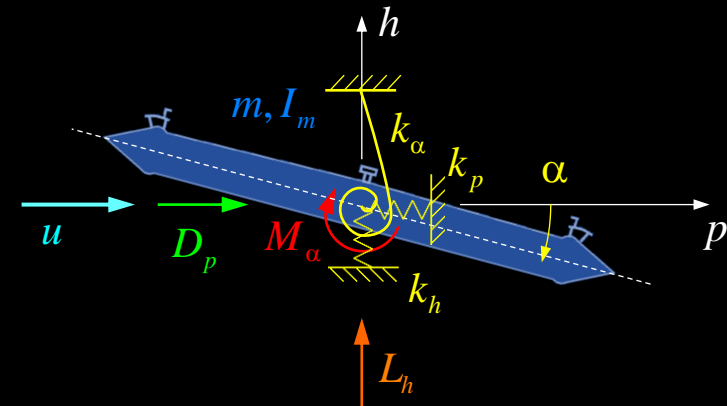
Cable-supported bridges – Dynamic effects: Wind-induced oscillations

Coupled flutter

- The aeroelastic forces can be determined using flutter derivatives, i.e., velocity-dependent force coefficients H^*_i, A^*_i and P^*_i (= relative changes of system damping and stiffness with regard to the wind speed variation)
(terms in grey = lateral motions often neglected)

$$\begin{Bmatrix} L_h \\ M_\alpha \\ D_p \end{Bmatrix} = \frac{\rho u^2 b}{2} \begin{bmatrix} \lambda_R H^*_1 & \lambda_R H^*_2 & \lambda_R^2 H^*_3 & \lambda_R^2 H^*_4 & \lambda_R H^*_5 & \lambda_R^2 H^*_6 \\ \lambda_R A^*_1 & \lambda_R A^*_2 & \lambda_R^2 A^*_3 & \lambda_R^2 A^*_4 & \lambda_R A^*_5 & \lambda_R^2 A^*_6 \\ \lambda_R P^*_1 & \lambda_R P^*_2 & \lambda_R^2 P^*_3 & \lambda_R^2 P^*_4 & \lambda_R P^*_5 & \lambda_R^2 P^*_6 \end{bmatrix} \cdot \begin{Bmatrix} \dot{h}/u \\ b\dot{\alpha}/u \\ \alpha \\ h/b \\ \dot{p}/u \\ p/b \end{Bmatrix}$$

with the so-called reduced frequency $\lambda_R = \dfrac{2\pi f b}{u} = \dfrac{\omega b}{u}$

- Based on plots of the flutter derivatives as functions of λ_R, obtained from wind tunnel tests, the flutter equations are obtained as follows:
  - assume that h, α and p are proportional to $e^{i\omega t}$ (harmonic oscillations)
  - insert expressions for h, α and p in equation of motion (previous slide) and set the determinant of the amplitudes of h, α and p to zero
  - $\rightarrow$ for each value of λ_R a complex equation in ω is obtained
  - $\rightarrow$ the lowest (nearly) real solution λ_{Rc} yields the flutter velocity: $\lambda_{Rc} = \dfrac{\omega_c b}{u} \rightarrow u_f = \dfrac{\omega_c b}{\lambda_{Rc}}$

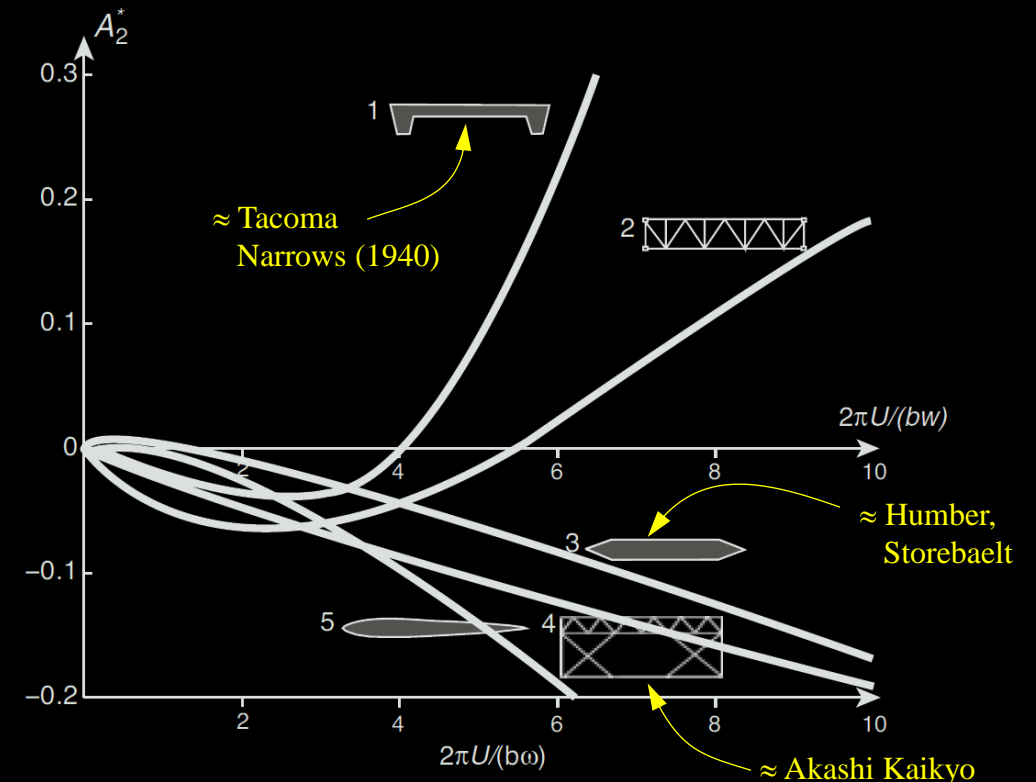Flutter derivatives of Kao-Ping Hsi bridge [Náprstek 2015]
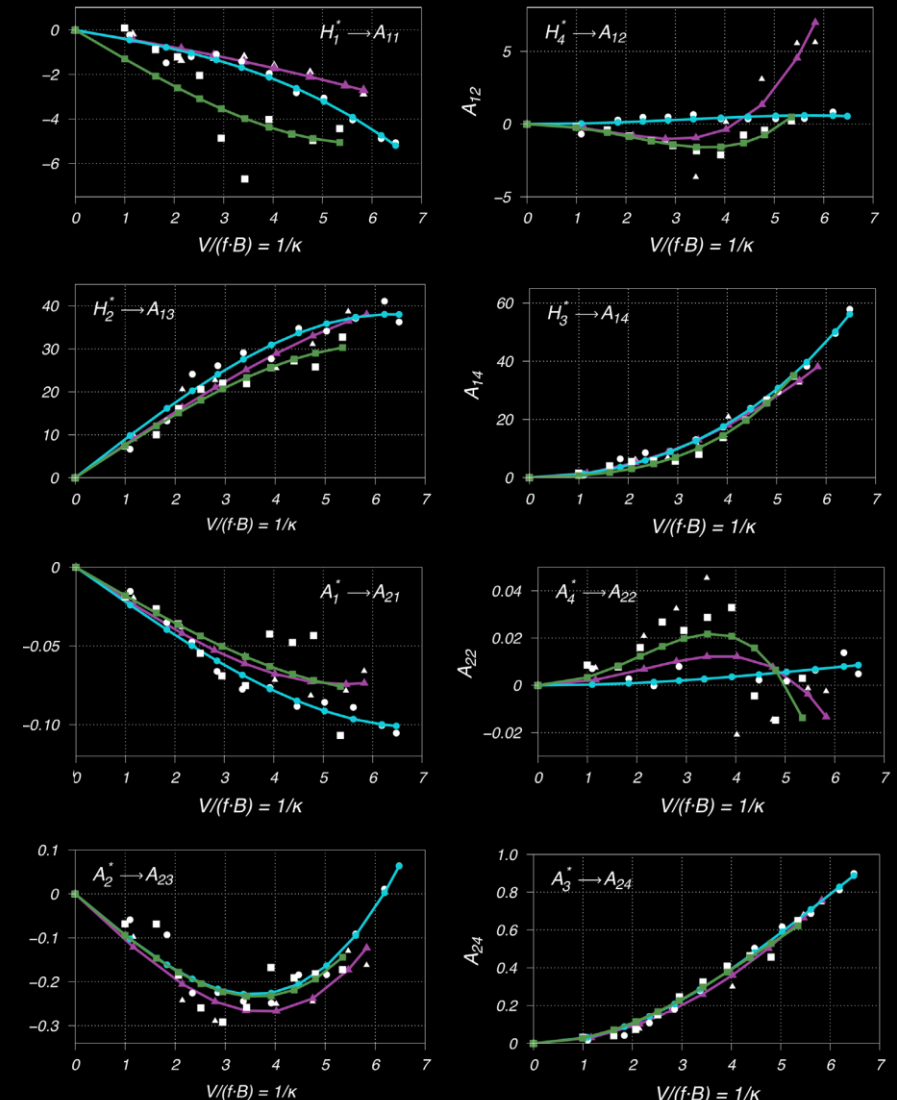
Cable-supported bridges – Dynamic effects: Wind-induced oscillations

Flutter derivatives ↔ Potential aeroelastic problems

- The flutter derivatives are also helpful to detect other potential aerodynamic problems, e.g. single mode flutter or oscillations caused e.g. by buffeting or vortex shedding.

- Here, the sign of the flutter derivatives associated with the velocity-proportional aeroelastic forces ($\dot{h}$, $\dot{\alpha}$) is particularly relevant, as a positive sign is equivalent to negative viscous damping = excitation:

  - $H_1^* > 0$ → susceptible to vertical oscillations ($\dot{h}$) (vertical flutter / "bending type galloping")

  - $A_2^* > 0$ → susceptible to torsional oscillations ($\dot{\alpha}$) (torsional flutter / "torsional galloping" → Tacoma Narrows collapse)

  - $H_2^* > 0$ and → coupling of $\dot{\alpha}$ and $\dot{h}$,
    $A_1^* > 0$ → danger of coupled flutter

- Realistic analysis of aerodynamic effects is complex and involves wind tunnel testing

  - → beyond "daily business" even for experienced designers
  - → consultation with experts common

Equations of motion and flutter (neglecting lateral components) and flutter derivative A_2^* for different bridge sections [Gimsing 2012]

$$\begin{Bmatrix} L_h = m\ddot{h} + d_h\dot{h} + k_h h \\ M_\alpha = I_m\ddot{\alpha} + d_\alpha\dot{\alpha} + k_\alpha\alpha \end{Bmatrix} = \frac{\rho u^2 b}{2} \begin{bmatrix} \lambda_R H_1^* & \lambda_R H_2^* & \lambda_R^2 H_3^* & \lambda_R^2 H_4^* \\ \lambda_R A_1^* & \lambda_R A_2^* & \lambda_R^2 A_3^* & \lambda_R^2 A_4^* \end{bmatrix} \begin{Bmatrix} \dot{h}/u \\ b\dot{\alpha}/u \\ \alpha \\ h/b \end{Bmatrix}$$
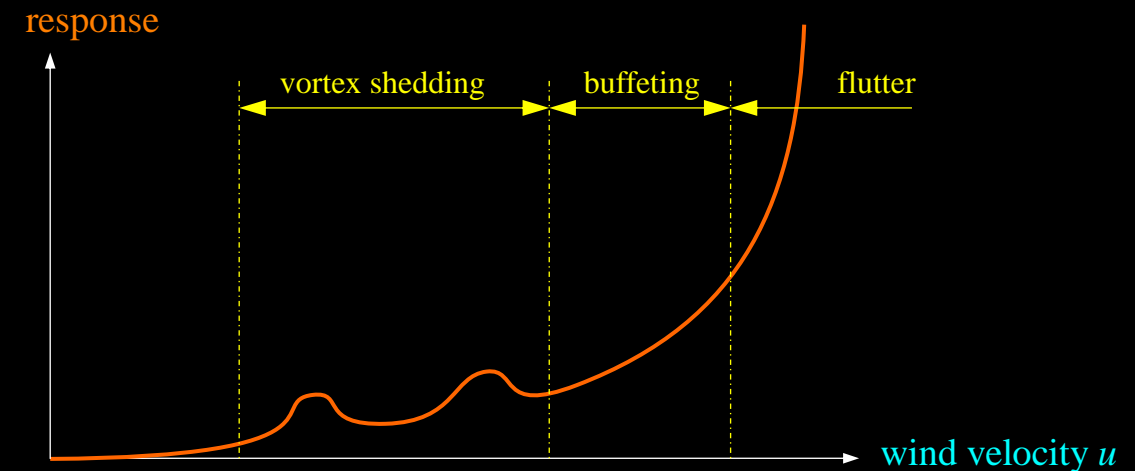
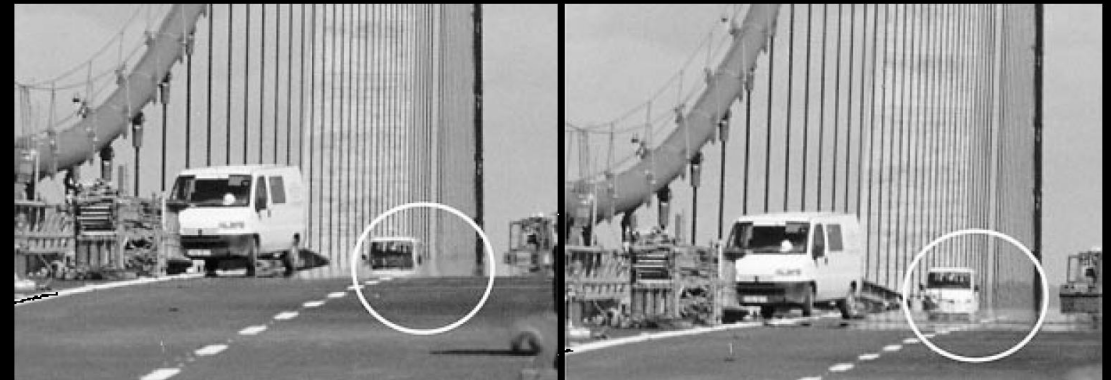# Cable-supported bridges – Dynamic effects: Wind-induced oscillations

Use of flutter derivatives for aeroelastic phenomena

- Even if aerodynamic stability is satisfied – i.e., the critical velocities for flutter and torsional divergence are higher than the design wind speed – large wind-induced oscillations may not be excluded.

- The most relevant phenomena potentially causing large, albeit self-limiting oscillations are
  - buffeting
  - vortex-shedding
  - galloping

- While galloping mainly affects cables, buffeting and vortex shedding also cause oscillations of the bridge girder. As seen in the upper figure, these mechanisms occur at lower wind velocities than coupled flutter.

- All these phenomena are fairly complex and can only be approximated analytically or numerically (computational fluid dynamics), requiring wind tunnel tests in general. They will only be briefly outlined in the following. As with flutter, consulting with wind experts is recommended.

Schematic response of a slender structure under wind (adapted from [Gimsing 2012])

Vortex-induced oscillations on the Storebælt bridge before mounting of guide vanes [Gimsing 2012]

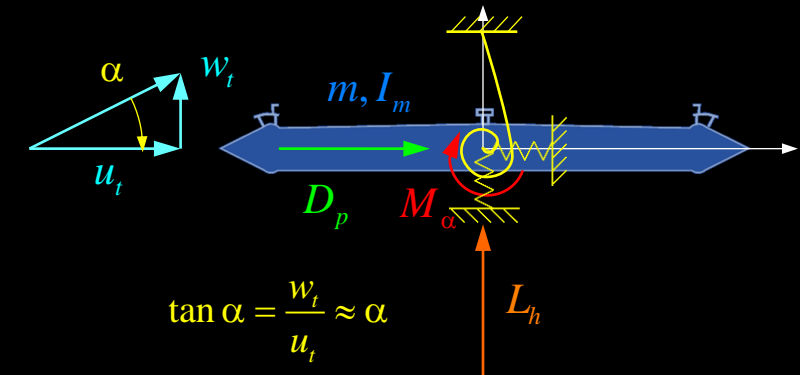# Cable-supported bridges – Dynamic effects: Wind-induced oscillations

Buffeting

- Buffeting is the forced, random vibrational response of a structure to random, turbulent wind. Turbulence can be due to topographical or structural obstructions or the bridge itself, the latter having minor importance.

- Using the horizontal and vertical turbulent wind components u_t and w_t (see *wind velocities and dynamic pressure* slide), normalised with respect to the mean wind velocity u), the buffeting forces may be expressed as

$$\begin{Bmatrix} L_{h,b} \\ M_{\alpha,b} \\ D_{p,b} \end{Bmatrix} = \frac{\rho u^2 b}{2} \begin{Bmatrix} c_L & \dfrac{\partial c_L}{\partial \alpha} + c_D \\ c_t b & \dfrac{\partial c_t}{\partial \alpha} b \\ c_D & \dfrac{\partial c_D}{\partial \alpha} \end{Bmatrix} \cdot \begin{Bmatrix} \dfrac{u_t}{u} \\ \dfrac{w_t}{u} \end{Bmatrix} \qquad \left(\frac{w_t}{u} = \tan \alpha \cdot \frac{u_t}{u} \approx \alpha \cdot \frac{u_t}{u} \right)$$

- These forces are inserted in the equations of motion of a two-dimensional section (see coupled flutter) to obtain the peak response of the structure

- The structure is then designed for the forces corresponding to the peak response (using e.g. RMS combinations of the modes).

Turbulent wind forces on bridge deck

$$\tan \alpha = \frac{w_t}{u_t} \approx \alpha$$

Exemplary wind spectrum (power spectral density)
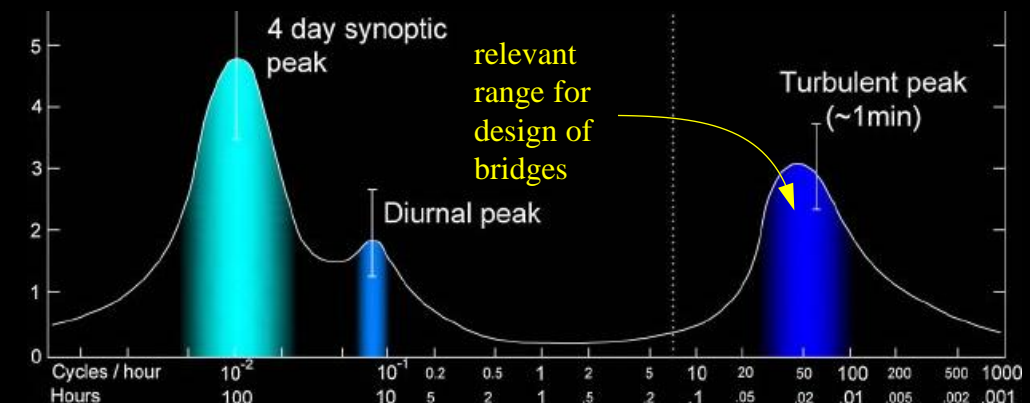
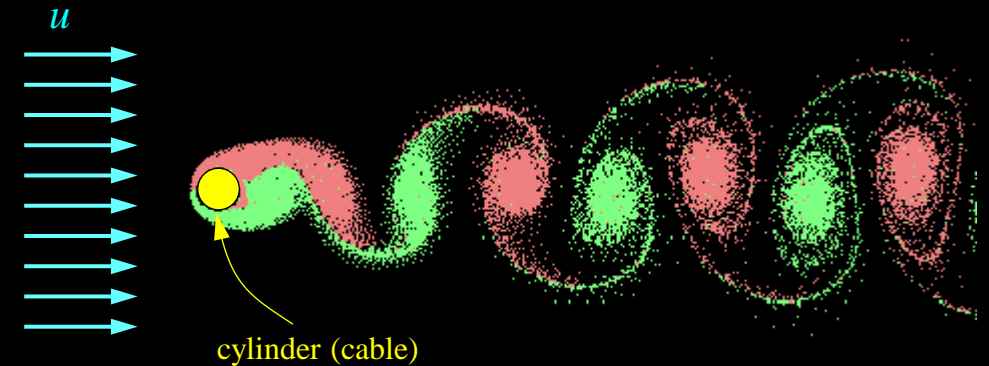# Cable-supported bridges – Dynamic effects: Wind-induced oscillations

Vortex shedding

- When air flows past a bluff (= not streamlined) body, vortices are created depending on the size and shape of the body, causing vibrations of slender bodies as observed by Strouhal in 1878. The Aeolian harp (Windharfe) makes acoustic use of this phenomenon.

- The shedding of vortices in the wake of circular cylinders was studied by Bénard and also studied by von Kármán, after whom the orderly array of vortices in the wake of a cylinder has been named (von Kármán street).

- For long prismatic bodies with a transverse dimension Ø (cable diameter, girder depth), the vortex shedding frequency is

$$f_s = S_r \cdot \frac{u}{\text{Ø}}$$

  where S_r = Strouhal number.

- Generally, the Strouhal number depends on the Reynolds number, but for long cylinders, $S_r \approx 0.21$ may be used. For bridge decks, it varies greatly; according to [Gimsing 2012], $S_r \approx 0.21$ was measured for Storebælt Bridge.

Shedding of vortices in the wake of a cylinder
(animation: C. de la Rosa Siqueira)

u

cylinder (cable)

Instantaneous vorticity magnitude field of a twin deck
(CFD analysis of Stonecutters bridge, effect of guide vanes)

guide vanes
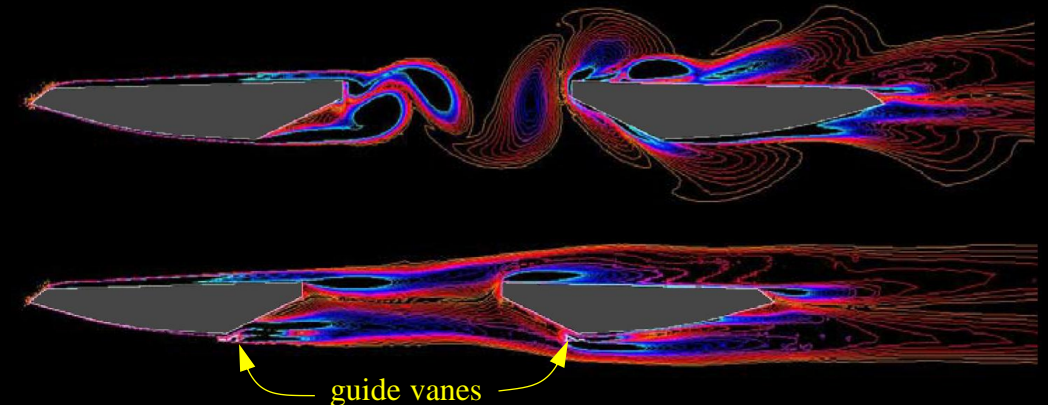
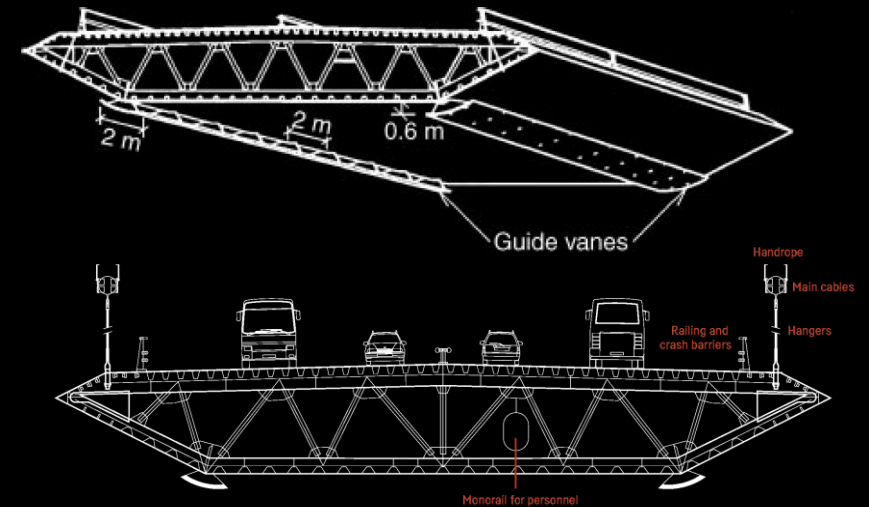# Cable-supported bridges – Dynamic effects: Wind-induced oscillations

Vortex shedding

- Large oscillations may occur in case of resonance, i.e., if the vortex shedding frequency coincides with a the frequency of a dominant eigenmode of the bridge cylinder f_i . Hence, the critical velocity is

$$u_{cr} = \frac{f_i \cdot \emptyset}{S}$$

- Even if the critical vortex-shedding velocity u_{cr} is reached, large oscillations only occur if all following conditions are met:
  - low structural damping
  - laminar wind flow with low turbulence intensity, nearly perpendicular to the girder axis (ca. $\pm 20°$)
  - u_{cr} high enough to excite bridge, but not too high such that narrowing of the wake disrupts the creation of vortices.

- Hence, only few cable supported bridges have exhibited excessive vortex-shedding oscillations though u_{cr} is often exceeded.

- The Storebælt Bridge experienced significant vortex-induced oscillations (photo on previous slide) before guide vanes were installed. As potential problems had been detected in the wind tunnel tests, provisions had been made in design to fit these elements to the bottom corners of the deck (figure and photo).

Guide vanes preventing vortex-induced oscillations on the Storebælt bridge [Gimsing 2012]

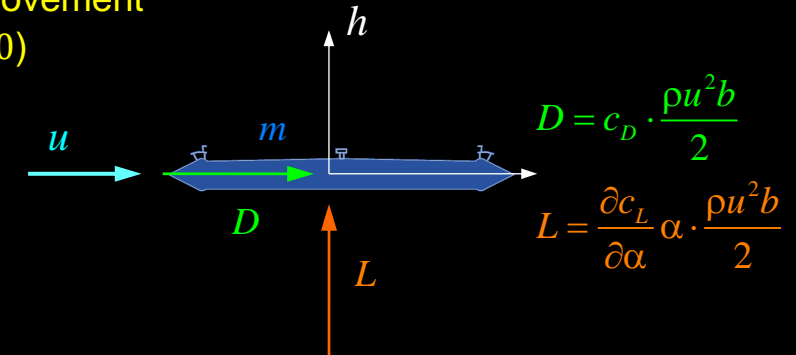# Cable-supported bridges – Dynamic effects: Wind-induced oscillations

Galloping

- Generally, two types of galloping are known: Wake galloping and across-wind galloping. The former refers to oscillations of a downstream body cylinder induced by the wake flow of an upstream cylinder. It is rarely relevant in bridges and therefore not further considered here.

- Across-wind galloping, simply referred to as galloping in the following, is a large amplitude oscillation in a plane normal to the wind flow velocity, by slender structures with bluff cross-section, such as ice-laden cables or – rarely – bridge decks (e.g. when loaded with traffic).

- The static lift and drag coefficients (c_L, c_D) as functions of the angle of attack α are sufficient for a satisfactory analytical description of galloping, but the variation of the angle of attack with the movement of the body (figure) needs to be accounted for. The equation of motion is thus

$$m\ddot{h} + d\dot{h} + kh = -\frac{\rho u^2 b}{2}\left(\frac{\partial c_L}{\partial \alpha} + c_D\right)\Bigg|_{\alpha=0} \cdot \frac{\dot{h}}{u} \qquad \left(\frac{\dot{h}}{u} = -\tan\alpha \approx -\alpha\right)$$
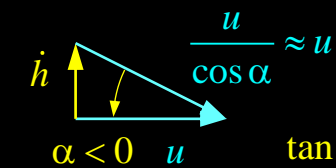
- The structure tends to instability if the total damping is negative:

$$d + \frac{\rho u b}{2}\left(\frac{\partial c_L}{\partial \alpha} + c_D\right)\Bigg|_{\alpha=0} \leq 0 \qquad \rightarrow \left(\frac{\partial c_L}{\partial \alpha} + c_D\right)\Bigg|_{\alpha=0} \leq 0$$
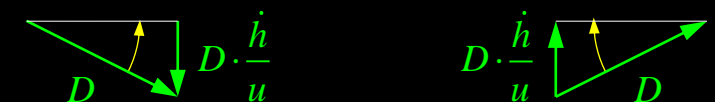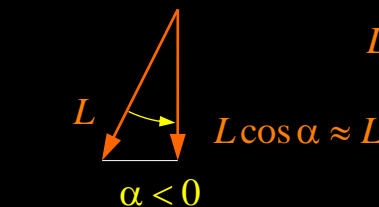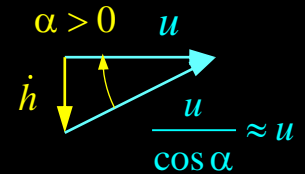
No movement ($\dot{h} = 0$)

$$D = c_D \cdot \frac{\rho u^2 b}{2}$$

$$L = \frac{\partial c_L}{\partial \alpha}\alpha \cdot \frac{\rho u^2 b}{2}$$

Relative velocity and forces:
Upward movement ($\dot{h} > 0$)   Downward movement ($\dot{h} > 0$)

$$\frac{u}{\cos\alpha} \approx u$$

$$\tan\alpha = \frac{\dot{h}}{u} \approx \alpha$$

$$\frac{u}{\cos\alpha} \approx u$$

$$L\cos\alpha \approx L$$

$$L\cos\alpha \approx L$$

$$D \cdot \frac{\dot{h}}{u}$$

$$D \cdot \frac{\dot{h}}{u}$$

Cable-supported bridges – Dynamic effects: Wind-induced oscillations

Cable vibrations

- Main cables of suspension bridges are rarely suffering from large vibrations. They may e.g. be excited by oscillations of their ends (Pylon tops).

- Hangers and stay cables are more frequently affected by vibrations. These may be caused by vortex shedding or galloping, where the latter is more frequent.

- While dry galopping may also occur, rain-wind induced vibrations of stay cables are the most frequent problem. The exact mechanism is still not well understood, but it appears that the creation of water rivulets along a significant length of a cable causes an apparent modification in cable shape, leading to the initiation of galloping (video)

- Cable vibrations may cause discomfort with users, and ultimately lead to fatigue failure of a stay cable or components of the cable. Mitigation can be classified as follows:
  - aerodynamic control (surface modification e.g. to avoid rivulets)
  - structural control (modify mass or stiffness)
  - mechanical control (e.g. viscous dampers, see video)

Cross-section of stay cable with upper water rivulet
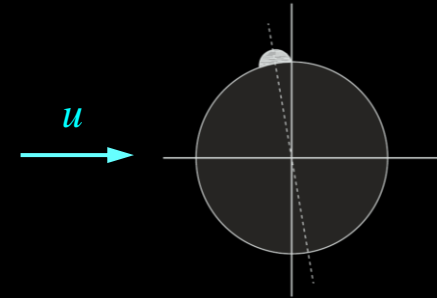
Indented HDPE stay tube (Stonecutters bridge)

u

Rain-wind induced vibrations of stay cables (Franjo Tuđman Bridge, Dubrovnik)